THE AN/AMQ-27 ( ) METEOROLOGICAL STATION, AUTOMATIC

Lee G. Buhr, et al

Packard-Bell Electronics Corporation
Newbury Park, California

6 August 1969

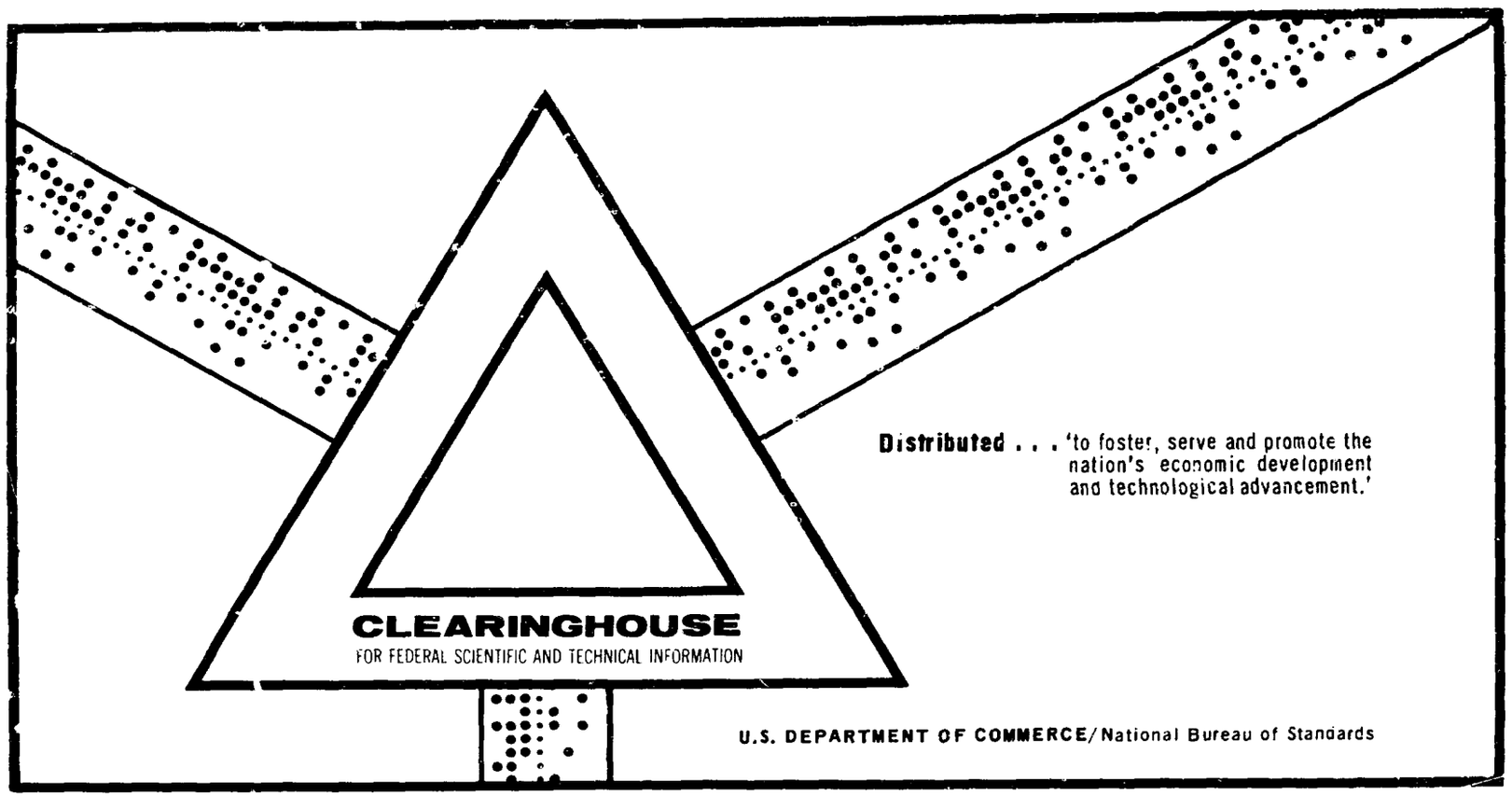

AFCRL - 69-0374

THE AN/AMQ-27 ( ) METEOROLOGICAL STATION, AUTOMATIC

by Lee G. Buhr - Octavio Galindo - Jan Rampacek

Packard Bell Electronics
Space and Systems Division
649 Lawrence Drive
Newbury Park, California 91320

Contract No. F19628-67-C-0174
Project No. 6670
Task No. 667002
Work Unit No. 66700201
FINAL REPORT

Period covered: February 1967 to August 1969

Date of Report - 6 August 1969

Contract Monitor - Russell M. Peirce
Aerospace Instrumentation Laboratory

Prepared for

AIR FORCE CAMBRIDGE RESEARCH LABORATORIES
OFFICE OF AEROSPACE RESEARCH
UNITED STATES AIR FORCE
BEDFORD, MASSACHUSETTS 01730

174

AFCRL - 69-0374

THE AN/AMQ-27 ( ) METEOROLOGICAL STATION, AUTOMATIC

by Lee G. Buhr - Octavio Galindo - Jan Rampacek

Packard Bell Electronics
Space and Systems Division
649 Lawrence Drive
Newbury Park, California 91320

Contract No. F19628-67-C-0174
Project No. 6670
Task No. 667002
Work Unit No. 66700201
FINAL REPORT

Period covered: February 1967 to August 1969

Date of Report - 6 August 1969

Contract Monitor - Russell M. Peirce
Aerospace Instrumentation Laboratory

Prepared for

AIR FORCE CAMBRIDGE RESEARCH LABORATORIES
OFFICE OF AEROSPACE RESEARCH
UNITED STATES AIR FORCE
BEDFORD, MASSACHUSETTS 01730

ABSTRACT

Packard Bell has successfully completed a program that developed an expendable, airdroppable weather station (the AN/AMQ-27 ( ) Meteorological Station, Automatic) for the Air Force Cambridge Laboratories (AFCRL) under contract number F19628-67-C-0174. The station grew out of a requirement for meteorological measurements in hostile or inaccessible areas. Packard Bell investigated this problem and devised a system that met the program's objectives of cost, reliability and covertness. The station's deployment vehicle mimics an autogyro when dropped from an aircraft. The main rotor blades control descent rate, while a set of counter rotating blades provide vertical stability. Upon touchdown, the impact spear embeds itself in the earth thereby keeping the system upright. Since there are no highly mechanized devices required for arming the system, the station is operational at impact. This report covers in detail, the problems and their solutions that were encountered as this program progressed to its completion.

TABLE OF CONTENTS

TABLE OF CONTENTS (Cont)

LIST OF ILLUSTRATIONS

LIST OF ILLUSTRATIONS (Cont)

LIST OF ILLUSTRATIONS (Cont)

LIST OF TABLES

SECTION I

INTRODUCTION

1.0 GENERAL

Packard Bell has successfully completed developing an expendable, airdroppable weather station (the AN/AMQ-27( ) Meteorological Station, Automatic) for Air Force Cambridge Research Laboratories under contract No. F19628-67-C-0174. This system grew out of a requirement for weather information in those areas where such information was limited, unreliable and/or denied by the enemy.

1.1 PROGRAM SUMMARY

The first design configuration was based on a soft-landing, achieved by dropping the vehicle from an aircraft with a parachute or autorotational device to slow its descent. Upon landing, tubular snap-locking legs, folded up during the drop, automatically engaged to raise the station to an upright position. A jack-in-the-box antenna extended automatically with the ejection of the cover plate, which occurred on impact. Conventional wind vane and three-cup anemometer designs were employed in the sensing elements.

During the study phase, however, it soon became apparent that this design did not lend itself to the program objectives of cost, reliability and covertness. The soft-landing feature required severe degradation of system performance which could not be offset by the effect of a low impact velocity upon the requirements of the sensor and electronic elements. This initiated the exploratory hardware development phase of the program.

The decision to alter the initial concept made it necessary to apply a good deal of imagination to sensor and packaging design which would with-

stand the high impact shock of a hard landing. The resultant design is the presently configured vehicle -- a slim, modular cylinder, using two sets of fixed-pitch airfoil blades which automatically unfold by spring action and provide a controlled, vertically-oriented descent. An impact spear retains the vertical vehicle orientation upon contact with the ground.

The sensor package is a module situated immediately above the stabilizing rotor plane. Solid state methods are used in measuring wind speed, wind direction, temperature, humidity, pressure, precipitation, and magnetic north reference. Conforming to vehicle shape, the sensor package is protected during vehicle descent by a split fairing which is released upon ground impact.

The wind vane and anemometer cups were discarded in favor of more rugged --- and more unconventional --- sensing methods. Wind speed and direction are sensed by a drag cylinder. The pressure of the wind against the cylinder causes a strain gage transducer to produce a voltage change proportional to wind speed. Four transducers are used. Wind direction measurements are obtained by placing the transducers in pairs at right angles. The wind speed voltages are therefore transmitted in such a manner as to indicate wind direction (the vector sum of the drag forces).

Precipitation sensing is also accomplished through an imaginative application of known techniques. The sound of the rain drops hitting the top of the sensor package is picked up by a microphone. The total count of drops hitting the package between interrogations is stored and transmitted to the base station on command.

Communications for the system is provided by a single frequency system operating in the range of 40 to 42 MHz and is capable of transmitting over at least 50 miles of range. The communication system operates in two modes; receive (active) and transmit. Basically, the system is always in the

receive (active) mode, drawing minimum battery power. If an interrogation is received, the transmit mode is used at relatively high peak power to provide a reasonable range of communication. Power is supplied by a 10-ampere-hour battery package.

All the measured parameters have been successfully transmitted via radio telemetry over 50 miles of mountainous terrain. The deployment vehicle has been dropped from altitudes ranging from [illegible] to 1500 feet.

With the completion of the exploratory hardware development phase, the follow-on flight testing and evaluation phase was initiated. The objective of this phase would be to develop an automatic, self-erecting dipole antenna; to test the deployment vehicle's compatibility of landing in terrain having different types of soil; and to evaluate its aerodynamic configuration to determine what system design changes would be required to extend its capabilities to a high speed launch.

SECTION II

SYSTEM DESCRIPTION

2.0 The study programs' evaluation of design concepts and final vehicle configuration will be covered in this section.

2.1 DEPLOYMENT VEHICLE

2.1.1 BACKGROUND

During the course of the study program, several conceptual approaches to the vehicle design were studied and analyzed from many standpoints. Basically, four designs and their associated deployment concepts were pursued. These were:

a. A balloon descent with a droppable anchor capable of providing a soft (low impact velocity) landing with a moderate descent rate until ground contact by the anchor.

b. A parachute controlled descent with auxiliary equipment to reduce the moderate in-flight descent rate to a soft landing.

c. An autorotative device with variable pitch control, providing relatively high speed descent and a landing at a moderate to low impact velocity.

d. An autorotative device of fixed pitch providing a relatively high descent rate and impact velocity.

The above four general approaches were utilized in evaluations because it became clear early in the study that there were, basically, two choices insofar as impact velocities were concerned -- either quite low (5-10 FPS) or relatively high (50 FPS or greater). Looking at sensors and electronics, moderate impact velocities, as opposed to high impact velocities, could not be justified although a low impact velocity could definitely be considered highly desirable.

In terms of cost, reliability, covertness, etc. it became evident as the study ensued that a soft landing would result in severe degradation of the system performance which could not be offset by the effect of a low impact velocity upon the requirements of the sensor and electronic elements. Upon rating the four basic concepts, it was concluded that the fixed-pitch autorotative vehicle was the only satisfactory solution to the problem. This conclusion was easy to arrive at in terms of vehicle analysis, but was useless unless sensor and electronic elements of the system could be configured to support the requirements imposed by such a vehicle.

As study was pursued towards evaluation of methodology for sensors and electronics in view of the autotOtative vehicle requirements, it was determined that the trade-off between soft and hard landings in these areas was not as severe as originally envisioned. Thus, the aotorotative fixed-pitch vehicle could indeed be justified, not only in terms of itself, but also in terms of the overall system.

2.1.2 TECHNICAL DISCUSSION

The use of rotating blades, both passive and active, to limit vertical descent velocity is quite feasible. With properly shaped airfoil sections, impact performance comparable to parachutes is possible. General helicopter aerodynamics are applicable for this problem of autorotative descent. In this particular case, however, only the factor of collective pitch was considered and, for obvious reasons, only passive rotating blades were considered. For relatively high descent velocities in which the rotor is in the windmill brake state, the Rankine Froude momentum theory is applicable. This theory assumes that the propeller acts as a continuous disk of rotating blades which sustains a pressure discontinuity and produces uniform streamline flow through the disk. The dependence of the thrust on both the free stream velocity and the resulting velocity difference are derived with the use of Beonoulli's relationship between pressure and velocity.

For lower order descent rates, momentum theory no longer holds and a turbulent windmill brake state develops. (See Figure 2-1.) For both these conditions, it becomes convenient to define two dimensionless thrust coefficients, $\bar{f}$ and $\bar{\bar{F}}$ which depend on the vertical velocity of the vehicle and the flow through the rotor respectively. If U is the wake velocity of flow through the rotor and V the vertical velocity of the vehicle, $\bar{f}$ and $\bar{\bar{F}}$ can be defined as follows,

$$\bar{f} = \frac{T}{2A\rho V^2} \tag{1}$$

$$\bar{\bar{F}} = \frac{T}{2A\rho U^2} \tag{2}$$

$$U = V \pm v \tag{3}$$

Where: T = Decelerating Thrust Force

A = Area of Rotor Disc

ρ = Air Density

v = Average Induced Flow Through the Rotor

For vertical descent during the windmill brake state, a simple relation between $\bar{f}$ and $\bar{\bar{F}}$ is obtained from Equations (1) and (2) with the use of the thrust equation $T = 2A(V-v)v$, derived from the Rankine Froude momentum theory.

$$F = \sqrt{\frac{\bar{\bar{F}}}{\bar{f}}} - 1 \tag{4}$$

$$\bar{f} = \frac{\bar{\bar{F}}}{(1 + \bar{\bar{F}})^2} \tag{5}$$

This relationship is illustrated in the upper portion of Figure 2-2.

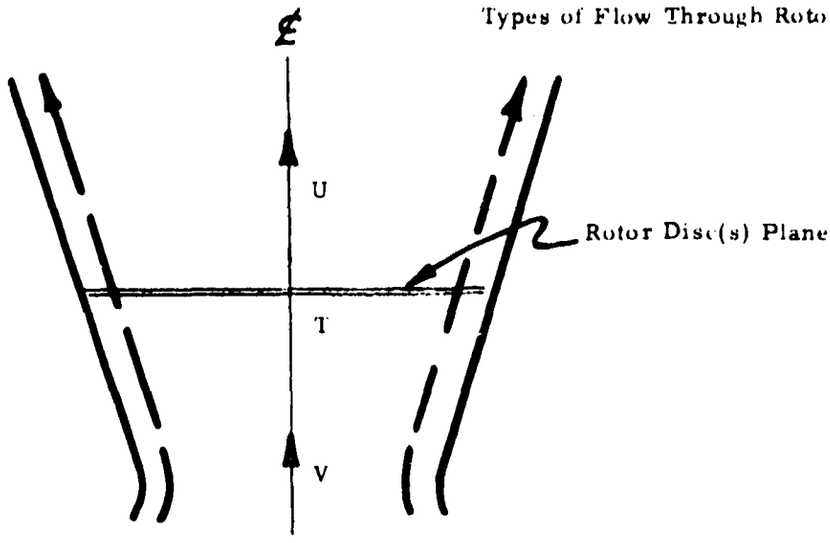

Windmill Brake State (Momentum Theory)

$\frac{U}{V} < 1 \qquad \bar{f} = \frac{\bar{F}}{(1+\bar{F})^2}$

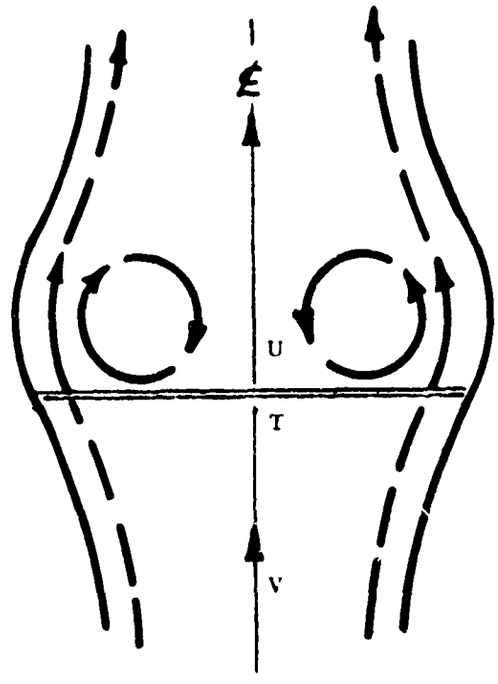

Turbulent Windmill Brake State

$0 < \frac{U}{V} < 1/2 \qquad 1/4 < \bar{T} < \infty$

Figure 2-1. Types of Flow-through Rotor

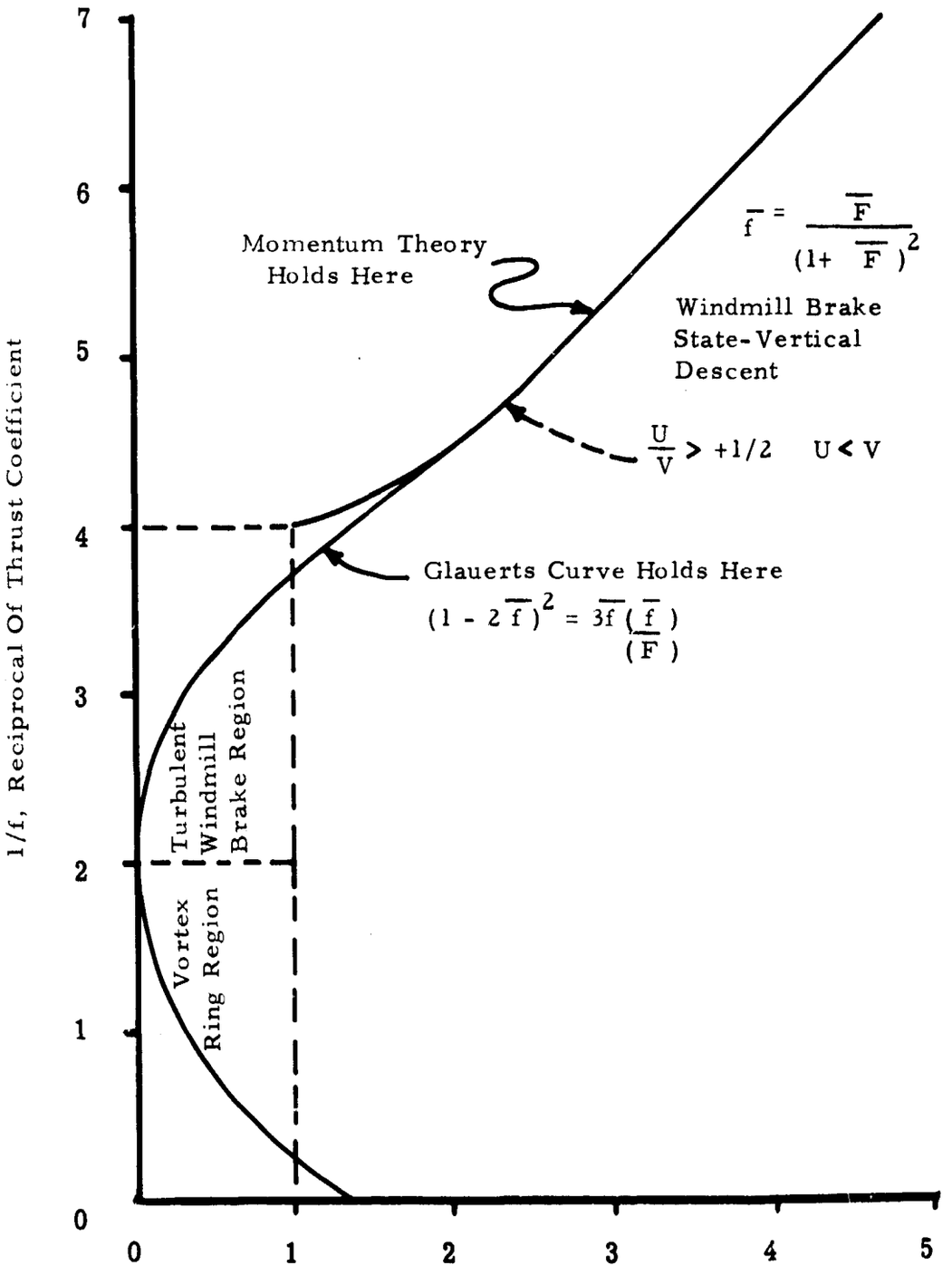

Figure 2-2. Reciprocal Thrust Coefficient Relations

For vertical descent during the turbulent windmill brake state, the wake velocity approaches zero. The corresponding limits of the thrust coefficients based on equations (3), (4) and (5), become

$$\bar{f} = \frac{1}{4} \qquad \bar{F} = 1$$

and is illustrated by the bounded area of Figure 2-2. For this region, Glauert's empirical curve $(1-2\bar{f})^2 = 3\bar{f}\left(\frac{\bar{f}}{\bar{F}}\right)$ is recommended. This curve is shown down to $\frac{1}{f}$ less than 2.0. The curve shown applies to power rotors only. The problem now becomes one of determining at what rates of descent the pure or turbulent windmill brake states apply.

To illustrate, consider the case of the 20-pound package and a two blade rotor whose diameter and mean chord are 6 and 0.1 feet, respectively. Equating the in-plane thrust and drag forces (constant descent velocity) yields

$$C_\ell \frac{U}{\omega r} = C_d \qquad (6)$$

Where C_ℓ and C_d are the respective lift and drag coefficients and U and ωr are the descent and rotor velocities. The thrust is defined as

$$T_{thrust} = W \int \frac{\rho}{2} (\omega r)^2 C_\ell \, dS$$

which with the use of (6) yields

$$F = \frac{W}{2A\rho U^2} = \frac{1}{4A} \int \frac{C_\ell^3}{C_d^2} dS = \frac{C_\ell^3}{C_d^2}_{AVG} \frac{\Sigma}{4} \qquad (8)$$

where Σ is defined as the ratio of blade area, S, to disk area, A. Assuming an average lift height and drag relation, $C_d = .015 + .045 C_\ell^2$, the condition of minimum descent velocity is achieved by maximizing $\bar{F}$ or $C_\ell^3/C_{d_2}^2$ which yields $.015 = .045 C_\ell^2/3$ or $C_\ell = 1$ and $C_d = .06$ such that $(C_\ell^3/C_d^2)_{max} = 278$. Noting also that $\Sigma = \frac{2 \times 0.1}{3\pi} = .0212$, we obtain from equation (8) $F = 278 \times \frac{.0212}{4} = 1.47$.

This value of $\bar{F}$ ($\frac{1}{\bar{F}}$ = .68) requires Glauert's Curve, (momentum theory not valid in this region) in Figure 2-2 which yields $\frac{1}{\bar{f}}$ = 3.4 or $\bar{f}$ = 0.294; hence the descent velocity is

$$Z = \sqrt{\frac{W}{2A\rho\bar{f}}} = \sqrt{\frac{20}{2(28.3)0.00238(.294)}} = 22.5 \text{ fps}$$

This value of the descent velocity is definitely on the low side in terms of the deployment vehicle concep.. The drag and lift factors used in the above analysis are taken from standard efficient rotor design. In the AN/AMQ-27 vehicle it is necessary to have increased impact velocity to insure reasonable spear penetration. This desire for increased impact velocity dovetailed very nicely with the desire to use relatively unsophisticated, easy to produce rotor blade design.

The mathematical analysis given above indicated that a reasonably wide tolerance on blade design and a potential weight/blade efficiency trade off existed which was well within the conceptual framework of the vehicle. In one extreme, using optimized, efficient rotor blade design such as used in the analysis, the vehicle weight can be increased to over 50 pounds and still not exceed the impact velocity range of 55-70 FPS necessary to insure good spear penetration. In the other extreme, retaining the estimated weight of 20 pounds, it can be seen that a relatively large degree of freedom existed in a rotor design that would provide a 55-70 FPS impact velocity. A final factor which required investigation was the factor of drop height as depicted in Figure 2-3. When the vehicle is deployed from the aircraft, a loss of altitude will be incurred befored autorotative descent is achieved.

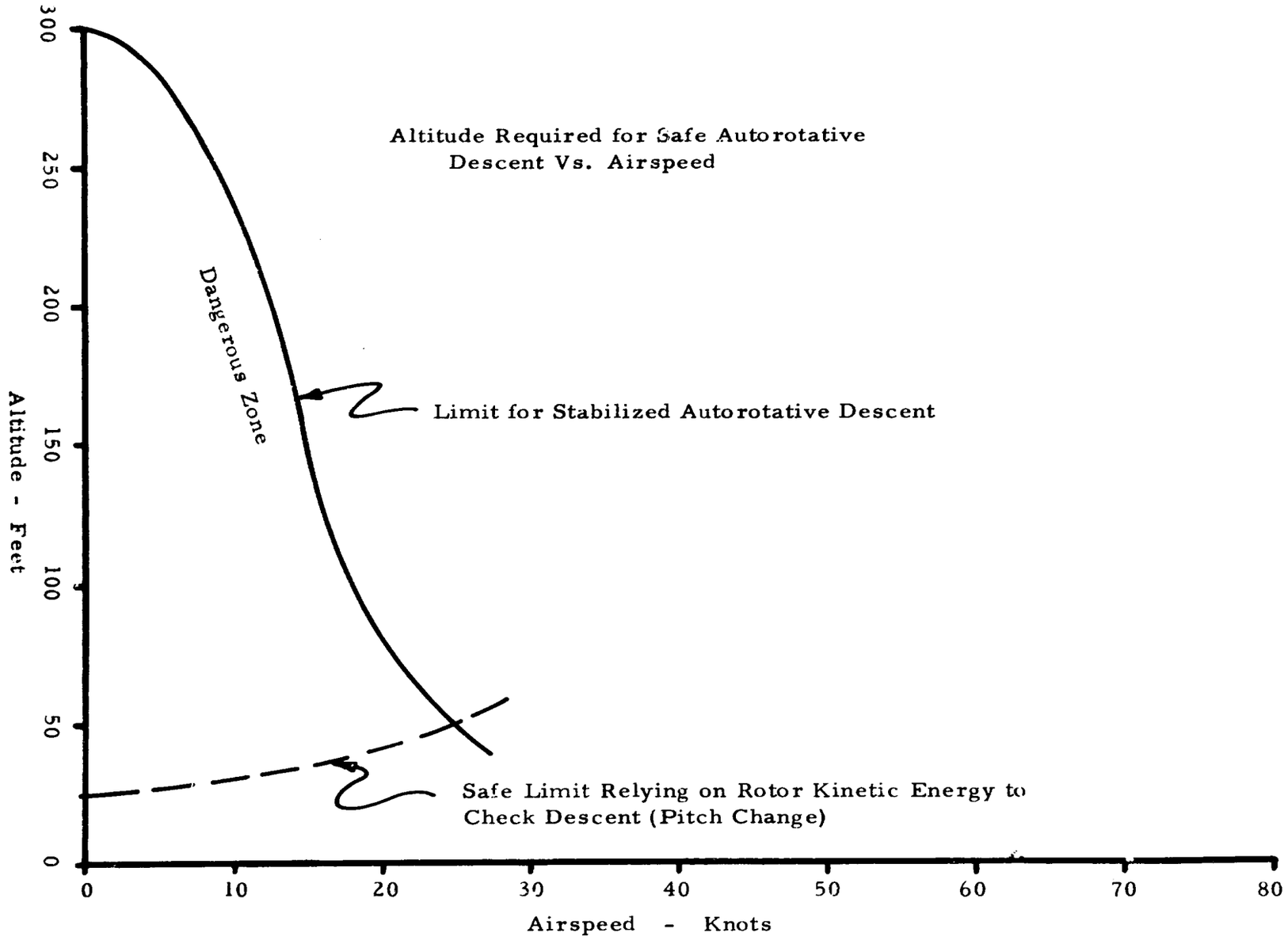

Figure 2-3. Altitude Required for Safe Autorotative Descent vs Airspeed

2.1.3 IMPACT SPEAR PENETRATION ANALYSIS

Following completion of the theoretical analysis of the vehicle concept, the mechanical detailed paper design was initiated. The main objective was to make the functional parts simple to fabricate. It was decided to fabricate only one model initially, since some changes would probably be necessary after the first flight test. This flight vehicle, as depicted in Figure 2-4, was six feet long with the main body 2.5 inches in diameter, simulated sensor package 5 inches in diameter, lower blades 32 inches long, upper stabilizing blades 16 inches long and a total weight of 20 pounds.

To gather more experimental data while the vehicle was being fabricated, a drop test experiment was devised for the impact spear.

The ground drop test, using the calculated vehicle impact velocity of 60 feet per second, simulated the vehicle impact conditions. This experiment produced information on the required spear penetration for vehicle stability in a medium to hard type soil. Using the dynamics equations

$$v^2 = 2gh \qquad (1)$$

$$\frac{w}{g} v = K \qquad (2)$$

the vehicle impact conditions were simulated. Assuming the weight (w) of the vehicle to be 20 pounds and the impact velocity (v) to be 60 feet per second, equation (2) was solved for K:

$$K = \frac{20}{32.2} 60$$

$$K = 37.3$$

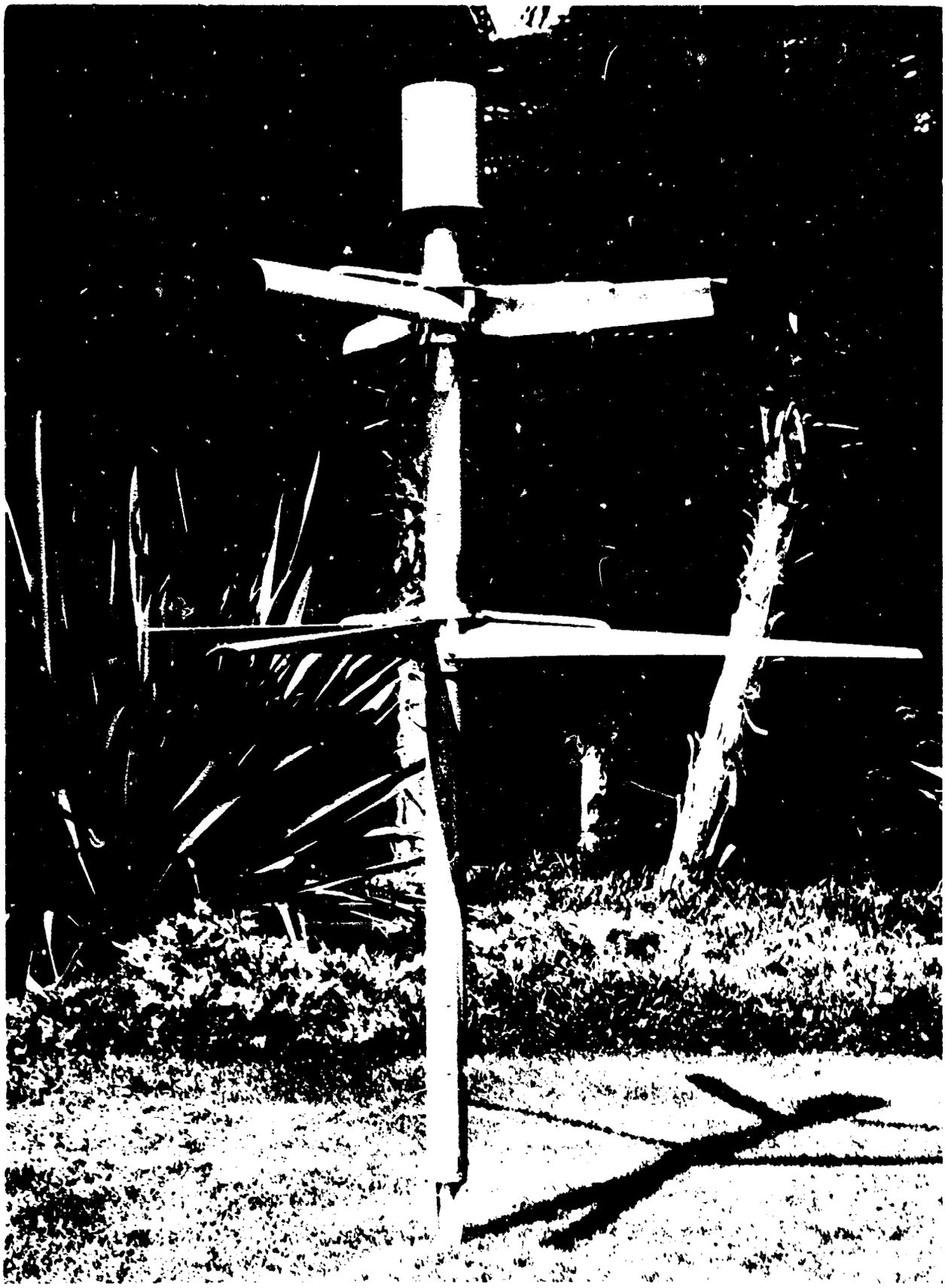

Figure 2-4. Flight Vehicle with Spear Impacted

By substituting this into equation (1), the experimental weight (w) to be used at a realistic height (h) was calculated as follows:

$$v^2 = 2gh \text{ or } \frac{w^2}{g} \quad 2gh = K^2$$

solving for h and substituting in the appropriate values

$$h = \frac{22,400}{w^2}$$

Choosing a weight (w) of 100 pounds, the drop height (h) became 2.3 feet.

Using this information, a 100-pound weight was attached to the impact spear with a harness to support it. The impact spear was attached to a pulley system which, in turn, was mounted on an A-frame support structure. The soil around the Packard Bell facility being rocky and quite compact was classified as a medium to hard type soil. The experimental equipment was set up and many test drops were conducted at different locations. A review of the test data indicated the best results were obtained when the weighted impact spear was released from a height of 30 inches. At this release height, the spear penetrated the ground to a depth of 7 inches and was quite stable. For vehicle stability, a spear penetration of 7 inches or more is needed. This type of penetration will be achieved if the vehicle's impact velocity is 60 feet per second or greater.

2.1.4 FINAL CONFIGURATION

The AN/AMQ-27 vehicle evolved into a slim modular cylinder (as depicted in Figure 2-5) using fixed pitch air foil blades to control its rate of descent and an impact spear for ground stability. The main body and the rotor blades of the vehicle were fabricated from light-weight tubular aluminum. This design configuration required the use of two sets of air foil blades. The lower rotor blades control the rate of vehicle descent, while the upper counter rotating blades assist in rate of descent control and provide vertical

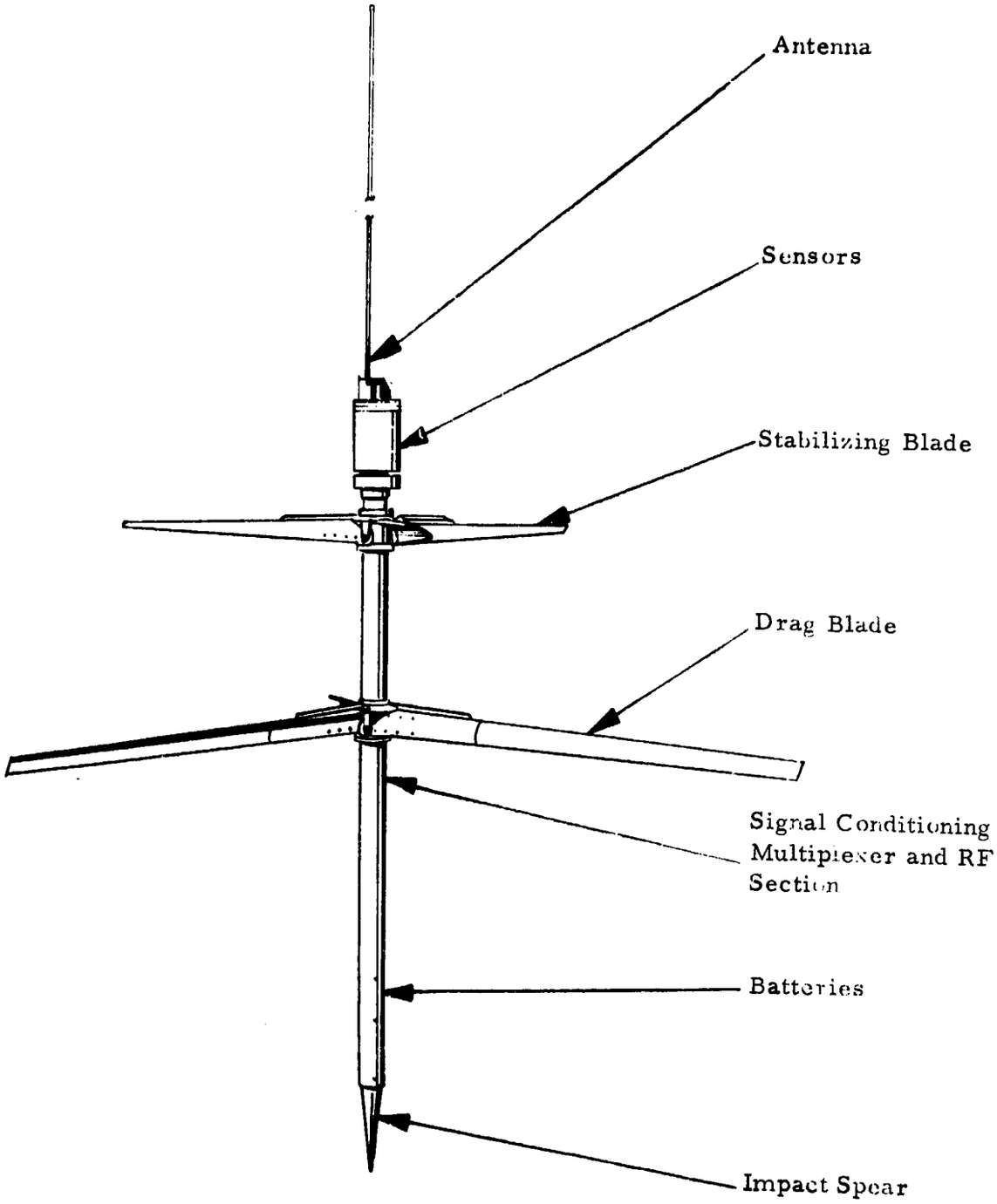

Figure 2-5. Tactical Air Droppable Automatic Meteorological Station

stability to the vehicle. Both sets of rotor blades are pivoted at their roots, permitting the blades to fold downward, thereby conforming to the cylindrical shape of the vehicle body for storage. Each set of blades is spring loaded at the pivot points to aid in their deployment during descent. The impact spear is a heat treated, one-inch diameter rod twenty four inches long.

The main body tube houses the batteries and support electronics as depicted in Figure 2-6. These modules are protected with sufficient energy absorbing material to protect them from excessive shock loads received when the vehicle impacts the ground.

The sensor package for the AN/AMQ-27 is a module situated immediately above the stabilizing rotor plane. Mounted to the top of this module is the delayed release antenna.

The final physical characteristics of the vehicle are listed in Table 2-1.

When the AN/AMQ-27 vehicle is released from an airplane as shown in Figure 2-7, the two sets of rotor blades automatically unfold by spring action and counter rotate during descent, providing the stability for a proper landing and spear penetration. While descending to earth, the vehicle offers a very small silhouette to a ground observer and, therefore, is not easily detected.

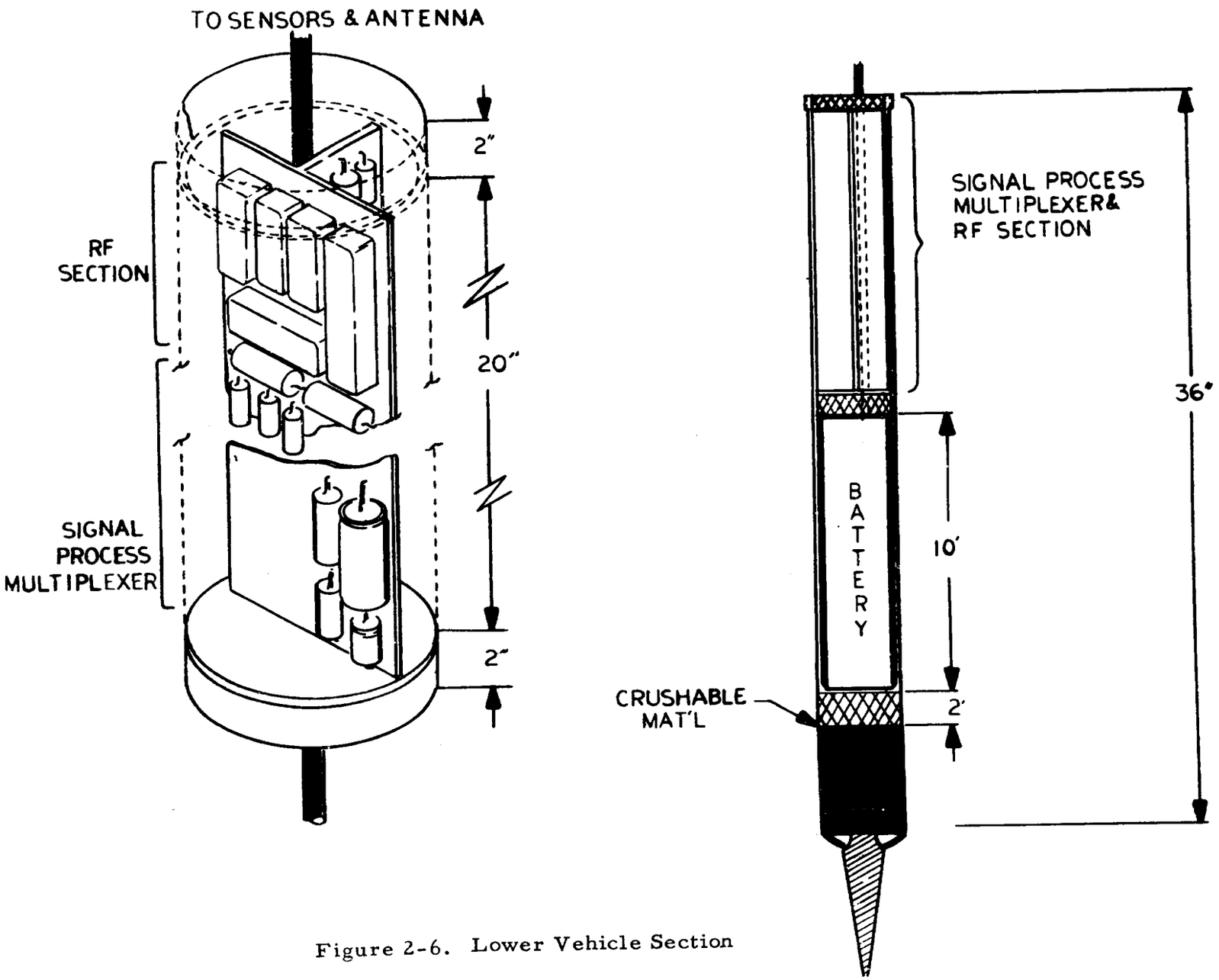

Figure 2-6. Lower Vehicle Section

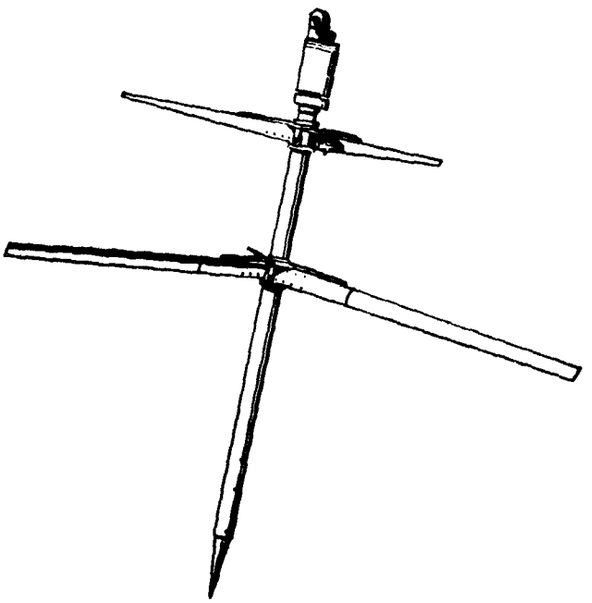

Figure 2-7. Airplane Release of AN/AMQ-27

Table 2-1. Physical Characteristics of Vehicle

Section	Length (inches)	Diameter (inches)	Weight (lbs)
Antenna	71	3/4	1.0
Sensor	6	4-1/2	4.0
Aerodynamic	20	4	5.0
Blades Folded	-	4-1/2	--
Blade Circle Dia.	-	90	--
Canister	36	4	2.0
Electronics	20	3-1/2	4.0
Battery	10	3-1/2	7.0
Shock Pads	-	--	1.0
Spear	24	1	5.0
Balancing Wts.	-	--	3.0

TOTAL LENGTH: 162 inches (deployed); 68 inches (stored)

TOTAL WEIGHT: 32 LBS.

2.2 ELECTRONICS AND COMMUNICATIONS ASSEMBLIES

2.2.1 TELEMETRY SYSTEM OPERATION

Figures 2-8 and 2-9 serve as guides to show the telemetry link as it was demonstrated and as it is intended to be used.

Initially, a one-second one-shot is triggered through a momentary pushbutton on the front panel of the base station. Two simultaneous tones then modulate an FM high-powered transmitter for a one-second period.

The command receiver in the vehicle then detects the rf, amplifies the two tones, and feeds them to the two tone decoders. The two tone decoders, after a 500-millisecond integration period, each produce a pulse. These two pulses are then fed into an AND gate which produces a single pulse turning on system power through a flip-flop. This simultaneously removes power from the receiver and switches a coaxial switch from a receive to a transmit mode. At this time, a mechanical multiplexer sequentially steps through each sensor data point, modulates the subcarrier oscillator with a dc signal and simultaneously keys the transmitter. The subcarrier also modulates the carrier frequency. The base station receives the data. At the end of the last data point, a pulse then resets the flip-flop removing system power, restoring power to the receiver and returns the coaxial switch to receive. The transmitted data are received by the base station receiver and the subcarrier is detected and fed into a subcarrier frequency. The subcarrier discriminator demodulates the carrier deviation frequency which is proportional to the dc input. The output data are proportional to the input data.

The electronic package space configuration is shown in Figure 2-10.

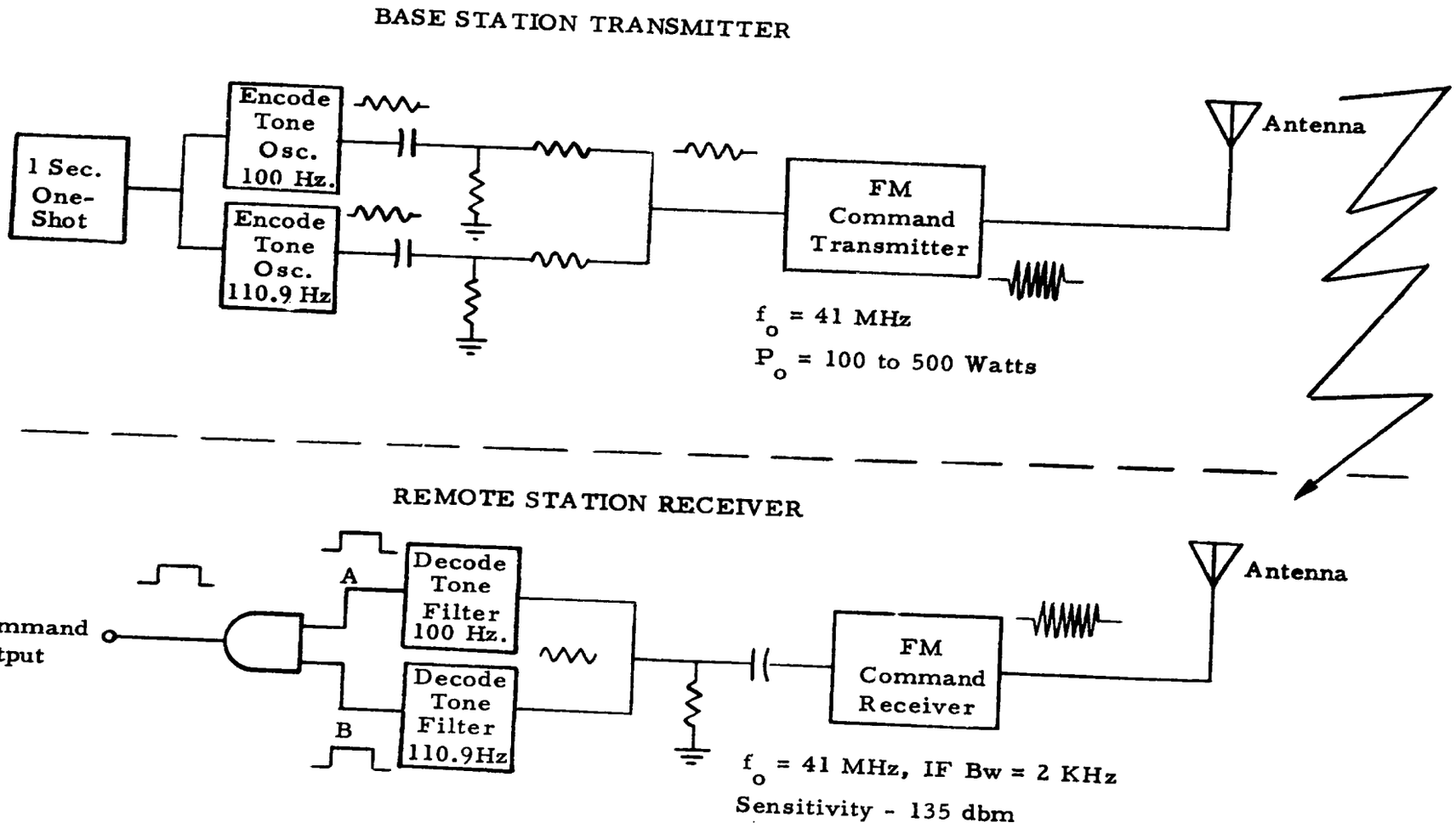

Figure 2-8. Base Station to Remote Unit RF Link

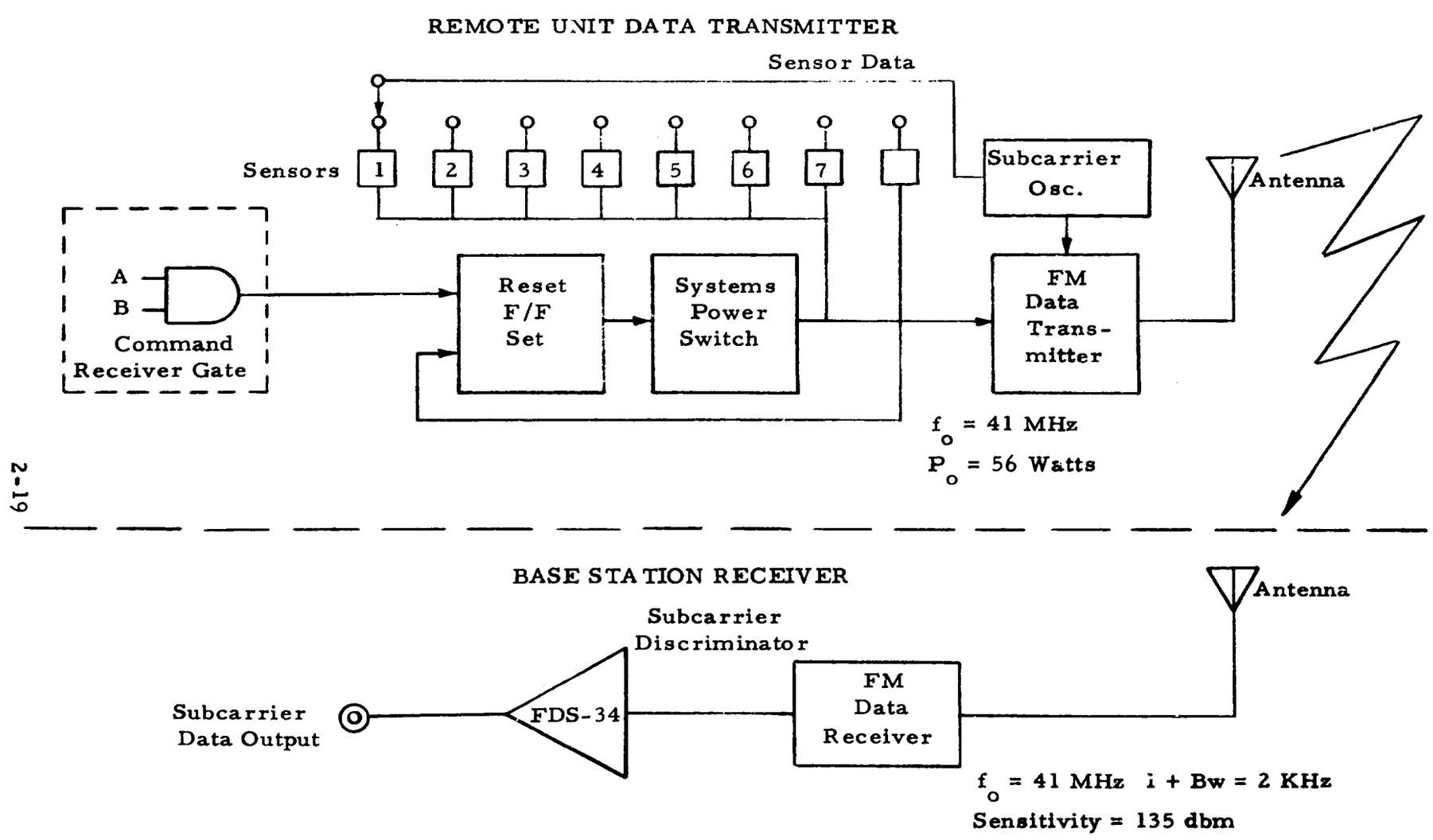

Figure 2-9. Remote Unit to Base Unit RF Link

REVISIONS						
ZONE	LTR	DESCRIPTION	DFT	CHK	DATE	APPR

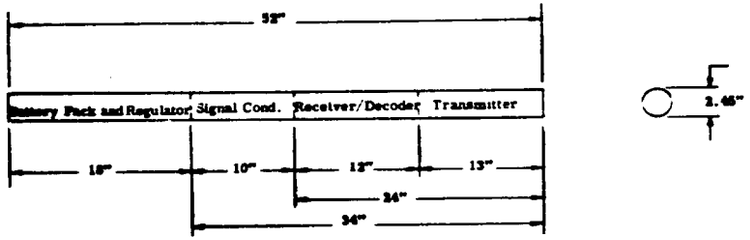

Functional Electronics:

1. Transmitter
2. Receiver
3. Signal Conditioner Circuits
4. Power Pack and Regulator Circuits

QTY REQD	PART OR IDENTIFYING NO.	NOMENCLATURE OR DESCRIPTION	CODE IDENT	REF DESIGNATION	SPECIFICATION	ZONE	ITEM NO.

LIST OF MATERIAL OR PARTS LIST

UNLESS OTHERWISE SPECIFIED DIMENSIONS ARE IN INCHES
TOLERANCES ON:
FRACTIONS ± 1/32
ANGLES ± 0°-30'
DECIMALS XX ± .02
XXX ± .010

MATERIAL:

FINISH:

NEXT ASSY | USED ON
APPLICATION

CONTRACT NO.

BY	NAME	DATE
DRAWN		
CHECK		
APPR		
APPR		

Packard Bell Space & Systems

Remote Unit Electronic Packard Space Configuration

SIZE C | CODE IDENT NO. 45413 | Figure 2-10

SCALE | SHEET

1. INTERPRET DRAWING IN ACCORDANCE WITH STANDARDS PRESCRIBED BY MIL-D-1000.
NOTES: UNLESS OTHERWISE SPECIFIED.

2.2.2 POWER PACK AND REGULATORS

The power pack for the system has been defined and absolute values for voltages and power levels have beer assigned. Packard Bell has evaluated (See Appendix A) the various types of batteries which best fit into the cost structure. The power requirements used for the evaluation were as follows:

Power Requirements	Current	Voltage	Regulation
(a) Transmitter	2.5 amps	28-30	None
(b) Receiver	10-12 ma	6-7.5	None
(c) Sensors	200 ma	+10	Not defined
	50 ma		

2.2.2.1 Power Pack Considerations

(a) Temperature, operational from -40°F to +120°F

(b) Storage and shelf life

(c) Size: limitations are imposed on battery pack due to existing package configuration

(d) The ability to sustain voltage levels under constant load

(e) Constant ampere-hour capacity over long periods

(f) Shock, vibration and acceleration resistance

(g) Low internal impedance

(h) High ampere capacity

(i) High discharge rates

2.2.2.2 Ampere-Hour Capacity

The ampere-hour capacity for the total system was based on the duty cycle and peak current requirements of each item listed under paragraph 2.2.2.

a. Receiver

Duty cycle 100%

10 days, 240 hours at 12 ma rate = 2900 ma hours

or 2.9 ampere hours

b. Xmtr

Duty cycle based on a 1.2 second transmission period every 4 hour for 10 days or 240 hours =

$\frac{240}{4}$ = 60 transmissions x 1.2 seconds = 72 seconds

Duty cycle = $\frac{1.6}{240 \times 60} = \frac{1.6}{14.4 \times 10^3} = \frac{1.6 \times 10^{-3}}{14.4} = .11 \times 10^{-3}$

$1.1 \times 10^{-4} \times 1 \times 10^{2} = 1.1 \times 10^{-2} \times .01 = 1.1 \times 10^{-4} \times$

$2.4 \times 10^{2} = 2.6 \times 10^{-2}$

.026 hours x 2.5 amps = .068 ampere hours.

c. Sensors

Duty cycle on the sensors is based on a 2-minute pretransmission warmup period to allow some of the sensors to stabilize coupled with the 1.2 second transmission period every 4 hours for 10 days or 240 hours =

$\frac{240}{4}$ = 60 transmissions x 1.2 seconds = 72 seconds

+80 prewarmup periods x 2 minutes = 1.6 + 160 = 161.2 minutes

$$\text{Duty cycle} = \frac{161}{14.4 \times 10^{3}} = \frac{161 \times 10^{-3}}{14.4} = 11 \times 10^{-3}$$

$$11 \times 10^{-3} \times 1 \times 10^{2} = 11 \times 10^{-1} = 1.1\% = 1.1 \times 10^{-2} \times$$

$$2.40 \times 10^{2} = 2.4 \text{ hours} \times .2 \text{ amps} = .480 \text{ hours.}$$

A multiple power pack system has been selected to eliminate the need of regulators due to the large number of voltages required of the system and also to eliminate the waste of watt-hours used up on regulators which would be on 100% of the time.

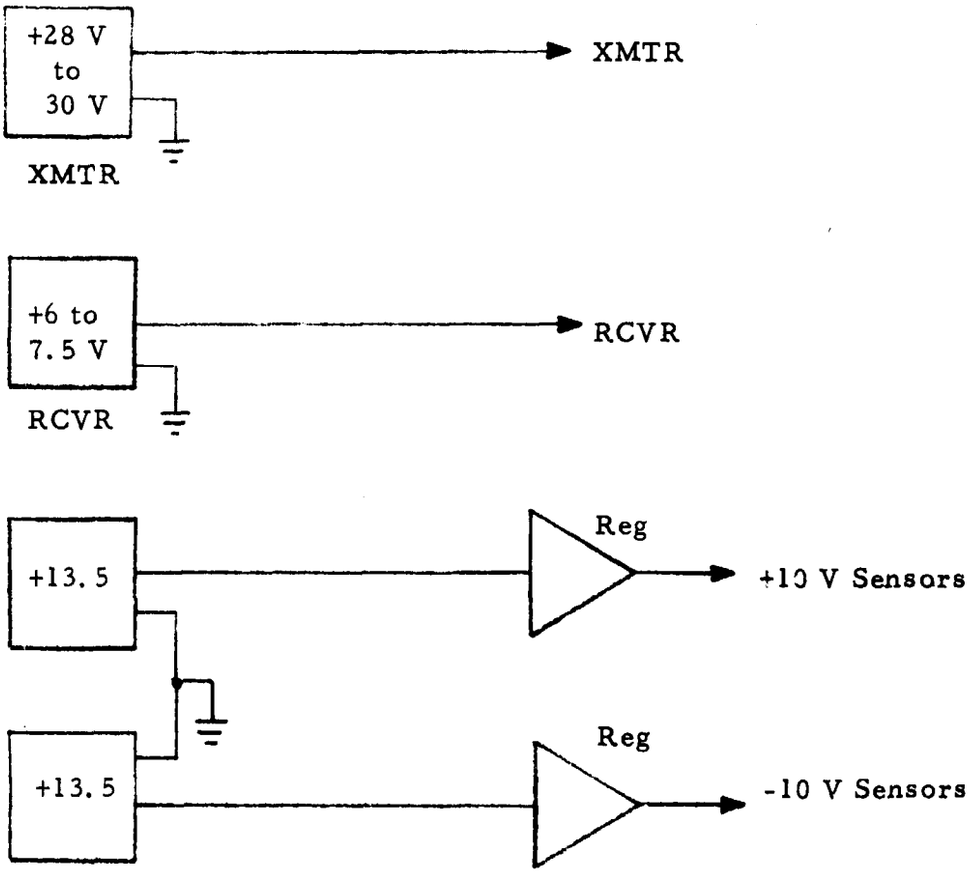

System Power Distribution

The transmitter and receiver do not require regulation. The normal decay characteristics of the battery curves were used and the selection of the ampere-hour capacity allowed an extended range over the required period.

High-discharge rate batteries, which exceed the battery power requirements by a 15 to 1 margin, were purchased for the transmitter power pack. Yardney silver-cells were used, due to their ability to withstand high discharged rates and also their size and low temperature characteristics.

The battery temperature limitation appeared to be inherent in the nature of battery construction but some options included: heaters to maintain battery temperature; pulsing the battery with heavy loads to warm it; and the use of other power sources such as propane, thermo-couple type generators in place of the battery.

Mercury batteries have been selected for sensor power and receiver power. Their size was a consideration here due to space limitations and also because of their inherent ability to deliver extremely large watt-hour capacity. These batteries, however, do not have good low-temperature characteristics. Battery manufacturers have been doing R & D work on low-temperature batteries for the Signal Corps and are more than willing to take on an R & D program for development of low-temperature cells for this program. Batteries are not presently available to fit our requirements. For the system evaluation, the Mallory Mercury Batteries were used. (See Appendix A)

The power pack has been packaged and was successfully shock tested at 75 g's without any detrimental effects on performance.

2.2.3 MULTIPLEXER

The mechanical multiplexer was designed and tested. (See Figure 2-11.)

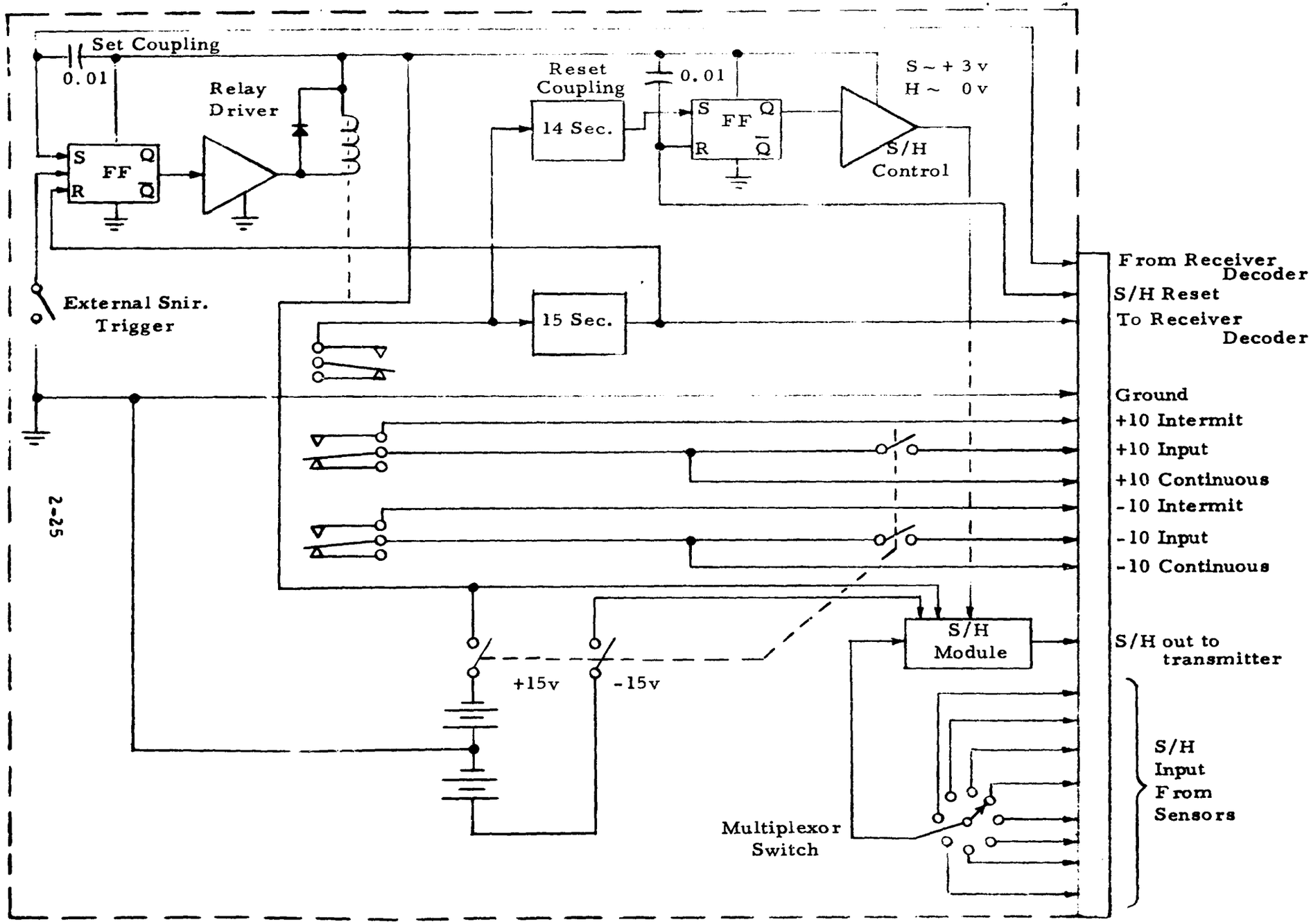

Figure 2-11. Multiplexer Block Diagram

2.2.4 DECODER

The decoder section was designed to (1) amplify, (2) discern the presence of two simultaneous predetermined tones with a time domain threshold determined by the bandwidth integration period, and (3) provide a trigger pulse to initiate system activity. See Figure 2-12 below.

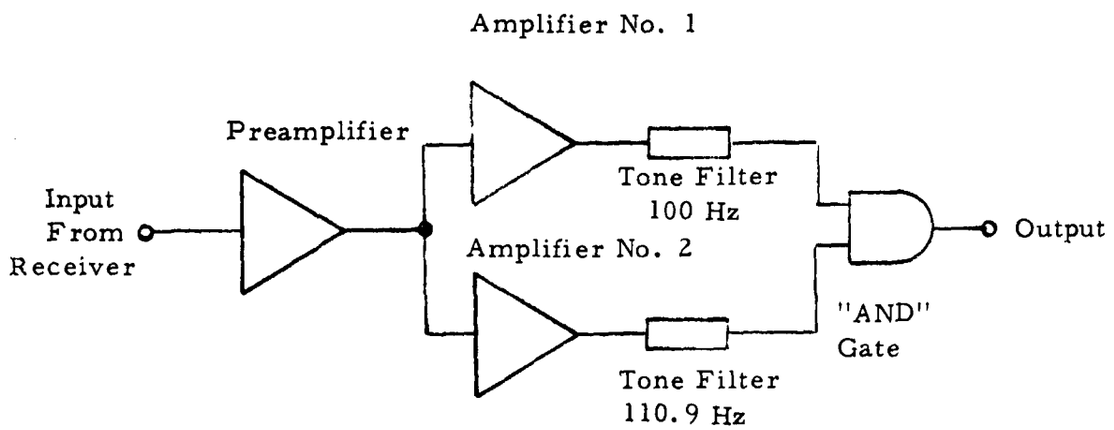

Figure 2-12. Decoder Block Diagram

The circuit employs two resonant reeds which are excited by the presence of their respective resonant frequencies. When this occurs, the reeds vibrate and an intermittant contact closure provides the simultaneous dc pulses for driving an "AND" gate which, in turn, gives the desired trigger pulse.

2.2.5 COMMUNICATION SYSTEM

Preliminary evaluation studies regarding telemetry range indicated that, by using very narrow transmitted bandwidths, increasing transmitted power, employing large antennas at the receiving end, and using low-noise, narrowband receiving equipment, it might be possible to transmit data over a 50-mile range a high percentage of the time. Range tests were strongly indicated as a next step to empirically determining the communications probabilities.

2.2.5.1 Final Design Philosophy

The communication subsystem was changed from the originally proposed two-frequency communication system to a single-frequency system. This feature eliminated the need of two separate antennas which would be required to receive the command or interrogation signal which is the low frequency channel, VLF, and the VHF antenna for the data transmission. The selection of a single frequency made the antenna problem more realistic in terms of simplicity and implementation and, of course, was more economically feasible. A single antenna served both the interrogate command RF link and also the data RF link.

The system was no longer dependent on discrete active periods before an interrogate command could be initiated. The command receiver, being active 100% of the time, could be interrogated at any given time within the active life of the system. The command signal consisted of two simultaneous tones generated at the base station of equal amplitudes and duration. These signals are in the 100 to 500 Hertz range with more than 0.1% stability. The receiver had, as part of the package, a tone discriminator decoder consisting of a set of discrete tones. This system reduced the probability of false recognition signals causing interrogation, not only because it required two simultaneous tones, but also because of the narrow

bandwidth characteristics of the decoders (approximately ± 2 Hertz) which require a finite interrogation period. In this case, the interrogation period was $\frac{1}{Bw}$ 500 msec which again reduced the probability of false recognition. With a minimum of tones within the bandpass of the receiver, a large number of units could be discretely interrogated, without any interaction between units.

The transmitter operated in a pulse modulated FM/FM mode because of the low data rates. The subcarrier oscillator was modulated by the data from the sensor package signal conditioners. The subcarrier oscillator then modulated the transmitter carrier. The transmitter transmitted each data point only at the time each data point was sampled. Transmitter power was only applied after an interrogate command had been received.

The frequency selected for the communication subsystem was considered carefully. (See Appendix B.) A study of those areas which would affect the transmission path were: the terrain and topography of the drop zone; the topography and conductivity between the drop zone and the base station; and, including the noise level for certain areas, receiver sensitivity and noise figure. Range capability is still predominantly a function of antenna height at the base station. As a result of all of these considerations, the receiver was designed to meet all of the noise and sensitivity requirements.

While all other parameters were being considered, the base station was by no means forgotten. Data acquisition and reduction using a simple stripchart recorder or meter is a feature of the FM/FM system. Due to the

low data rates, a stripchart recorder could respond to prf's of 8-10 cps giving a permanent record of the data for later analysis or correlation with other units. Demodulation of the data only required the addition of a sub-carrier discriminator.

The system, as previously discussed, meets the requirements of a suitable communication link for the droppable unit. The system components on the remote station are:

a. Tramsitter
   (1) Mode; PM, FM/FM

b. Receiver
   (1) Mode; FM

c. Decoder
   (1) Two simultaneous different frequency tones

d. Antenna
   (1) Single dipole

2.2.5.2 Receiver

A receiver has been designed to operate at an operational frequency between 40 and 42 MHz with an IF bandwidth of 2 KHz and a noise figure of 4 to 6 db. The command receiver is illustrated in Figure 2-13.

Receiver sensitivity for the base station is:

KT	-174 dbm/cycle
KW_{if} (2 KHz)	33
NF	10
Threshold S/N_{if}	3
	-128 dbm = Pr = power to receiver

Radio wave propogation analysis showed, that, in order to deliver -128 dbm to the base station receiver, the following requirements had to be met.

REVISIONS					
ZONE	LTR	DESCRIPTION	DFT	CHK	DATE	APPR

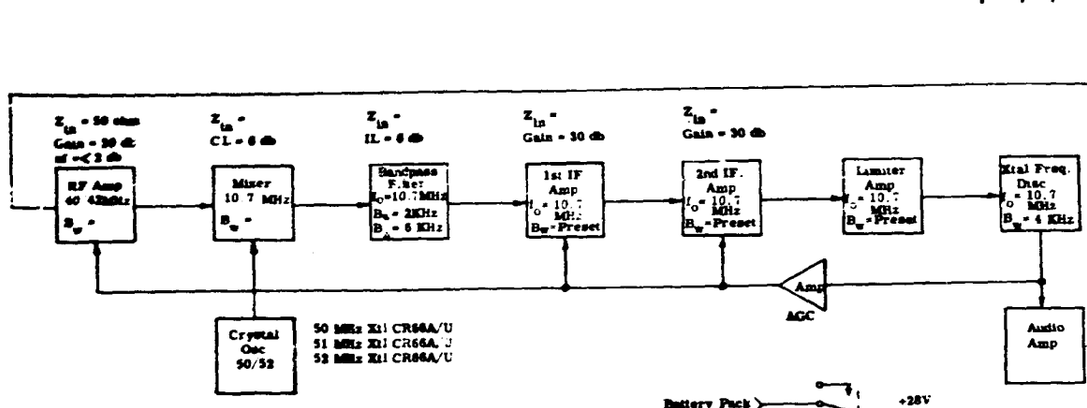

1. System Pwr Relay
2. Bandpass Filter
3. Xtal from Disc.
4. Tone Decoders
5. Xtal 50, 51, 52 MHz
6. Coaxial Switch

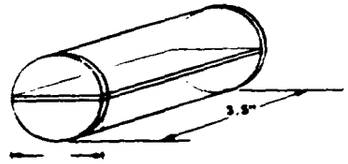

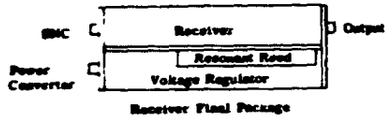

Receiver Final Package

Note: 1. RF coils shall be wound on coil forms. No exceptions.

QTY REQD	PART OR IDENTIFYING NO.	NOMENCLATURE OR DESCRIPTION	CODE IDENT	REF DESIGNATION	SPECIFICATION	ZONE	ITEM NO.
LIST OF MATERIAL OR PARTS LIST							

UNLESS OTHERWISE SPECIFIED DIMENSIONS ARE IN INCHES
TOLERANCES ON:
FRACTIONS ± 1/32
ANGLES ± 0°-30'
DECIMALS XX ± .02
XXX ± .010

MATERIAL:

FINISH

NEXT ASSY | USED ON
APPLICATION

CONTRACT NO

BY	NAME	DATE
DRAWN		
CHECK		
APPR		
APPR		

Packard Bell Space & Systems

AN/AMQ-27 Command Receiver

SIZE	CODE IDENT NO	Figure 2-13
C	45413	

SCALE | SHEET

1. INTERPRET DRAWING IN ACCORDANCE WITH STANDARDS PRESCRIBED BY MIL-D-1000.
NOTES: UNLESS OTHERWISE SPECIFIED.

Transmitter power, Pr = 50 watts	+47 dbm
Remote Unit antenna gain, Gr =	0 db
Base Station antenna gain, Gr =	+13 db
Space loss calculated =	-103 db
Ground wave loss =	-85 db
	-128 dbm Pr = Power to Receiver

The receiver was designed for a sensitivity of -135 dbm with a signal to noise figure of 6 to 8 db and an IF bandwidth of 2 KHz. Sensitivity was increased to give a 7 db safety margin. The receiver was breadboarded and tested. The tests showed that the receiver met the sensitivity requirements.

2.2.5.3 Transmitter

A transmitter has been designed to operate over a frequency range between 40 and 42 MHz with the capability of delivery between 50 and 60 watts into a 50-ohm matched load.

The prototype transmitter has also been tested and meets the power requirements with an additional 6 watts to spare. Total output power 56 watts. The data transmitter is illustrated in Figure 2-14.

2.2.6. ANTENNA

2.2.6.1 Preliminary Study

The initial effort was concentrated on the design and development of a suitable antenna to operate between 3 and 7 MHz for ground wave propagation as proposed and capable of a transmission distance of 50 miles.

The approach taken at that time was the evaluation of a square loop antenna. Loop antennas of various materials, material diameters, and loop sizes were constructed. This was to determine and optimize the radiation effiency of the antenna.

REVISIONS					
ZONE	LTR	DESCRIPTION	DFT	CHK	DATE	APPR

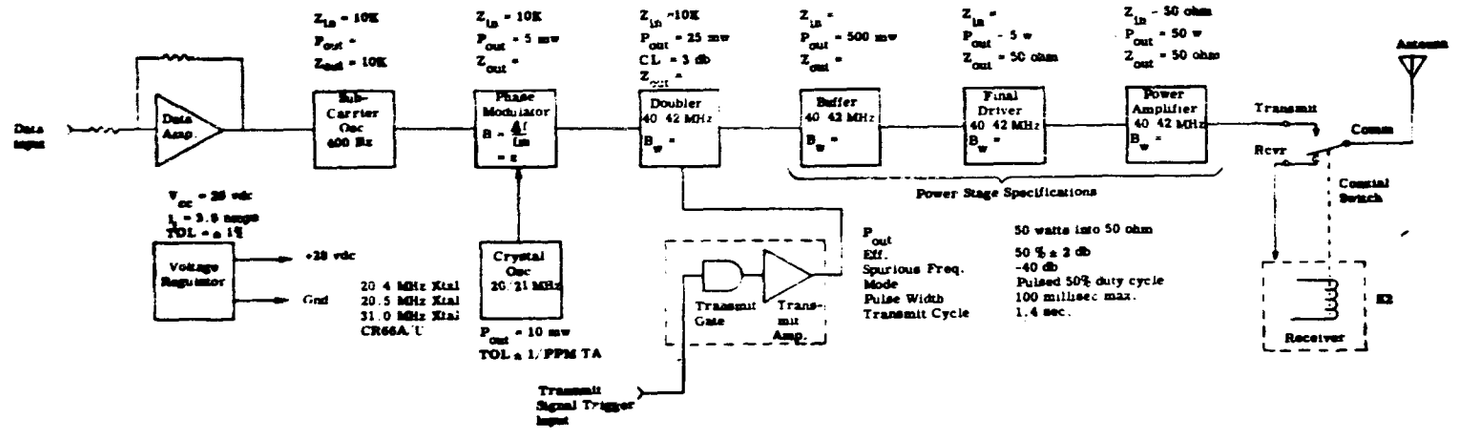

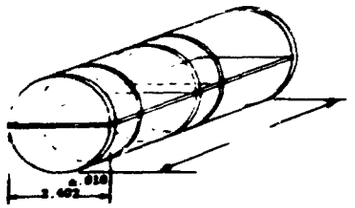

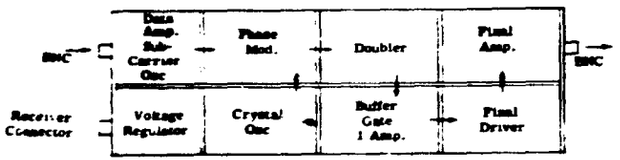

QTY REQD	PART OR IDENTIFYING NO.	NOMENCLATURE OR DESCRIPTION	CODE IDENT	REF DESIGNATION	SPECIFICATION	ZONE	ITEM NO.

LIST OF MATERIAL OR PARTS LIST

NEXT ASSY	USED ON
APPLICATION	

UNLESS OTHERWISE SPECIFIED DIMENSIONS ARE IN INCHES
TOLERANCES ON:
FRACTIONS ± 1/32
ANGLES ± 0°-30'
DECIMALS XX ± .02
XXX ± .010

MATERIAL

FINISH

CONTRACT NO.

BY	NAME	DATE
DRAWN		
CHECK		
APPR		
APPR		

Packard Bell Space & Systems

AN/AMQ-27 Data Transmitter

SIZE	CODE IDENT NO	
C	45413	Figure 2-14

SCALE | SHEET

1. INTERPRET DRAWING IN ACCORDANCE WITH STANDARDS PRESCRIBED BY MIL-D-1000.
NOTES: UNLESS OTHERWISE SPECIFIED.

When the radiation efficiency of the antenna was optimized, best operational frequency and power levels were evaluated.

Selection of a loop antenna as the radiator was based on various electrical and mechanical characteristics and considerations best suited for application to an air droppable system such as the one proposed.

Electrical

a. Opposed to a dipole antenna the loop antenna does not require a critical ground plane.

b. Height does not degrade the radiated energy as does the dipole when placed at close proximity to the ground, due to the incident reflected wave which has a cancelling effect to the radiated wave. The reflected wave from a loop antenna combines with the incident wave in an in-phase condition resulting in an increase of radiated energy.

Mechanical

a. Storage - The antenna can be hinged at all four corners when not in use by folding into a length equal to one of the sides.

b. Deployment - Deployment should not require motors, but could be spring-loaded and deployed upon impact.

c. Size - The size of the antenna would probabily not be greater than one meter on a side.

Field strength measurements were taken with one antenna configuration and indications showed that antenna efficiency was low. Improvements were made to increase efficiency. Tests were also conducted to determine radiation pattern characteristics of this antenna.

After intensive testing and evaluation of a loop antenna, the test results showed that the efficiency of the antenna could be increased only by

increasing the diameter of the loop and also the conductor itself to the point that it became impractical in size for use as a radiator in the proposed vehicle. Another undesirable characteristics was tuning. Tuning became critical when placed on locations other than where the antenna was originally tuned. To overcome this problem, electronic tuning would have to be included in the package, adding additional drain to the batteries which would then lead to a larger battery pack. This would then impose space limitations for the electronics. For these reasons, the loop antenna as the radiator was abandoned.

A different approach, after careful consideration and study, was implemented and tested. It was decided that a dipole antenna could be used, if a high enough frequency was selected so that a quarter wave length whip antenna would be equal to 3/4 the length of the vehicle barrel. This would give essentially a center-fed, fullwave antenna and, using the rotor blades as the ground plane for increasing antenna efficiency, would provide a practical antenna for use in the vehicle.

2.2.6.2 Preliminary Design

The frequency selected for range testing was between 50 and 52 MHz. This however, would not be the operational frequency intended for the MET system. The operational frequency would have to be in the 40 to 42 MHz range, which is allocated for armed forces use.

A telescopic antenna was used for adjusting the antenna to the required antenna length to properly load a transmitter for minimum VSWR. The tests indicated that the antenna required various lengths to reduce the VSWR for good antenna matching when operated with the rotors extended or collapsed. Also, there was an interaction between the lower and upper rotor blades when one or the other was collapsed, again changing the antenna requirements. To overcome this interaction a fixed ground plane had to be developed such that the length of the radial elements would not interfere with the rotation

of the upper rotor blades and yet give a fixed antenna length. The number of ground plane elements was reduced to three elements 18 inches long and spaced 120° apart at the base of the antenna which is the bottom of the sensor package.

Additional tests (See Appendix C) were conducted to determine the effects the penetration of the vehicle in the ground would have on VSWR and antenna length. Tests showed that the vehicle could penetrate the ground to the lower blades without significantly effecting the VSWR and antenna length.

Also, of importance was the off-vertical angle characteristics of the signal strength. Range tests indicated that the antenna can operate as much as 35° off-vertical without critically effecting the signal strength. Signal strength at 45° off-vertical approached 6 db.

Propagation signals at distances of 30 to 50 miles using this antenna configuration on the vehicle indicated that the power levels and signal strength were compatible with the system requirements.

2.2.6.3 Final Configuration

As a result of the exploratory hardware development phase, the final antenna configuration requirements were defined. During this phase of the program an automatic, self-erecting dipole antenna was designed, fabricated and tested for compatibility with the existing communications system of the station.

A specification control drawing was made and negotiations were started with Spar Aerospace Products Limited for the development of the antenna. Of major concern was the strength requirements and considerable evaluation was given to the behavior of the antenna under the 60-knot wind condition.

2.2.6.3.1 Electrical And Mechanical Design Requirements

The electrical and mechanical design requirements for this antenna were formulated with the following specifications:

a. Scope

This specification is for the design and development of an extendable vertical dipole antenna. This device will be of the "jack-in-the-box" type and, therefore, will not require electrical power to raise or lower the antenna.

b. Electrical Characteristics - Design Goals

(1)	Frequency Range	39-42 MHz
(2)	Power Gain (Over 1/2 wave dipole)	0.00 db
(3)	Bandwidth VSWR	1:5:1 @ 3 db Points
(4)	Normal Input Z	50Ω
(5)	Minimum Power Input	100 watts
(6)	Termination	Subminiature Screw-on Connector for RG 196/U Cable (Micro Dot, Inc. Type No. 031-0050 or equivalent.)
(7)	Wave Length Mode	1/4λ

c. Mechanical Characteristics

(1)	Mounting	2 threaded inserted holes or studs
(2)	Size	2" Square X 3" High
(3)	Weight	1/2 Pound Maximum
(4)	Antenna Release Mechanism	Spring Loaded adjustable "G-Release Mechanism" that will release between 40-50 g's.

d. Environmental Conditions

(1)	Temperature	-50° F to +150°F
(2)	Wind	60 knots
(3)	Impact Shock Loads	60-80 g's
(4)	Salt and Sand Atmosphere	Antenna will continue to be functional when operating in this type of atmosphere.

2.2.6.3.2 Antenna Design And Development

Initially, the basic STEM (storable, tubular, extendible member) type considered for the antenna was the "Jack-in-the box", as depicted in Figure 2-15. Evaluation of this type of STEM proved to be faulty when trying to extend in a 60-knot wind environment due to its weak root section, Figure 2-16c. Many alternatives were explored in the evolution of the tip drum type (TDM) device, shown in Figure 2-17. This device represents a design that will meet the requirements of the AN/AMQ-27 system.

2.2.6.3.2.1 Antenna Description

It was determined that a four element BI-STEM device would be used in this application (Figure 2-18b). Calculations indicated that this would ensure survival of the antenna in a 60-knot wind. This meant, however, a total weight of about one pound, or, twice the desired weight. If a maximum survival wind speed of 45 knots was satisfactory, then a two element BI-STEM could be used and the weight reduced to about 0.65 pound.

The elements of the BI-STEM are wound onto a storage spool which is then loaded into a roller cassette (Figure 2-19). This cassette is mounte . on top of a fixed base structure with a vee-shaped register to ensure a rigid attachment, shown in Figures 2-17 and 2 20.

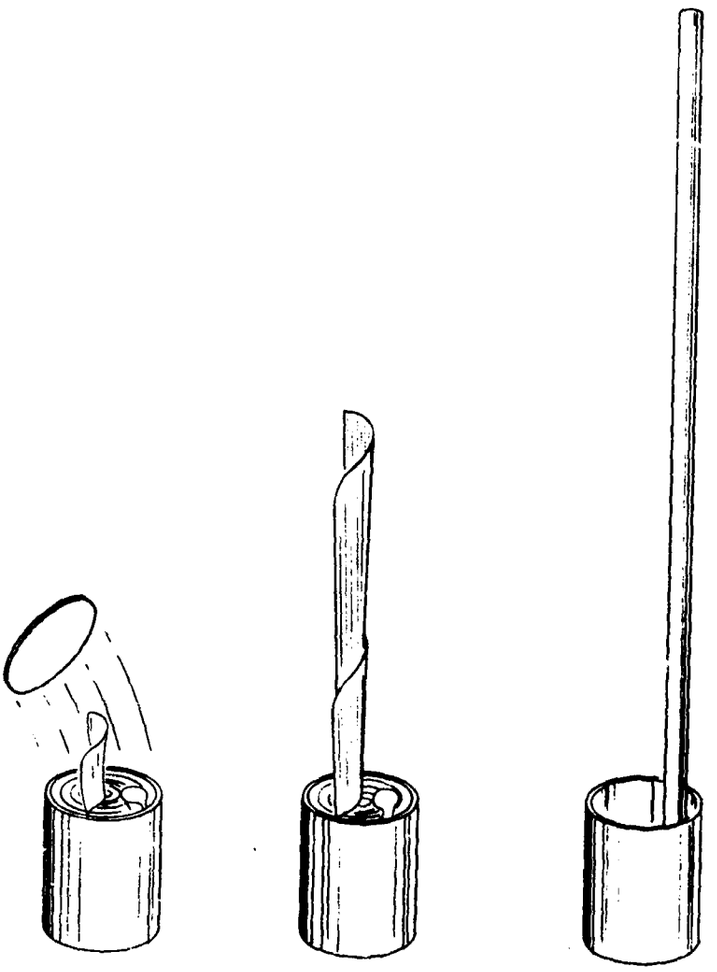

Figure 2-15. "Jack In The Box" Extension Process

One of the most unusual machine elements to appear in some time, the STEM is also one of the simplest. It was developed specifically for use as an extendible boom in spacecraft but has found increasing use in down-to-earth applications. Here's a complete guide to designing the STEM.

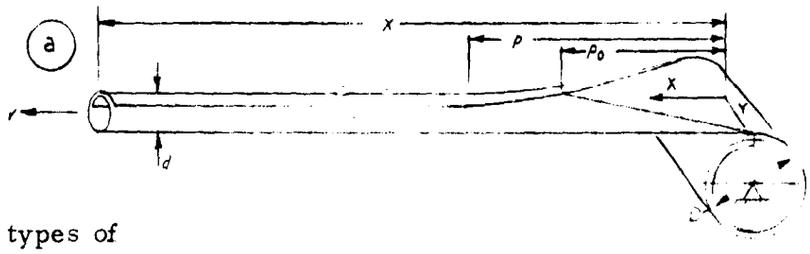

Figure 1 - Three basic types of STEM with applicable design parameters and dimensions. The root-drum model (RDM) a, is the most common type. This unit unfurls from a drum, and is retractable. It is used in lengths up to 1000 ft. The tip-drum model (TDM), b, is basically similar to the RDM except that the drum rolls off the tip of the tube. A one-shot unit, this type is self-extending. Strain energy of the coiled tube as it is released from the drum provides force necessary for extension. Jack-in-the-box model (JBM), c, is also self extending, the necessary force being provided in the same manner as in the TDM. This type has a constant ejection speed, of about 20 ft/sec for typical units. Because the STEM rotates during extension, it has considerable stability.

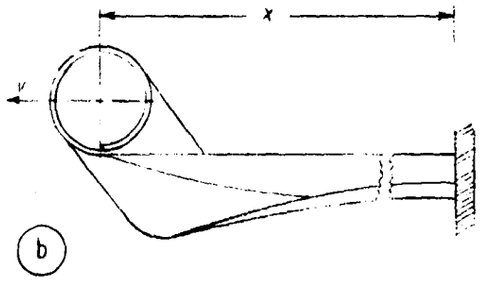

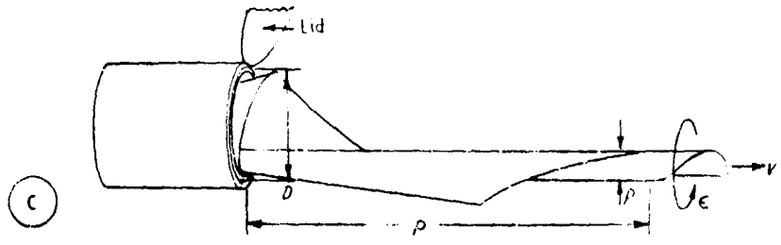

Figure 2-16. STEM Configuration

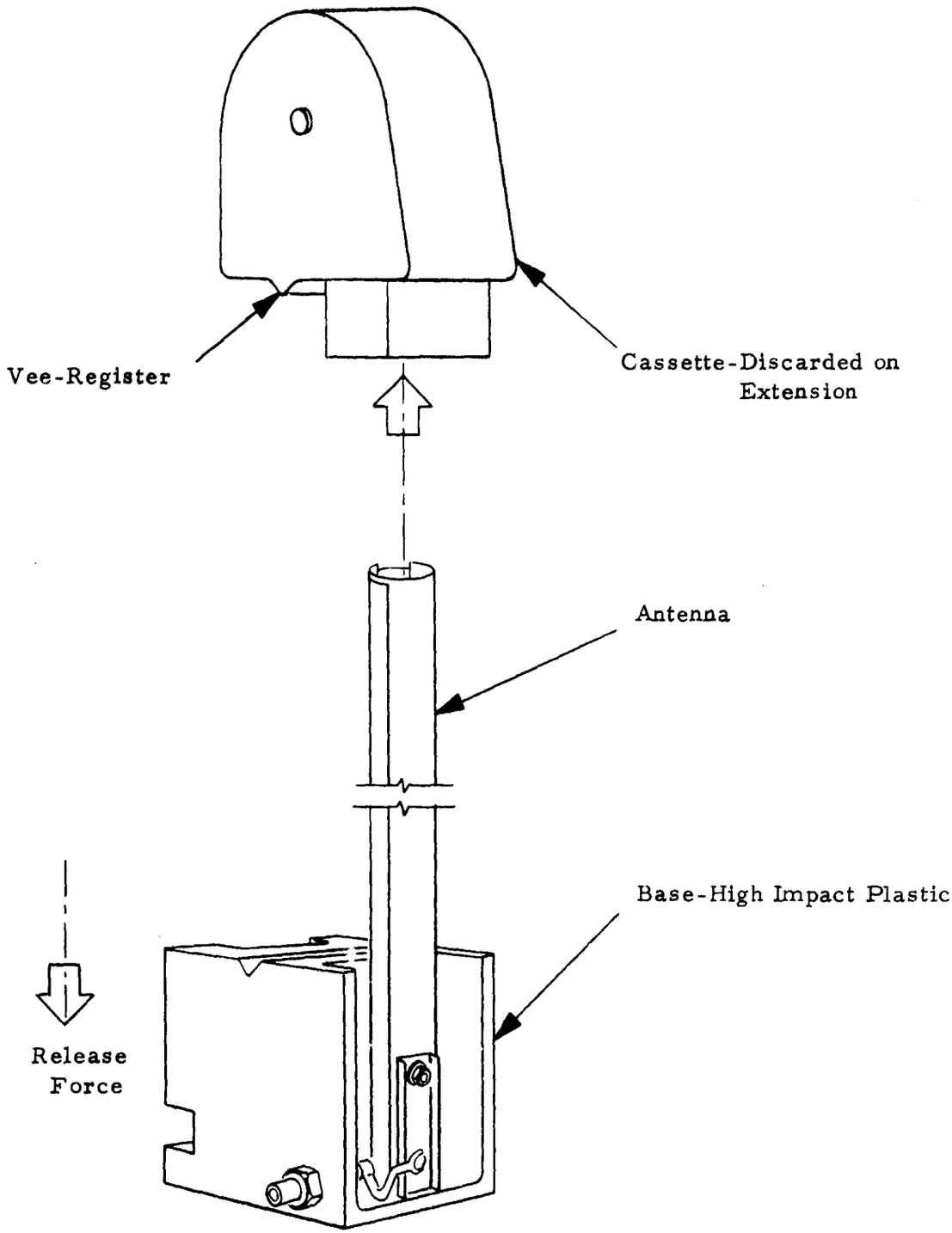

Antenna-Extended - NTS

Figure 2-17. Tip Drum Type Antenna

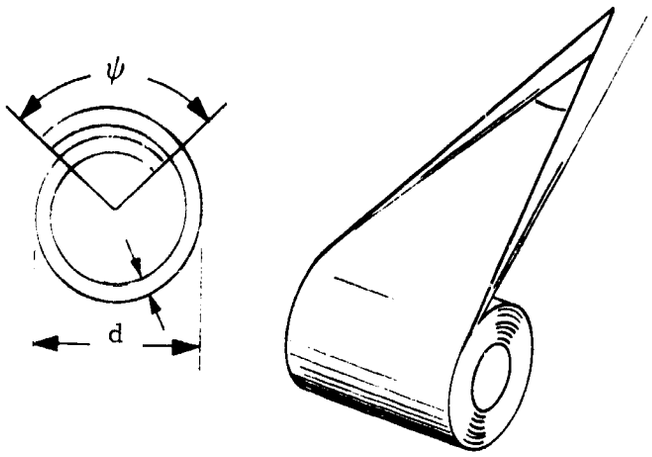

A. The STEM principle

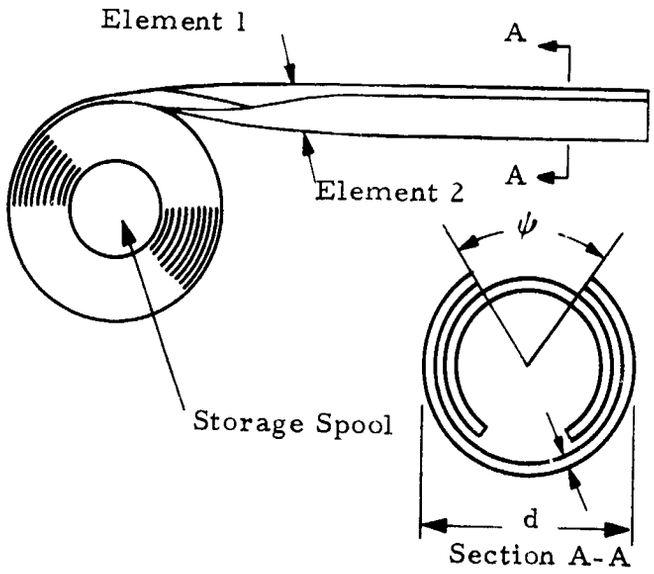

B. The BI-STEM principle

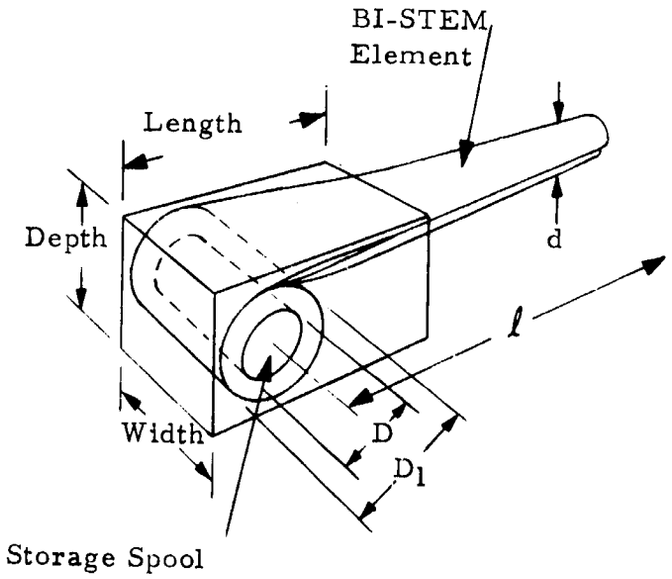

C. BI-STEM dimensions

Figure 2-18. BI-STEM Device

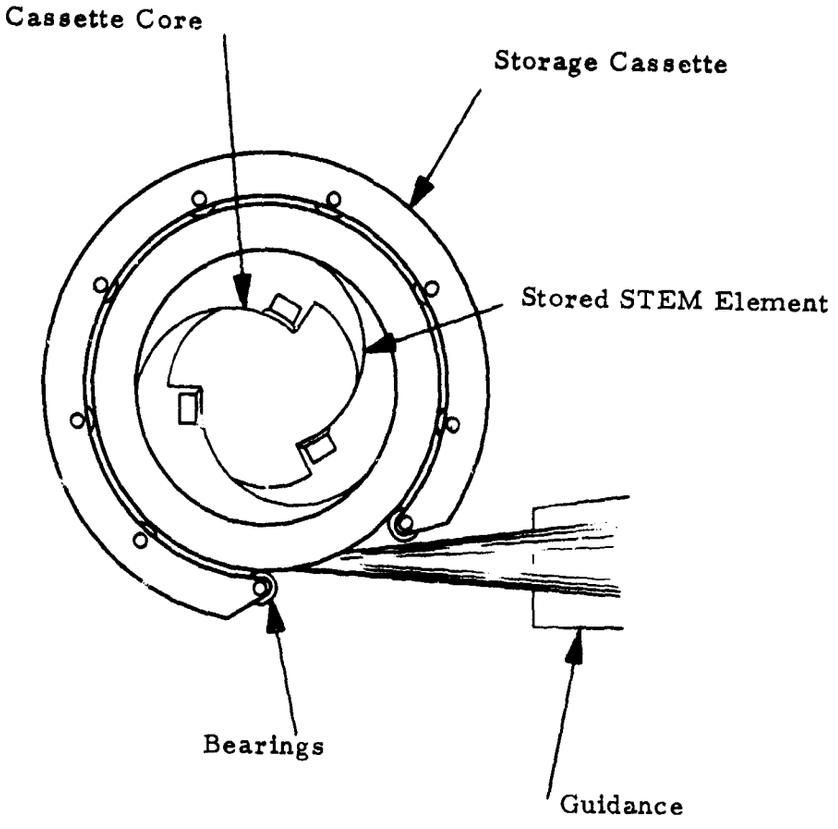

Figure 2-19. Cassette Principle

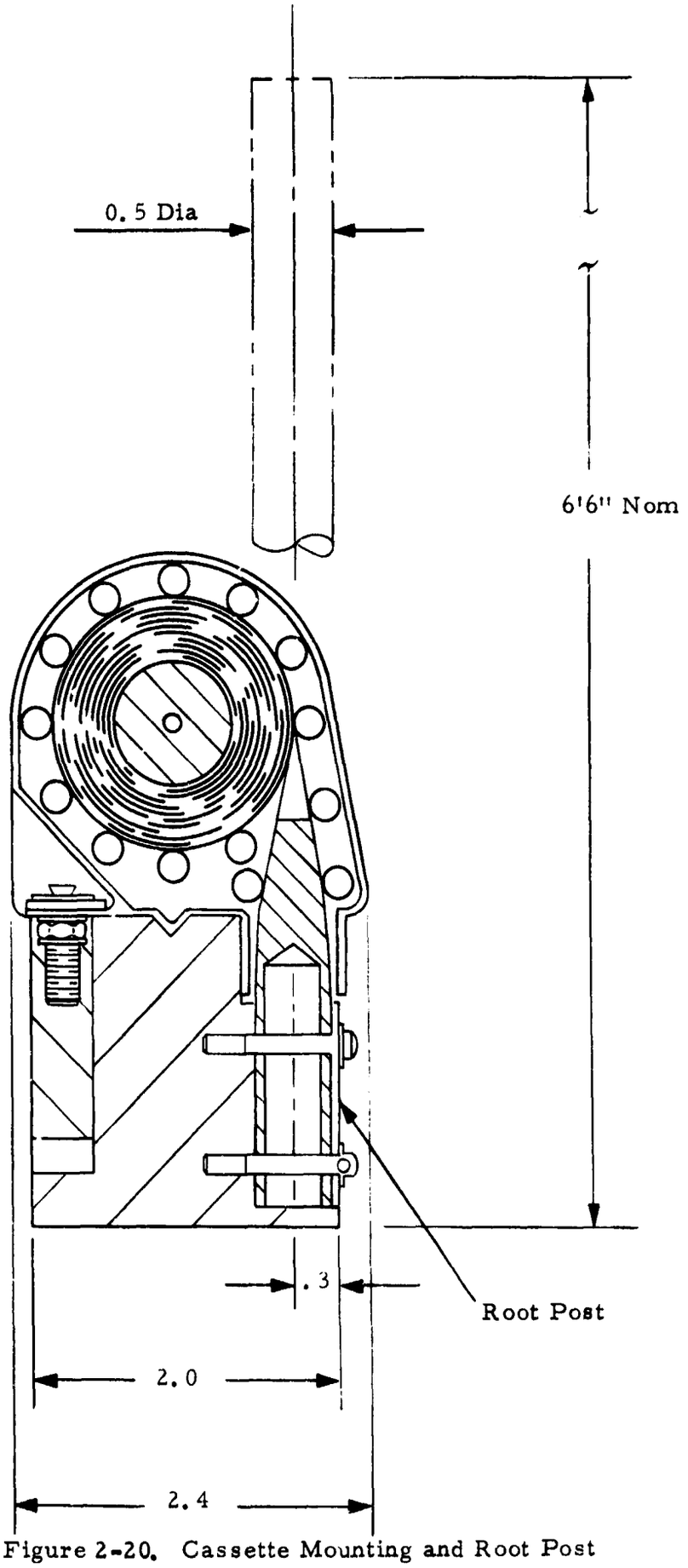

Figure 2-20. Cassette Mounting and Root Post

The ends of the antenna elements projecting from the cassette are attached to a root post (Figure 2-20) which, in turn, is attached to the base with two screws and a root clamp. Under the head of the lower screw is a solder lug which is connected to the Microdot connector by a short wire braid to form an RF pick-up (Figure 2-21).

The cassette is retained in the position shown by a special "G" latch (Figure 2-22). This consists of a threaded plunger attached to a comparatively large actuating mass. The top of the plunger is waisted and engages with a thin metal diaphram washer resting on a reinforced land in the cassette.

Upon impact of the parent vehicle, the "G"-latch mass is accelerated toward the base and pulls the plunger through the diaphram washer. The spring under the mass is compressed and, upon completion of the downward stroke of the mass, provides an upward return force to assist the cassette in lifting off the base. The stored strain energy of the BI-STEM elements then completes the lift off and, upon full extension of the antenna, the cassette is forcibly discarded. The mounting configuration and overall parameters of the antenna are shown in Figure 2-23.

2.2.6.3.2.2 Antenna Development

A four element BI-STEM device was developed for this application. A confidence test was successfully completed on the stem part of this device. The mylar elements that form the base section of the antenna were subjected to tensile tests over the required temperature range and showed good repeatability.

Upon receipt of the BI-STEM self extendible antenna from Spar Aerospace, the release mechanism was redesigned to include two spring loaded pins held in a latched position by a release mass plate and a Mylar latch as shown in Figure 2-24. This mechanism was designed to actuate under a downward "G" force of 40 to 50 "G's". Upon application of

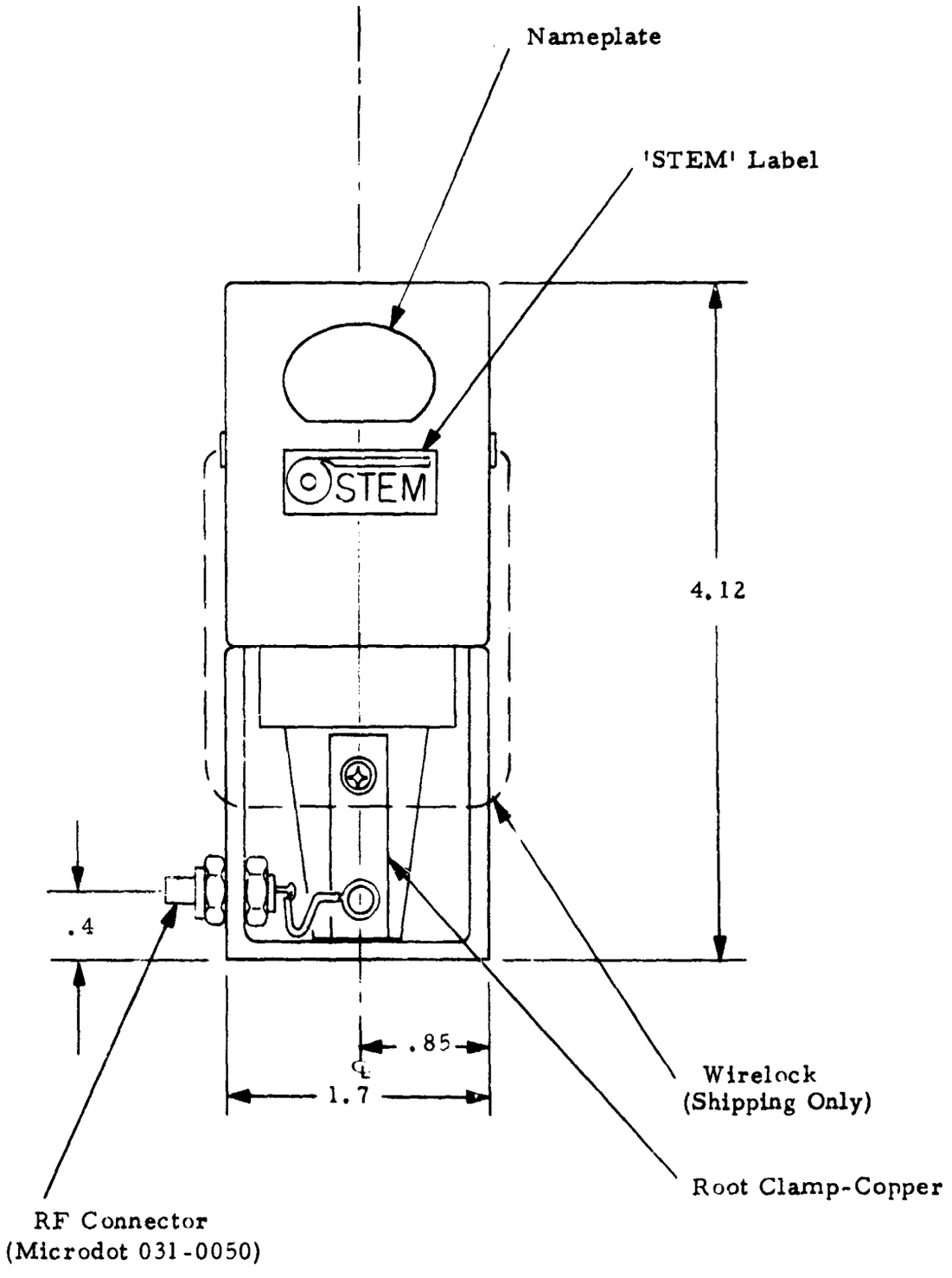

Figure 2-21. RF Pick-Up

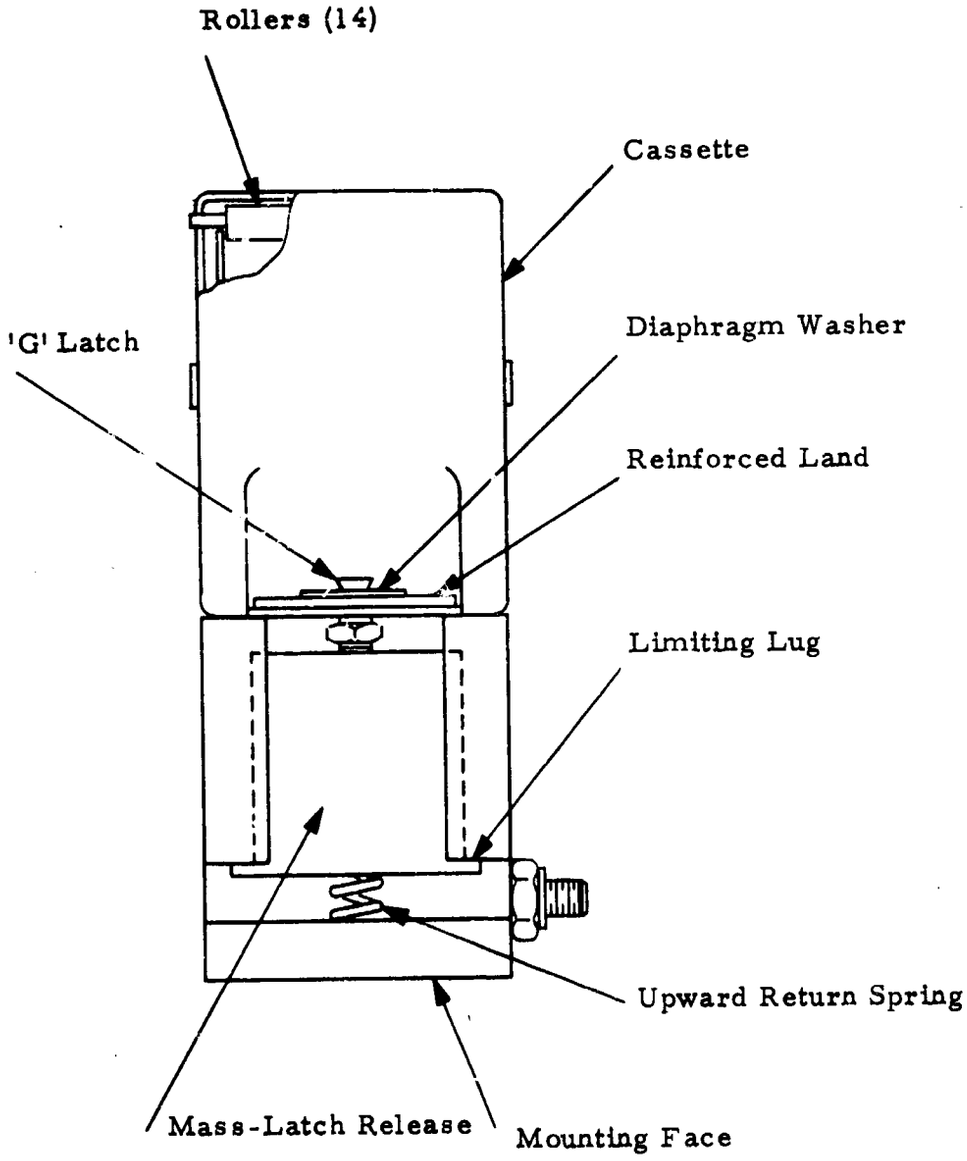

Figure 2-22. Cassette Retainer

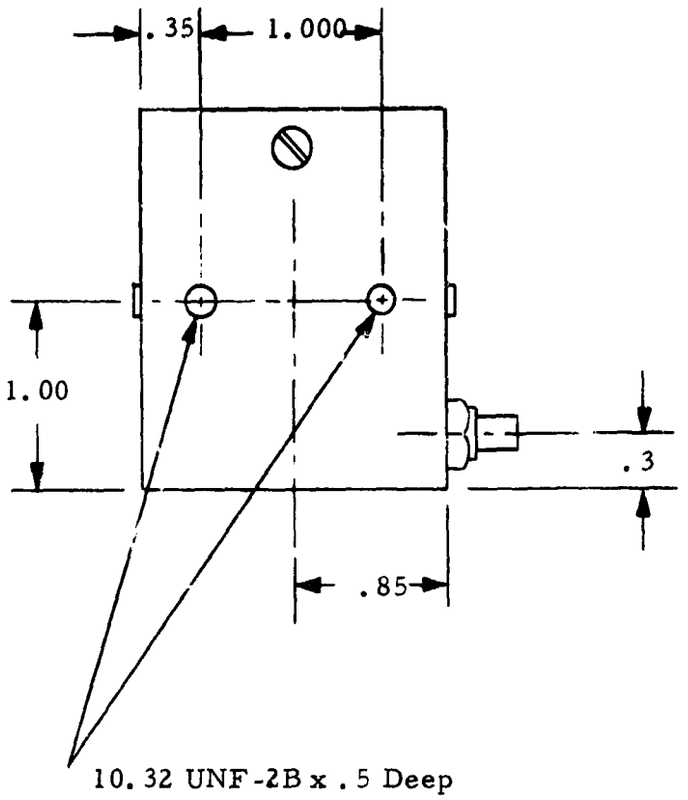

Notes

1. All Dimensions for installation purposes only
2. Antenna Specifications:
   - 2.1 Diameter - - - - - - - - - - - - .5 in
   - 2.2 Material - - - - - - - - - - - - Stainless Steel (.003" Thk)
   - 2.3 No. of Elements - - - - - - - - 4
   - 2.4 Type - - - - - - - - - - - - - - 'BI-STEM'
3. Weight - - - - - - - - - - - - - - - - - - 1.0 lb.
4. Release Force Required - - - - - - - - 40 - 50G (Adjustable)

Figure 2-23. Mounting Configuration

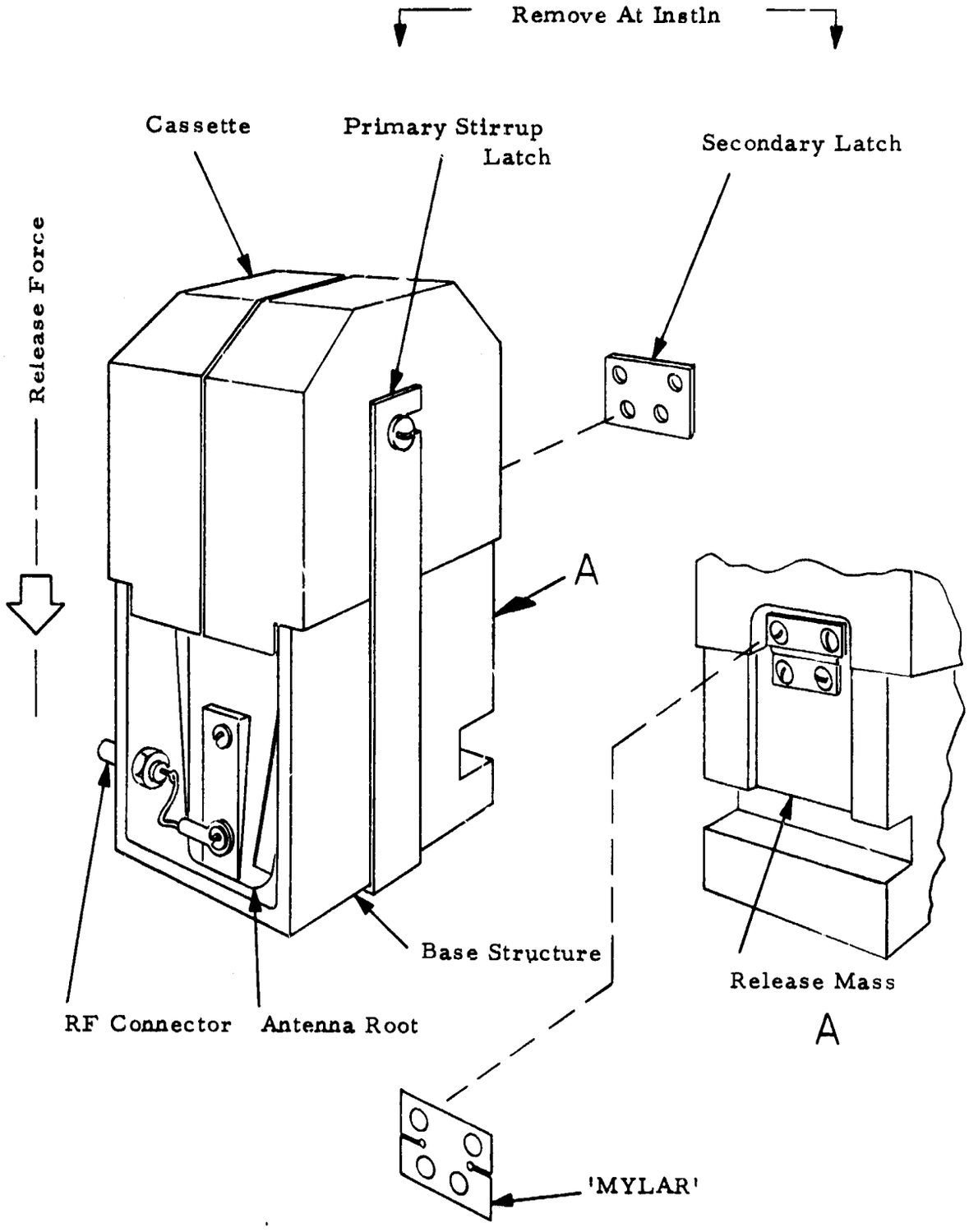

Figure 2-24. BI-STEM Device - Type 877

this "G" force, the release mass is accelerated downwards causing the mylar latch to fall in tension. The displacement of the mass exposes the two spring loaded pins which secure the cassette. The pins then disengage the cassette and the stored strain energy of the BI-STEM elements causes immediate erection of the antenna mast. Upon reaching the full mast height, the cassette is thrown clear in a random arc.

The BI-STEM device was mounted to a shock testing machine at Packard Bell to check out the shock release mechanism. The antenna was induced to a 45 "G" shock load and it failed to release. An investigation of the release mechanism revealed that the spring loaded pins did not release when the release mass dropped and exposed them. A closer look at the spring pins revealed that they were covered with adhesive and, therefore, glued in place so that they could not be released. This happened when the plastic retaining washers were glued in place to hold the spring pins captive. Packard Bell could not satisfactorily re-glue these retaining washers in place so the unit was shipped back to Spar for a re-evaluation of the design of the release mechanism.

Prior to shipping the antenna back to Spar, it was subjected to an electrical test mounted on the deployment vehicle. It was cut to 70.5 inches, which is the correct electrical length for 42 MHz, and it functioned quite well in both the transmit and receive modes.

The antenna was modified by Spar Aerospace and returned to Packard Bell. The plastic retaining washers that were installed with adhesive had been replaced with a machined plate held in place by three screws. This device was set up on the shock machine and tested numerous times. The shock release mechanism worked and the antenna released each time. The release mechanism could be adjusted in the range of 40 to 47 g's.

2.2.6.3.3 Antenna Delay Release Mechanism

The last series of flight tests conducted in April 1969 indicated that the antenna would not properly release without some kind of delayed release mechanism. The initial parameters established for such a device were:

a. Capable of a one minute delay.

b. Ruggedized to withstand a 100 g vertical shock and a 50-60 g horizontal shock.

c. Low cost.

Having these parameters as guidelines, various delay release type mechanisms were evaluated.

These conceptual devices included various designs with electromagnetic relays, oil and air dashpots and CO_2 cartridges. All of these concepts seemed to fall outside of the previously established guidelines. They would either result in a complicated design that would be costly to produce or too flimsy to withstand the high impact conditions during vehicle landing. Finally, a model airplane enthusiast suggested using an item common to this hobby known as a "TICK-OFF". This is a mechanical timer, adjustable from 0 to 5 minutes, used to control the flight time of model airplanes in a free flight pattern.

One of these "TICK-OFF" devices was purchased for laboratory testing and evaluation. The initial evaluation indicated that the device was well built, very compact and light weight. A fixture was made to hold this device on the shock testing machine for endurance testing in the vertical and horizontal axes. This device received a dozen shocks of 100 g's in both axes and survived without any failures or degradation in performance.

Since the testing proved the device's capability of functioning in a 100-g environment, the next step was to couple it to the release mechanism of the antenna. This was accomplished as depicted in Figures 2-25, 2-26 and 2-27. The "TICK-OFF" was mounted close to the antenna and coupled to the antenna through the arm latch (item 6, Figure 2-25). New parts were fabricated to support this design, as indicated in Figure 2-25. A functional description of this delaying mechanism follows using Figure 2-25 as a reference.

The antenna with the delaying mechanism was mounted on the top plate of the sensor package, as shown in Figure 2-28. The vehicle was loaded into the deployment tube, the timer set for one minute and the timer actuating clip placed in position (item 10). When the deploying airplane reached the drop altitude of 1000 feet over the target area, the vehicle was released. As the vehicle exited from the deployment tube, a lanyard removed the actuating clip and therefore started the timer. The flight time of the vehicle is normally 9 to 10 seconds, therefore, leaving 50 seconds of delay prior to antenna erection. After a minute had elapsed, the timer allowed the arm latch (item 6) to drop, releasing the release pin assembly (items 7, 8, 11 and 12) which allowed the cassette (item 3) to extend the antenna.

This completed assembly had been repeatedly tested on the laboratory shock machine (100 g's vertical, 50-60 g's horizontal) without degrading its performance. This device was considered satisfactory for flight testing.

2.2.7 ELECTRICAL SPECIFICATIONS

2.2.7.1 Transmitted Electrical Specifications

Power output	50 watts nom.
Frequency stability	±0.002 %
Linearity	±2% of best straight line
Deviation (carrier)	10 mv/rms at MI = 2

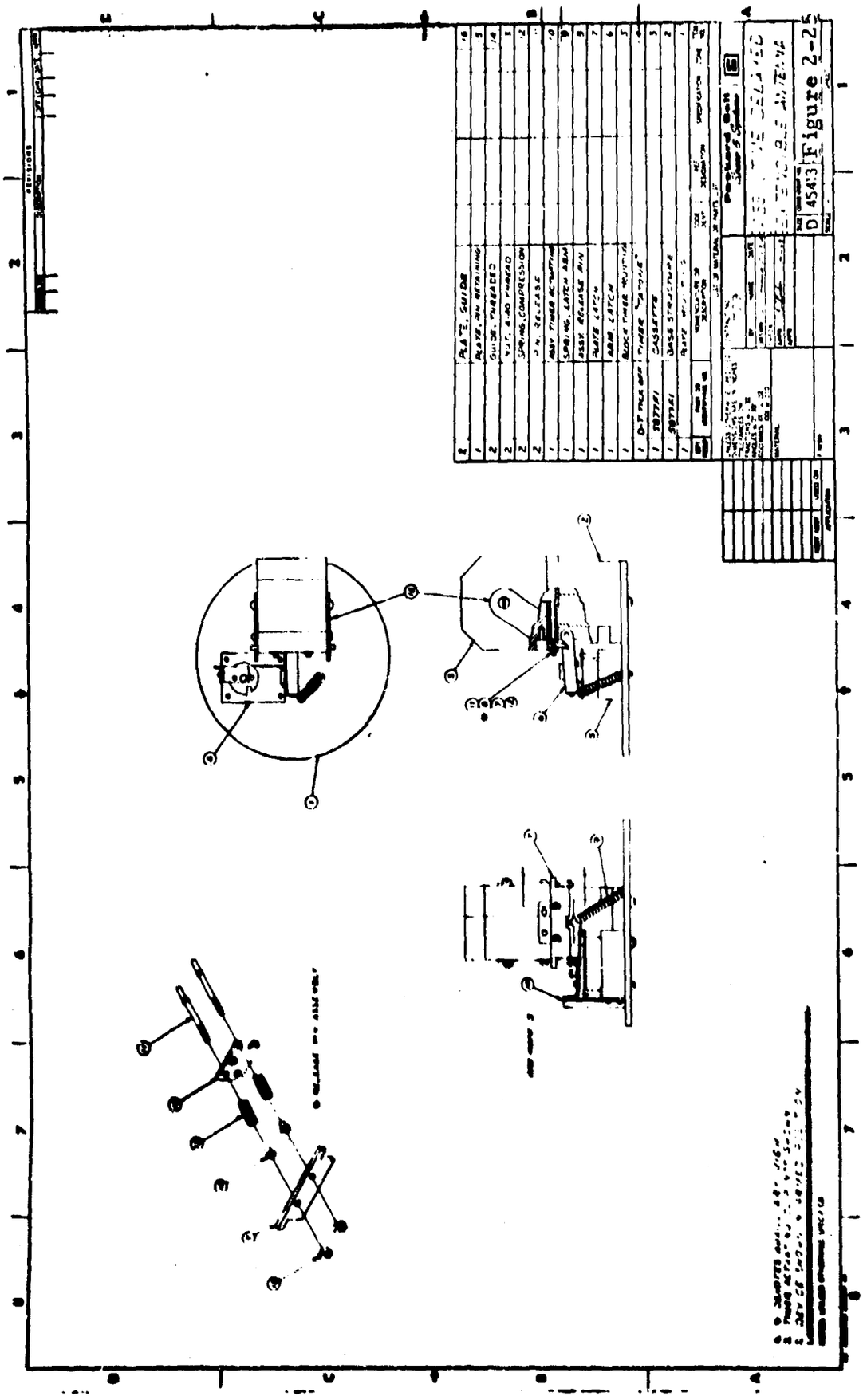

Figure 2-25

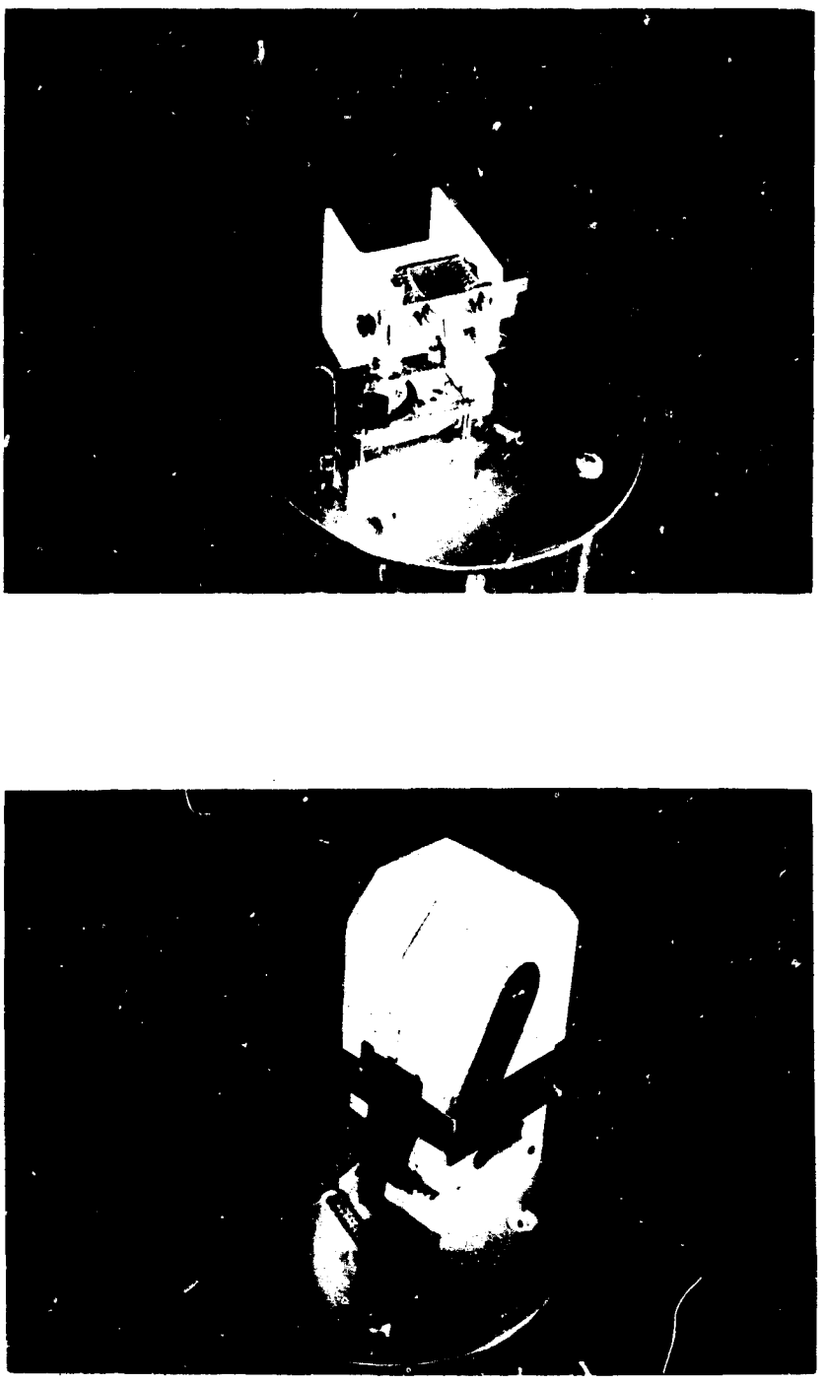

Figure 2-26. Antenna Delayed Release Mechanism - Front View

Figure 2-27. Antenna Delayed Release Mechanism - Side View

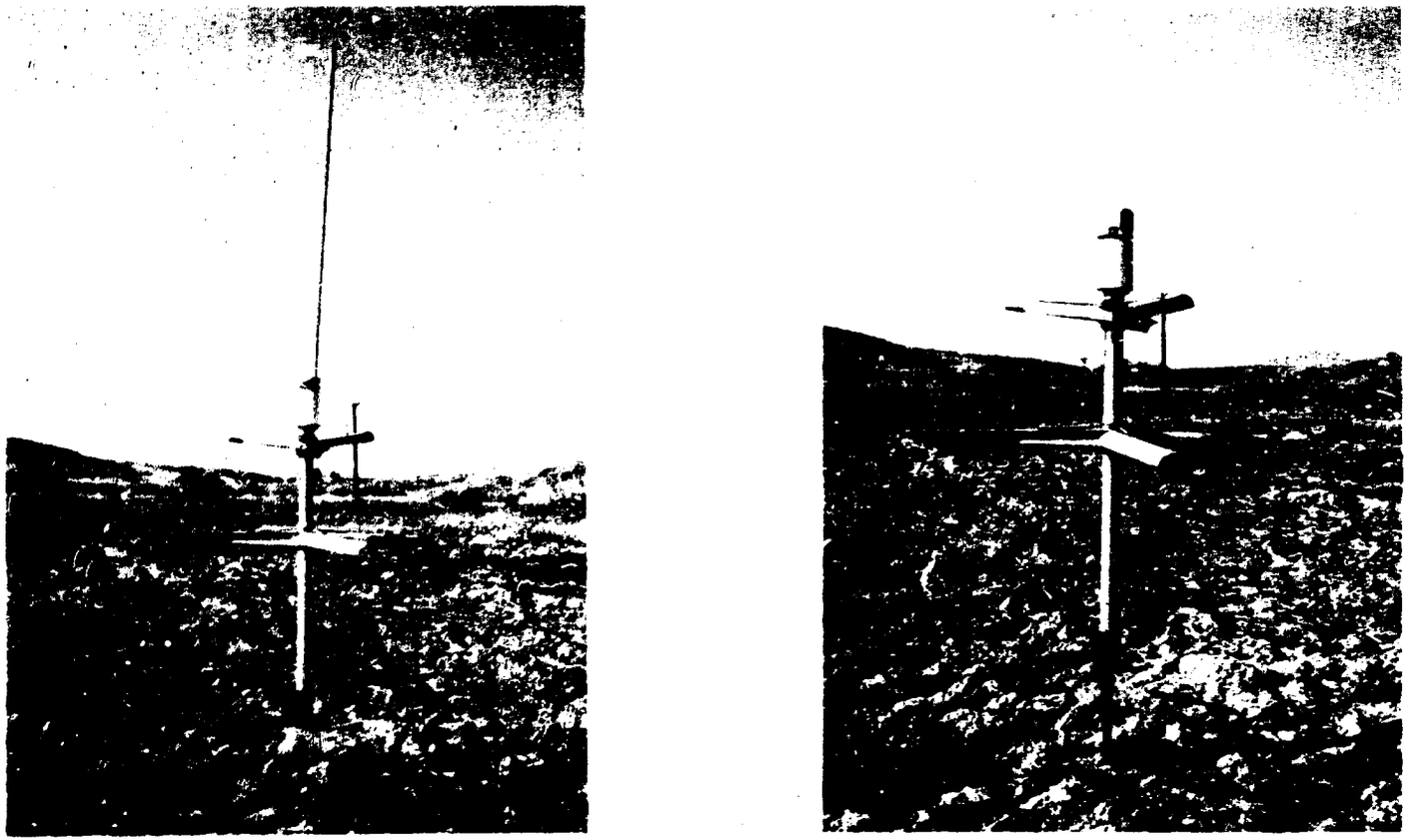

Figure 2-28. Deployment Vehicle Deployed

Deviation (subcarrier)	± 7% at ± 2.5 vdc
Input impedance	50 ohms
Harmonic distortion	2%
Modulation	Pulse, FM/FM
Frequency	40-42 MHz crystal controlled
Power requirements	+28 vdc nom ± 3 volts
Spurious output	60 db
Current	3 amps average

2.2.7.2 Receiver Electrical Specifications

Receiver type	FM
Frequency stability	± 0.002% crystal controlled
Input impedance	50 ohms
Noise figure	6 db
Image rejection	60 db
Spurious resonse	60 db
IF. rejection	80 db
IF. Bw	2 KHz crystal IF. filter
Discriminator lin.	± 2%
Limiter	Limits on noise
Sensitivity	-128 dbm
Frequency	40-42 MHz
Power requirements	+7.5 volts nom. ± 1 vdc
Current	12 ma

2.2.7.3 Decoder Specifications

Type	Tone decoder
Frequency	Tone No. 1 100 Hz Bw = 2 Hz
	Stability ± 0.1%
	Tone No. 2 110.9 Hz Bw = 2 Hz
	Stability ± 0.1%
Integration period	500 milliseconds

Command response	Presence of two simultaneous tones ("and" gate function)
Input impedance	50 k ohms
Sensitivity	35 mv/rms
Power requirements	7.5 vdc nom. ± 1 vdc
Current	1.2 ma nom.

2.2.7.4 Discriminator Specifications

Input frequency range	Standard units are available for center frequencies between 300 Hz and 185 KHz and for deviations between ± 3% and ± 40%
Input sensitivity	10 mv to 10 v rms without adjustment
Input impedance	100,000 ohms shunted by less than 25 pf
AM rejection*	A 20 db step in input amplitude will result in a peak output transient of less than 1% of bandwidth.
Adjacent channel rejection*	With the desired channel at center frequency, presence of adjacent channel band edges up to 16 db greater in amplitude will produce crosstalk of less than 0.1% of bandwidth.
Output signal	Adjustable from ± 1 v peak at 10 ma to ± 10 v peak, at 2 ma, single ended referred to ground. Continuous short circuit of output will cause no damage.
Output impedance*	Less than 1 ohm at minimum gain setting to less than 5 ohms at maximum gain.

Output voltage limit	Less than 15 volts peak.
Capacitive loading	Capacitive loading of output will cause no instability. Parallel RC load must not exceed maximum rated load.
Linearity	Less than 0.1% departure from best straight line.
Output ripple and noise 0-10 KHz*	Less than 0.1% of bandwidth
Data frequency response	Low pass cutoff frequencies from 6 Hz to 20 KHz. Roll off asymptotic to 18 db/ octave. Constant amplitude filters down 0.5 db ± 0.25 db and linear phase filters down 3 db ± 0.5 db at rated maximum intelligence frequency.
Harmonic distortion*	Less than 0.5% for any frequency up to channel cut off.
Zero stability	Within ± 0.075% of center frequency for 24 hours after a 20 minute warmup.
Tape speed compensation	A minimum improvement of 20 db is achieved for wow and flutter as great as ± 3%.
Counter output	A square wave with frequency identical to the carrier input appears at the front panel "CTR" test point. Amplitude is approximately 3.0 volts P-P independent of input voltage. Minimum load impedance 50k shunted by 1000 pf.

Temperature range	Operating:	0°C to +55°C
	Storage:	-40°C to +80°C
Power requirements	+18 vdc at 140 ma (max.) and -18 vdc at 70 ma (max.). Supply must be highly regulated:	
Weight	1.5 lb. max.	

*Specifications refers to performance when used with IRIG proportional bandwidth system employing a modulation index of 5.0.

2.3 SENSOR PACKAGE

2.3.1 SENSOR PACKAGE MECHANICAL DESIGN

In arriving at a final mechanical design, the various areas analyzed, breadboarded and evaluated in the sensor package (temperature, humidity, precipitation, pressure, wind speed and direction) were reviewed. Much effort was spent on obtaining and evaluating manufacturers' specifications on key component elements, such as the temperature thermistor, microphone for use in the precipitation sensor, strain gages, etc.

In order to conserve battery power, an evaluation of the sensor package was made with the sensors and their signal conditioners switched off during the quiescent period. Also, the time required for the sensors to warm up before being sampled was approximated.

The feasibility of using common signal conditioning amplifiers for a multiplicity of sensors to reduce power requirements was also studied.

The design of the sensor package has been completed and is shown in Figure 2-29. The signal conditioners were fabricated as flat circuit board assemblies, and potted as individual modules 2.25 inches in diameter and 1-inch thick. The prototype modules were all potted in foam potting compound, and assembled into the complete sensor package.

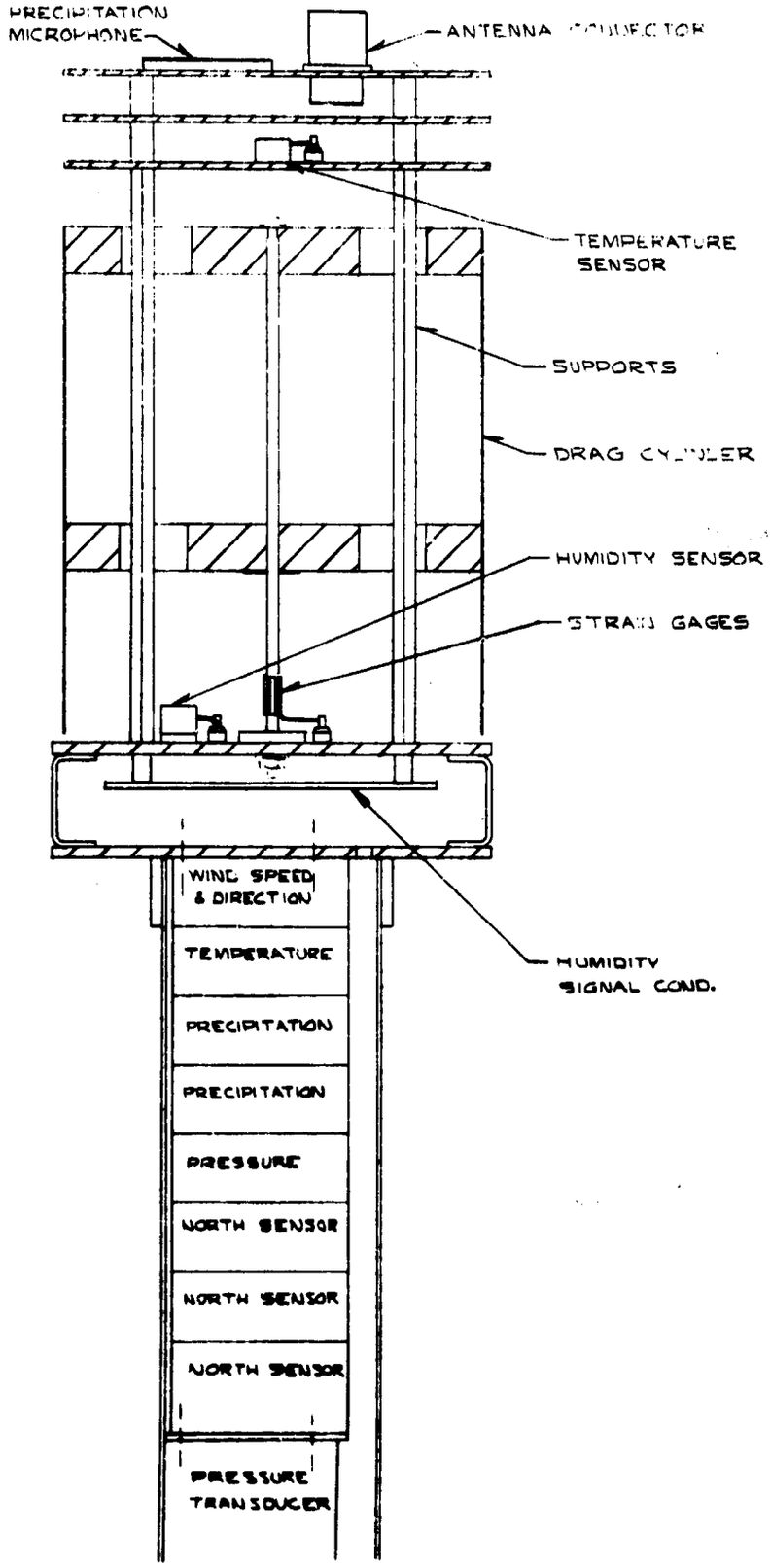

Figure 2-29. Sensor Package

2.3.1.1 Prototype Interface Connections

Figure 2-30 illustrates the interface connections in the sensor package.

2.3.1.2 Sensor Package Power Requirements

The following data delineates the power requirements of the sensors.

Sensor	+10 ± 0.1 vdc	-10 ± 0.1 vdc
Wind Speed and Direction	1.7 ma	18 ma
Temperature	10.2 ma	1.3 ma
North	87 ma	7.4 ma
Pressure	40 ma	- -
Humidity	6.5 ma	6.2 ma
Precipitation	16.7 ma (Readout) 12.2 ma (Cont.)	4.6 ma (Readout) 3.2 ma (Cont.)
	182.1 Int. 12.2 Cont.	37.5 Int. 3.2 Cont.

2.3.2 WIND SPEED AND DIRECTION

A solid-state anemometer was used for wind speed and direction. Due to package size limitations, the dynamic characteristics and threshold of the "mini-vane" approach previously proposed for wind direction measurement were undesirable. Heat flow shielding and associated problems indicated that implementation of the heated thermistor approach would lead to difficulty. The solid-state anemometer appeared to be a simplified approach with the present package. Modification and adaptation of techniques already demonstrated in previous developments yielded a simplified configuration for the composite measurement of wind speed and direction in rectangular coordinates. Design techniques were used to minimize the effects of "off vertical" operation to within the accuracy tolerance (Figure 2-31). The basic

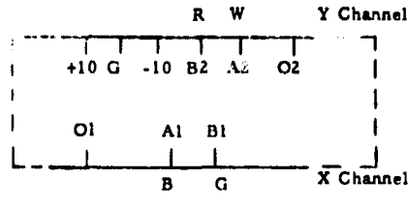

Wind Speed and Direction

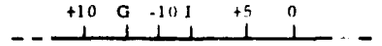

Barometric Pressure

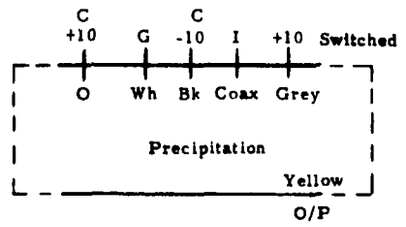

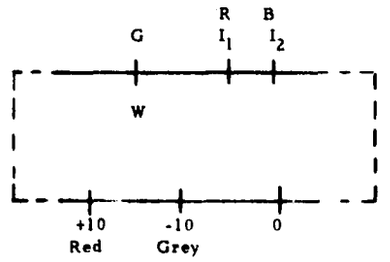

I_1 = Center of 18.7K and 35.25K

Air Temperature

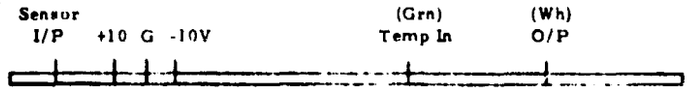

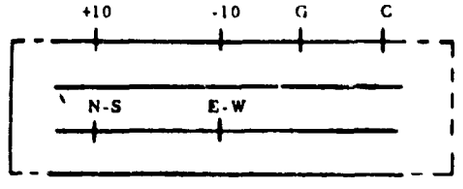

North Sensor

Green - E_o1

Yellow - E_o2

Final Values

N-S	E-W
S - 5.01	S - 2.50
W - 2.50	W - 0.11
N - 0.09	N - 2.50
E - 2.50	E - 4.99

Figure 2-30. Prototype Interface Connections

Weight of Drag Cylinder	0.0575 Lbs.
Drag Force at 2 Knots	0.0030 Lbs.
Drag Force at 5 Knots	0.0185 Lbs.
Specification	2 to 50 Knts ± 5 Knts
Maximum Off-Vertical Angle	$\theta = \text{Sin}^{-1} \frac{0.0185}{0.0575} = 18°$

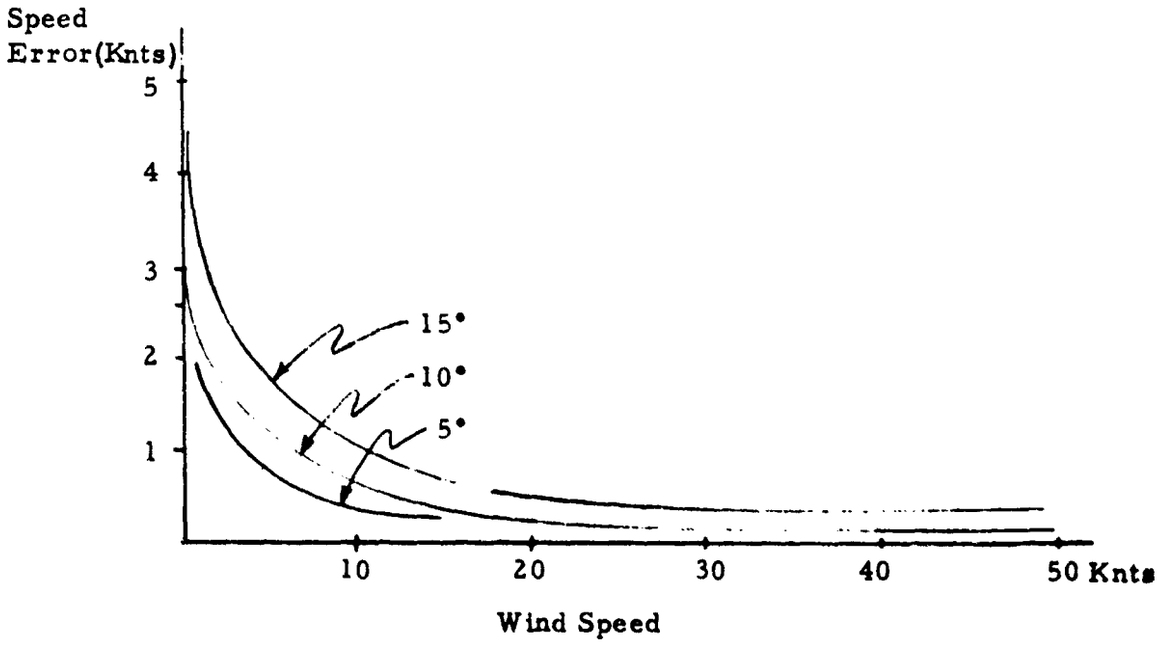

Figure 2-31. Wind Speed Error Due to Off-Vertical Orientation

approach was to use a limited-length cylinder and high sensitivity strain gages to measure drag-imposed deflection in the two horizontal directions (Figure 2-32). Special design, including excursion limiters, led to a device readily adaptable to the drop package.

A drag cylinder, 4.75 inches in diameter and 5.5 inches long stresses a 0.125-inch square brass bar (Figure 2-33). The orthogonal components of strain are sensed by semiconductor strain gages. The strain output is amplified and transmitted as two signal components as shown in Figure 2-34.

Because of the square law characteristic of the pressure velocity curve, accuracy requirements are most stringent at low-wind velocities. The error due to off-vertical landing was computed to be less than five knots at wind speeds near zero for angles of less than 15 degrees. Since flight experience indicated that the landing attitude did not exceed these limits, it was decided to eliminate the off-vertical correction from the prototype package.

Static loading tests (Table 2-2) on the wind/speed direction sensor demonstrated that errors of less than ± 20 degrees and ± 5 knots could be achieved. Wind tunnel tests did not reveal a need for spoilers on the drag cylinder. The drag cylinder is constructed of polystyrene foam and Mylar to reduce weight. This reduction of weight to 30 grams raised the natural resonance frequency to 30 Hz where the signal conditioner could successfully filter the oscillations.

2.3.3 AIR TEMPERATURE

The air temperature breadboard, which had been previously tested, was approved for prototype fabrication (Figure 2-35). Sun shields and sensor mounts were designed as part of the sensor package mechanical design. Sensor accuracy over the temperature range tested was ±1 degree F.

APPLICATION		REVISIONS					
NEXT ASSY	USED ON	LTR	DESCRIPTION	DFT	CHK	DATE	APPR

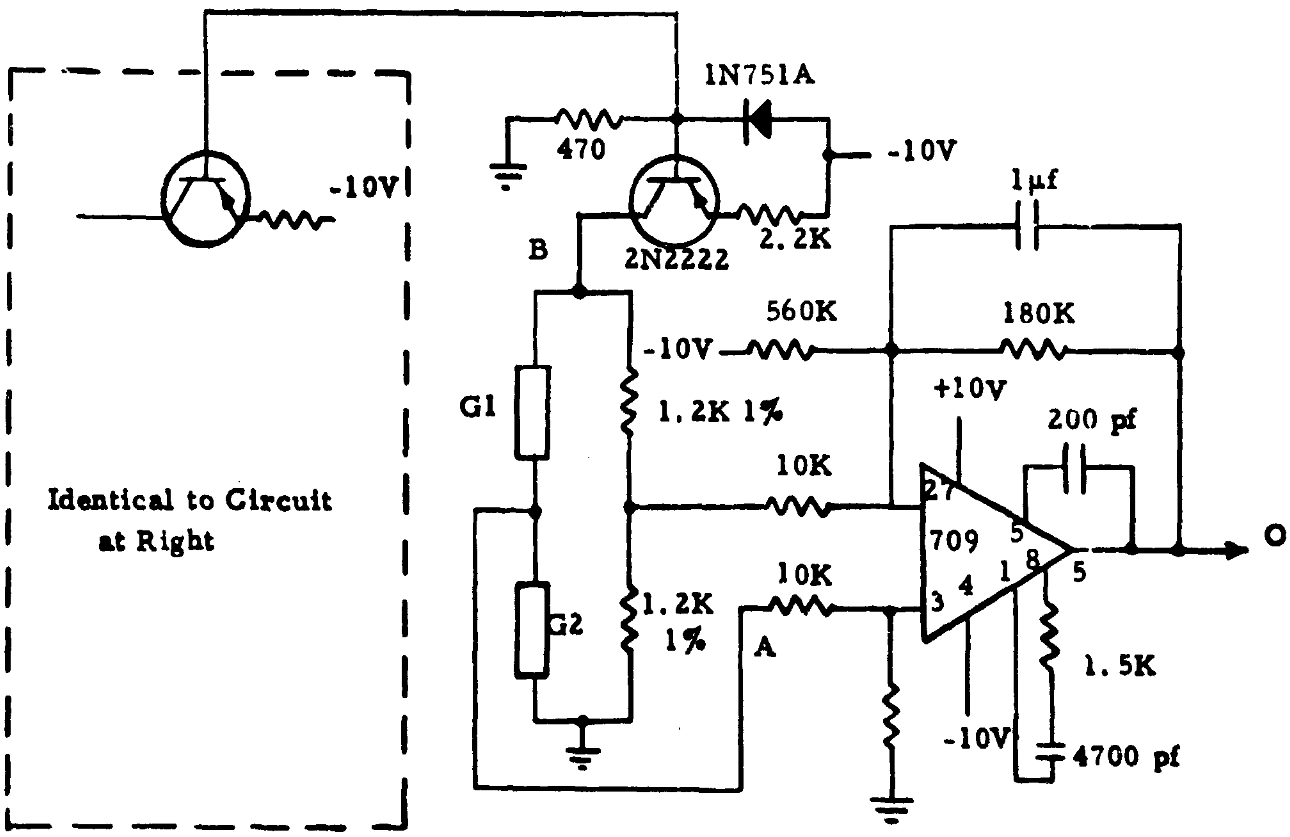

REV STATUS OF SHEETS	REV
	SHEET

UNLESS OTHERWISE SPECIFIED DIMENSIONS ARE IN INCHES

TOLERANCES ON:
FRACTIONS ± 1/32
DECIMALS XX ± .02
XXX ± .010
ANGLES ± 0°-30'

MATERIAL:

CONTRACT NO.

DRAWN		
CHECK		
APPD		

Packard Bell Space & Systems

Wind Speed and Direction Sensor

SIZE	CODE IDENT NO.	
A	45413	Figure 2-32

SCALE		SHEET	OF

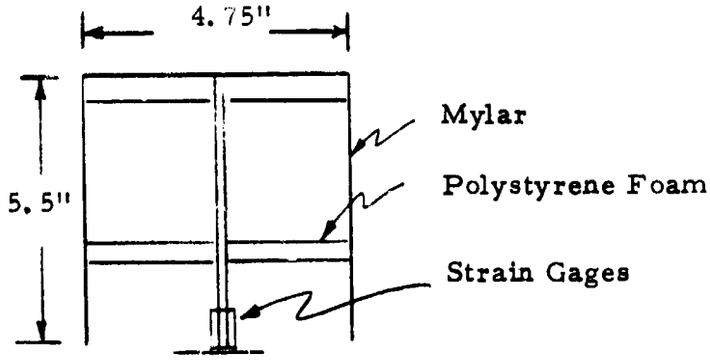

$A = 4.75'' \times 5.5'' = 0.182\ ft^2$

$D = \frac{1}{2}\rho V^2 A C_D = \frac{1}{2} \times 2.38 \times 10^{-3} \times 0.182 \times 1.2\ V^2_{(fps)} = 2.6 \times 10^{-4} V^2_{fps}$

$= 1.56 \times 10^{-4} V^2_{fps}$

at 50 Kts, D = 1.82 Lbs.

Spec. W/S 2 - 50 Kts ±5 Kts

W/D ±20° for W/S > 2 Kts

V_{kts}	D_{lbs}	V_o Volts
±2	.00063	0.0044
±5	.0039	0.025
±15	.0352	±0.225
±30	0.14	±0.9
±50	0.39	±2.5

Figure 2-33. Wind Speed and Direction Sensor Pictorial View

APPLICATION		REVISIONS					
NEXT ASSY	USED ON	LTR	DESCRIPTION	DFT	CHK	DATE	APPR

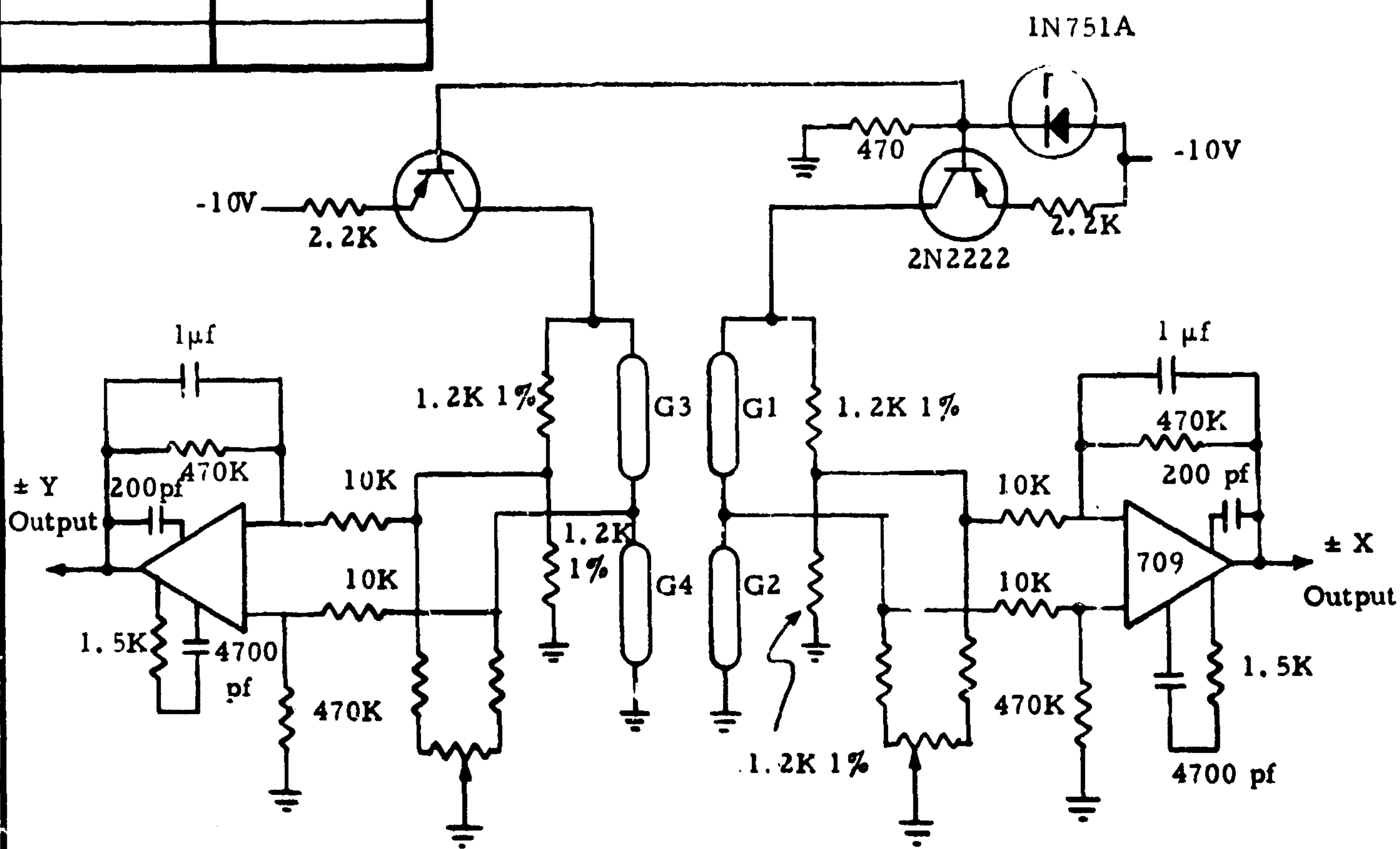

REV STATUS	REV
OF SHEETS	SHEET

UNLESS OTHERWISE SPECIFIED DIMENSIONS ARE IN INCHES
TOLERANCES ON:
FRACTIONS ± 1/32
DECIMALS XX ± .02
XXX ± .010
ANGLES ± 0°-30'
MATERIAL:

CONTRACT NO.

DRAWN
CHECK
APPD

Packard Bell
Space & Systems

Wind Speed and Direction
Signal Conditioner

SIZE	CODE IDENT NO.	
A	45413	Figure 2-34

SCALE | SHEET OF

Table 2-2. Wind Speed and Direction Sensor Prototype-Static Loading Tests

ΔV_x at 50 Kts = 2.68V

ΔV_y at 50 Kts = 2.63V

V_{ox} = 2.473 V_{oy} = 2.454

$$\Delta V = \sqrt{\Delta V_x^{\,2} + \Delta V_y^{\,2}} \qquad \bar{V} = 50\sqrt{\frac{\Delta V}{2.65}}$$

$$\theta = \mathrm{Tan}^{-1}\ \frac{\Delta V_y}{\Delta V_x}$$

TEST at 15 Kts

θ	V_x	V_y	ΔV_x	ΔV_y	ΔV	θ'	$\bar{V}$
90°	2.499	2.703	0.026	0.349	0.25	84°	15.3
120°	2.352	2.684	-0.121	0.230	0.26	118°	15.7
150°	2.282	2.611	-0.191	0.157	0.248	141°	15.3
180°	2.241	2.477	-0.232	0.023	0.234	174°	15.1
210°	2.256	2.341	-0.217	-0.113	0.244	208°	15.2
240°	2.317	2.223	-0.156	-0.221	0.270	235°	16.0
270°	2.434	2.180	-0.039	-0.274	0.277	262°	16.2
300°	2.572	2.225	0.099	-0.229	0.250	293°	15.3
330°	2.637	2.299	0.164	-0.155	0.226	313°	14.6
360°	2.739	2.439	0.266	-0.015	0.266	357°	15,8
30°	2.712	2.561	0.239	0.107	0.262	24°	15.7
60°	2.626	2.662	0.153	0.208	0.262	54°	15.7
90°	2.507	2.689	0.034	0.235	0.237	82°	15.0

Final Values

X_o = 2.48

ΔV_x at 50 Kts = 2.48 Volts

$R_g = 180^k || 680^k$

$R_o = 390^k || 430^k$

Y_o = 2.57

ΔV_y at 50 Kts = 2.53 Volts

$R_g = 180^k || 620^k$

$R_o = 390^k || 330^k$

REVISIONS					
ZONE	LTR	DESCRIPTION	DFT	CHK	DATE	APPD

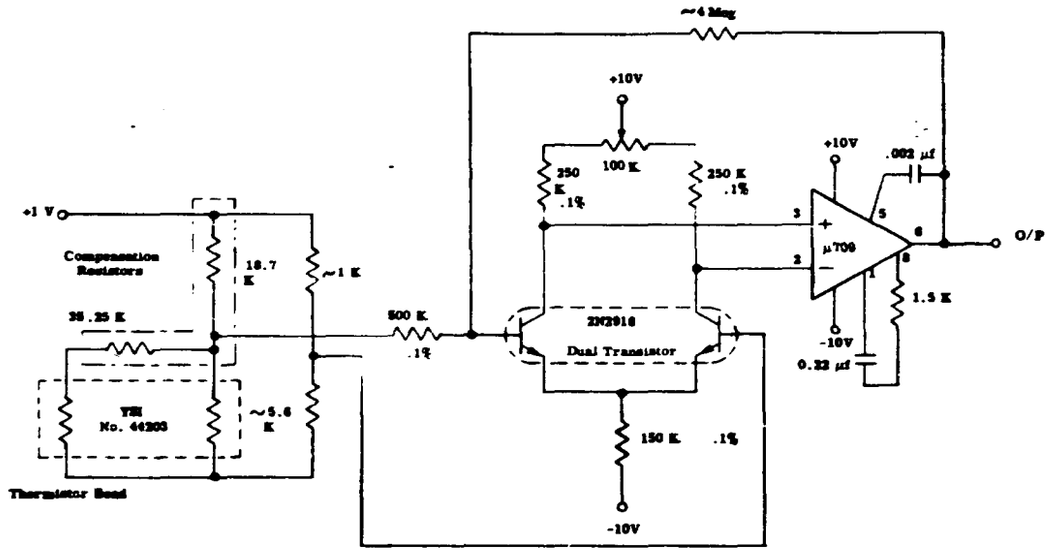

QTY REQD	PART OR IDENTIFYING NO.	NOMENCLATURE OR DESCRIPTION	CODE IDENT	REF DESIGNATION	SPECIFICATION	ZONE	ITEM NO.

LIST OF MATERIAL OR PARTS LIST

UNLESS OTHERWISE SPECIFIED DIMENSIONS ARE IN INCHES
TOLERANCES ON:
FRACTIONS ± 1/32
ANGLES ± 0°-30'
DECIMALS .XX ± .02
.XXX ± .010

MATERIAL

FINISH

NEXT ASSY | USED ON

APPLICATION

CONTRACT NO.

BY	NAME	DATE
DRAWN		
CHECK		
APPR		
APPR		

Packard Bell Space & Systems

Temperature Sensor

SIZE C | CODE IDENT NO. 45413

Figure 2-35

SCALE | SHEET

1. INTERPRET DRAWING IN ACCORDANCE WITH STANDARDS PRESCRIBED BY MIL-D-1000.
NOTES: UNLESS OTHERWISE SPECIFIED.

Development of a special thermistor which meets the accuracy requirements over the -50°F to +130°F range was not undertaken.

A YSI type 44203 compensated thermistor bead was used as the initial temperature sensing device. The dynamic range of this thermistor is -20°F to +120°F, (Figure 2-36) slightly less than that required for the final model.

The differential output of the thermistor over the temperature range is approximately 640 millivolts/volt excitation. The load on the thermistor network must be around the one-megohm region to maintain the specified accuracy. The preceding two factors dictate the available current value to tenths of a μamp. The amplification stages are required to be very stable at these low currents over the full temperature range, increasing the cost of the signal conditioner.

The prototype submitted is a compromise of cost versus accuracy for the thermistor bead used. If a more suitable thermistor can be found providing additional advantages in cost and/or accuracy, then it can replace the type currently utilized.

2.3.4 RELATIVE HUMIDITY

The relative humidity sensor was breadboarded using a variable resistance humidity sensor. The logarithmic nature of the output with humidity and the high temperature coefficient presented design problems in meeting the accuracy requirements.

Further testing indicated that the polarization of the relative humidity sensor was negligible at the duty cycles encountered in the AMQ-27. This allowed the use of dc biasing and simplified the non-linearity and drift correction problems.

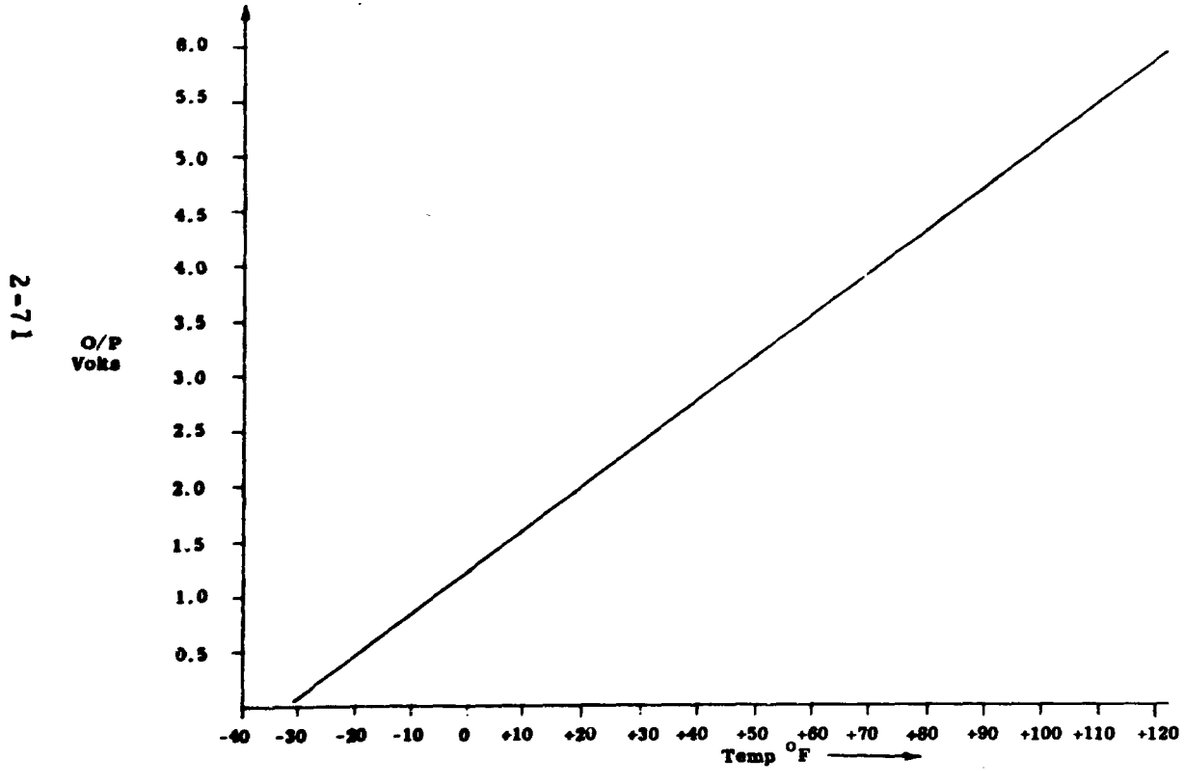

Results	
Temp °F	O/P Volts
-40	0.095
-35	0.035
-30	0.19
-25	0.34
-20	0.51
-15	0.69
-10	0.86
-5	1.06
0	1.25
+5	1.44
+10	1.63
+15	1.83
+20	2.02
+25	2.21
+30	2.39
+35	2.58
+40	2.77
+45	2.96
+50	3.15
+55	3.34
+60	3.53
+65	3.72
+70	3.92
+75	4.12
+80	4.323
+85	4.51
+90	4.72
+95	4.92
+100	5.123
+105	5.31
+110	5.504
+115	5.696
+120	5.887

Figure 2-36. YSI No. 44203 Thermistor Bead

A successful basic design for relative humidity (R. H.) has been achieved. The accompanying graph (Figure 2-37) shows the linearity using a simulated R. H. sensor (a custom-made decade box) at a constant temperature.

Experimentation indicated that the PCRC-55 R. H. sensor can be used with dc power reducing the circuit cost significantly because of the low duty cycle proposed. Initial tests indicated that, by feeding the temperature channel output into the R. H. channel, successful temperature compensation can be effected.

2. 3. 5 PRECIPITATION SENSOR

No changes were made in the precipitation sensor approach, where a rain intensity type of sensor was used to provide a qualitative measurement of liquid precipitation.

The precipitation sensor design and prototype construction was completed. The rainfall measurement is subjective, consisting of counting the number of raindrop "hits" on a barium titanate crystal. A charge, proportional to the number of drops hitting the crystal, is stored in an E-cell and read out on demand. Details of the timing were resolved.

The accompanying block diagram Figure 2-38 portrays the basic operation of the precipitation sensor. For this application, a subjective measurement of rain is all that is required, enabling the utilization of relatively low cost components.

Referring to the block diagram, rain drops hitting the sensing element generate voltage pulses which are amplified and rectified by the first operational amplifier stage. The resulting unidirectional pulses are now integrated by the second stage and fed via a voltage controlled current generator into an *E-cell, where information is stored accumulatively.

*An E-cell is an electro-chemical device which stores a current/time integral by physical transference of silver from one electrode surface to another.

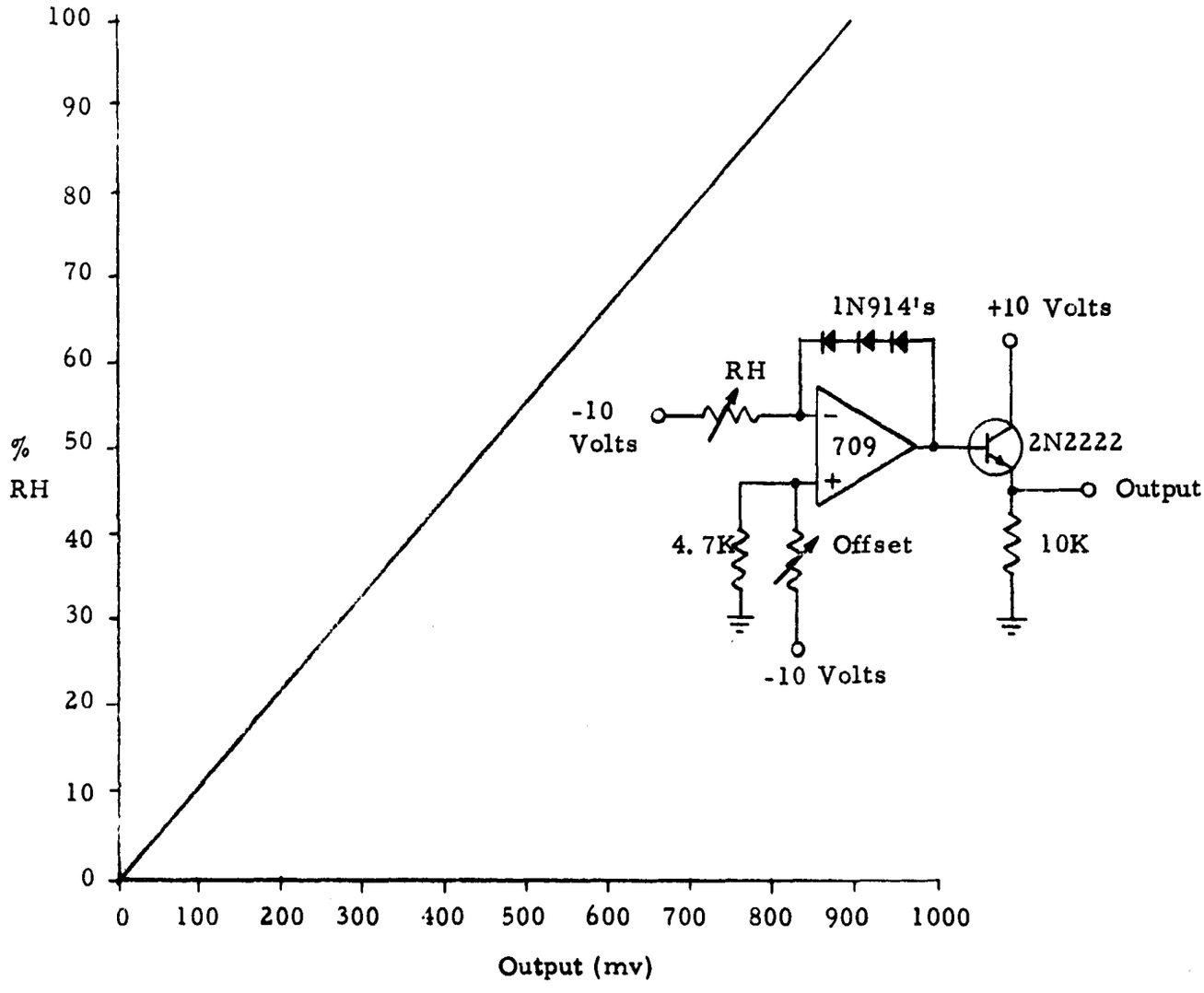

Figure 2-37. Relative Humidity Linearity Curve

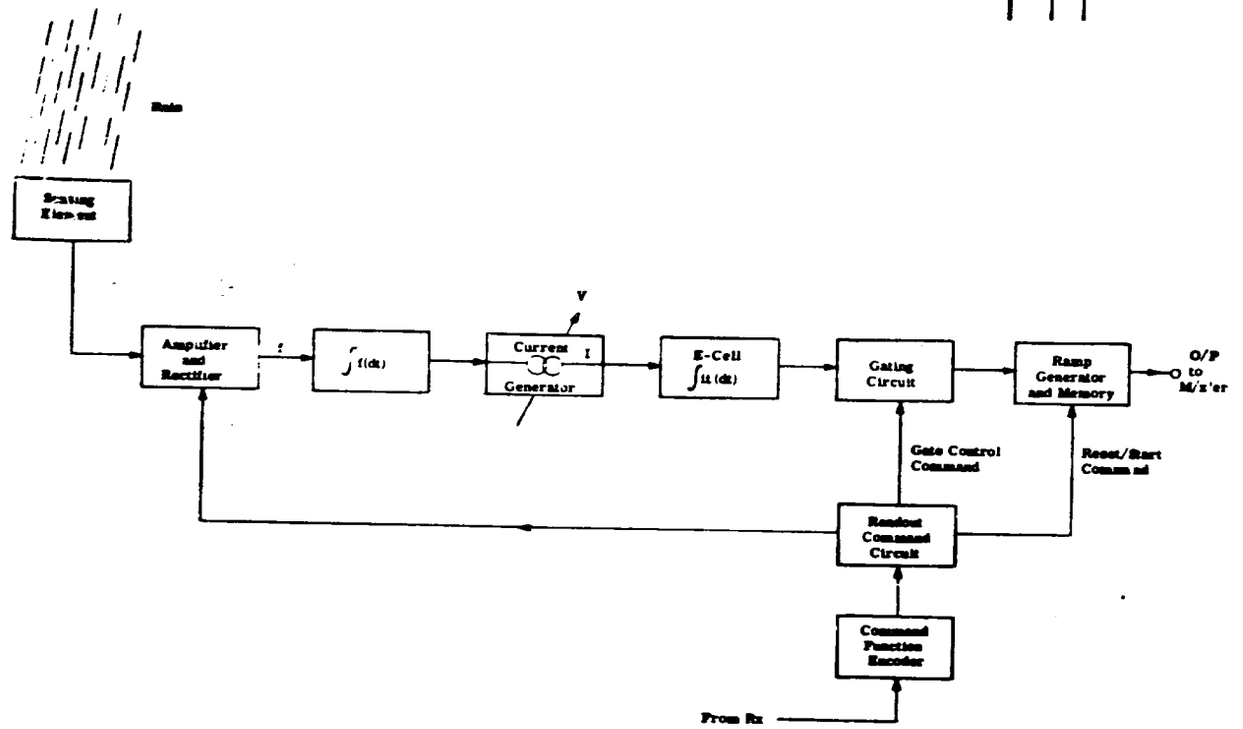

REVISIONS					
ZONE	LTR	DESCRIPTION	DFT	CHK	DATE	APPR

QTY REQD	PART OR IDENTIFYING NO.	NOMENCLATURE OR DESCRIPTION	CODE IDENT	REF DESIGNATION	SPECIFICATION	ZONE	ITEM NO.

LIST OF MATERIAL OR PARTS LIST

UNLESS OTHERWISE SPECIFIED DIMENSIONS ARE IN INCHES
TOLERANCES ON:
FRACTIONS ± 1/32
ANGLES ± 0°-30'
DECIMALS XX ± .02
XXX ± .010

MATERIAL:

FINISH:

NEXT ASSY | USED ON
APPLICATION

CONTRACT NO.

BY	NAME	DATE
DRAWN		
CHECK		
APPR		
APPR		

Packard Bell Space & Systems

Precipitation Sensor Block Diagram

SIZE C | CODE IDENT NO. 45413

SCALE | SHEET

1. INTERPRET DRAWING IN ACCORDANCE WITH STANDARDS PRESCRIBED BY MIL-D-1000.
NOTES: UNLESS OTHERWISE SPECIFIED.

Figure 2-38

After a known time interval, a command signal arrives reversing the direction of silver flow in the E-cell and starting a 10-second ramp voltage generator. When all the silver has been transferred back to its original electrode, the impedance of the E-cell rises sharply, activating a transistor switch which clamps the rising ramp voltage to the instantaneous value.

The voltage level now stored is a measure of the rain which fell in the previous time interval. As soon as the information has been read, the circuit is reset to begin the cycle over again.

2.3.6 BAROMETRIC PRESSURE

Atmospheric pressure was measured by a metal membrane element. Several models of existing transducers including strain-gage bridge and variable resistance types were evaluated for system suitability. Two of these transducers were prototypes developed for this program. One barometric pressure transducer, constructed to commercial specifications, was received enabling design and testing of the associated signal conditioners (Figure 2-39). On the basis of this evaluation, a lightweight, rugged version of this transducer developed by Computer Instruments Corporation was selected for the prototype package. This transducer is a potentiometer type and produces a high level signal which can be buffered and sent directly to the transmitter.

The Computer Instruments Corporation (C.I.C.) pressure transducer type 2000 was chosen by careful consideration of total cost, accuracy, packaging, weight, size, environmental ruggedness, and the reputation of the manufacturer in the field of pressure measurement.

The transducer functions by utilizing the movement of a pressure sensitive capsule to vary the slider arm of a thin film potentiometer, requiring a minimum of signal conditioning. The accompanying graph displays the linearity of the device (Figure 2-40).

APPLICATION		REVISIONS					
NEXT ASSY	USED ON	LTR	DESCRIPTION	DFT	CHK	DATE	APPR

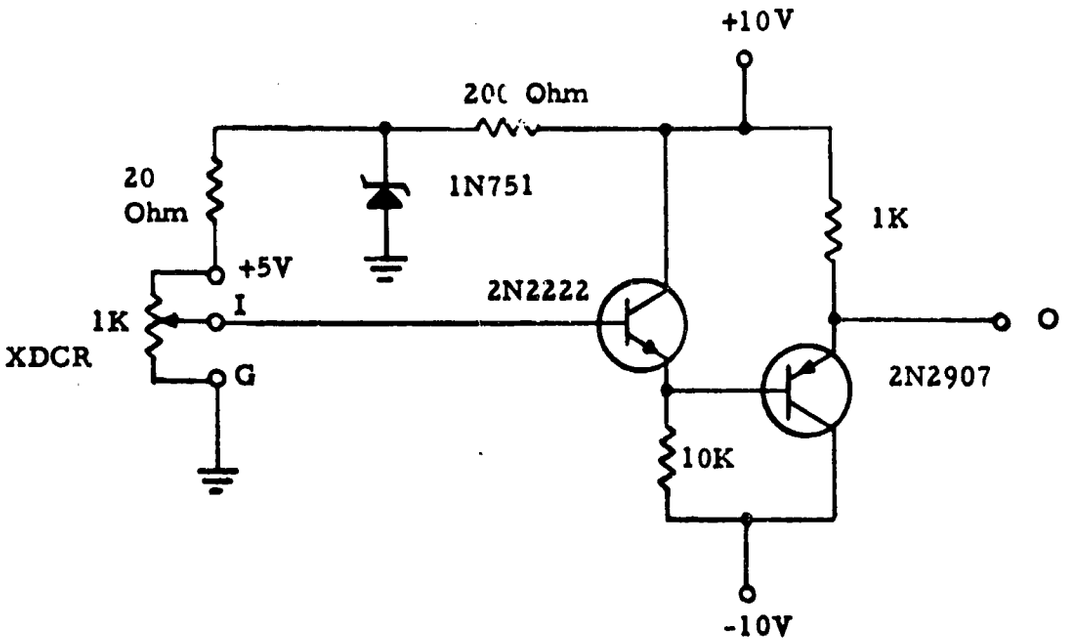

REV STATUS	REV																													
OF SHEETS	SHEET																													

UNLESS OTHERWISE SPECIFIED DIMENSIONS ARE IN INCHES TOLERANCES ON: FRACTIONS ± 1/32 DECIMALS XX ± .02 XXX ± .010 ANGLES ± 0°-30'	CONTRACT NO.	Packard Bell Space & Systems	PB
	DRAWN / CHECK / APPD	Barometric Pressure Signal Conditioner	
MATERIAL:		SIZE A / CODE IDENT NO. 45413	Figure 2-39
		SCALE	SHEET OF

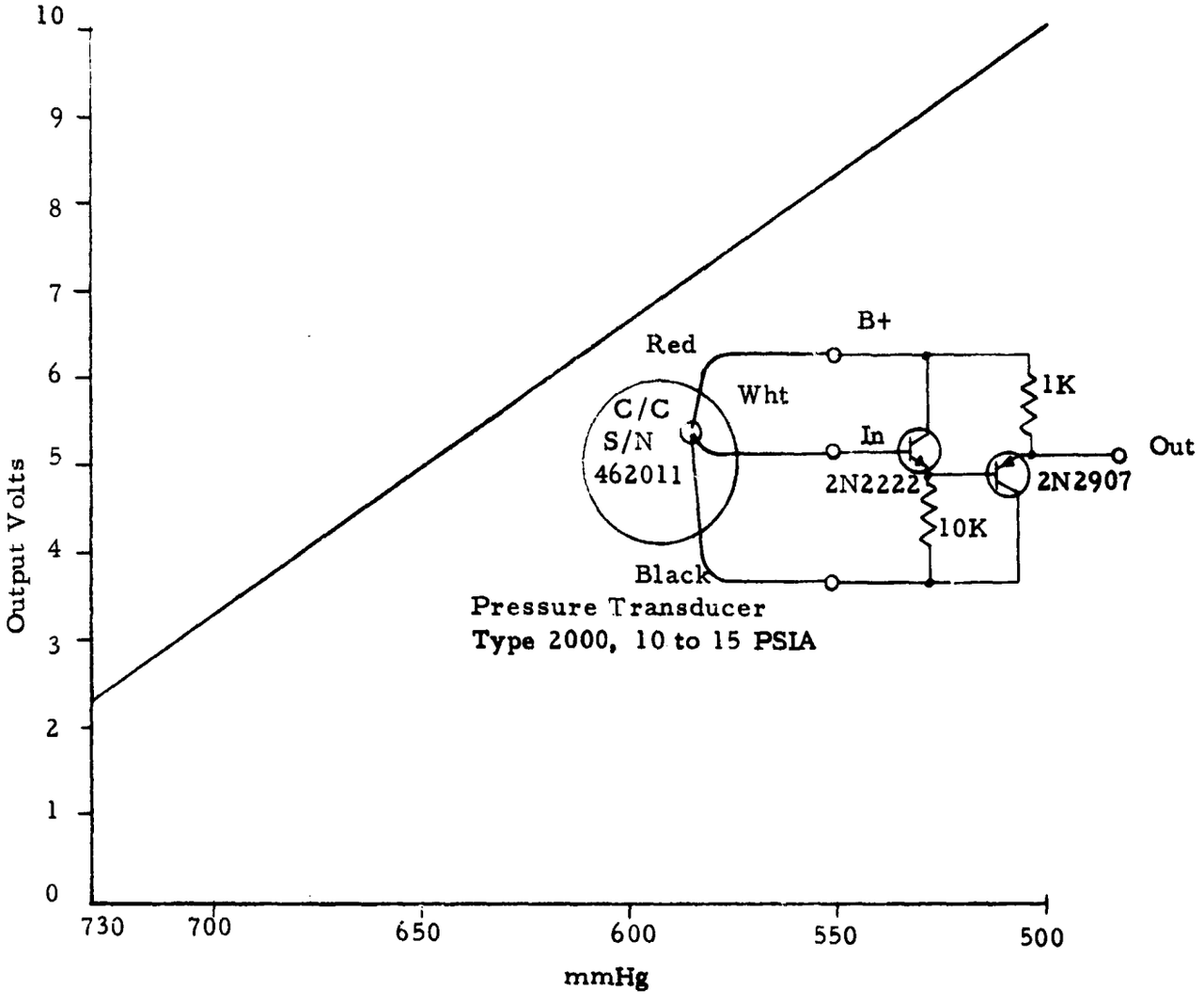

Figure 2-40. Barometric Pressure Graphic Presentation

2.3.7 NORTH SENSOR

A north sensor suitable for use in the meteorological package appeared to be the most challenging requirement. It appeared that the practical approach was to use a Hall-effect device to sense the earth's magnetic field. Basic sensors have been used for this type of measurement and were readily available; however, special design techniques were required for use in this system. A tentative design allowed the use of relative rather than absolute values and facilitated implementation.

One candidate north sensor subsystem was breadboarded (Figures 2-41 thru 2-44). This sensor met the accuracy requirements but required a long warmup time. Other techniques were pursued and another configuration was selected.

This second north sensor configuration was breadboarded and tested. This second design was found to be inferior to the previous design in terms of accuracy and complexity. Steps were successfully taken to improve the warm-up time of the first design. Stabilizing the accuracy over the temperature range remained the only problem area. Preliminary tests showed that an accuracy of ±5° could be anticipated.

The north sensor consists of a liquid-filled compass and two orthogonal Hall-effect position sensors. The Hall-effect devices respond to the sine and cosine of the angle between the north pointing compass magnet and the north sensor reference position. The data is transmitted as two orthogonal components and is, therefore, compatible with the wind speed/direction data readout.

APPLICATION		REVISIONS					
NEXT ASSY	USED ON	LTR	DESCRIPTION	DFT	CHK	DATE	APPR

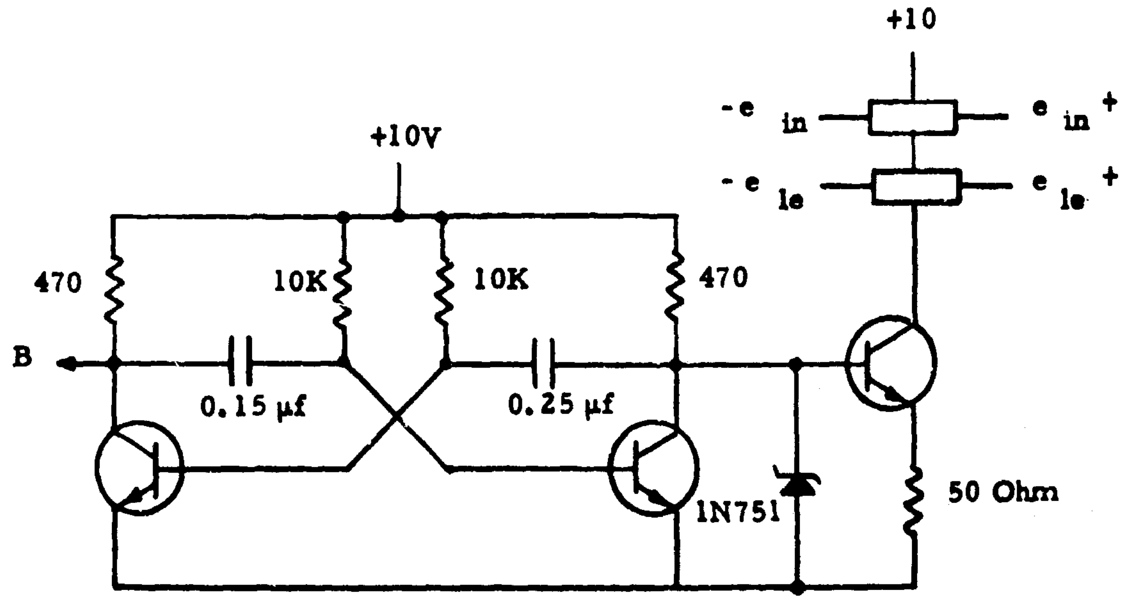

REV STATUS OF SHEETS	REV
	SHEET

UNLESS OTHERWISE SPECIFIED DIMENSIONS ARE IN INCHES
TOLERANCES ON:
FRACTIONS ± 1/32
DECIMALS XX ± .02
XXX ± .010
ANGLES ± 0°-30'
MATERIAL:

CONTRACT NO.

DRAWN		
CHECK		
APPD		

Packard Bell Space & Systems

Current Generator

SIZE	CODE IDENT NO.	
A	45413	Figure 2-41

SCALE | SHEET OF

APPLICATION		REVISIONS					
NEXT ASSY	USED ON	LTR	DESCRIPTION	DFT	CHK	DATE	APPR

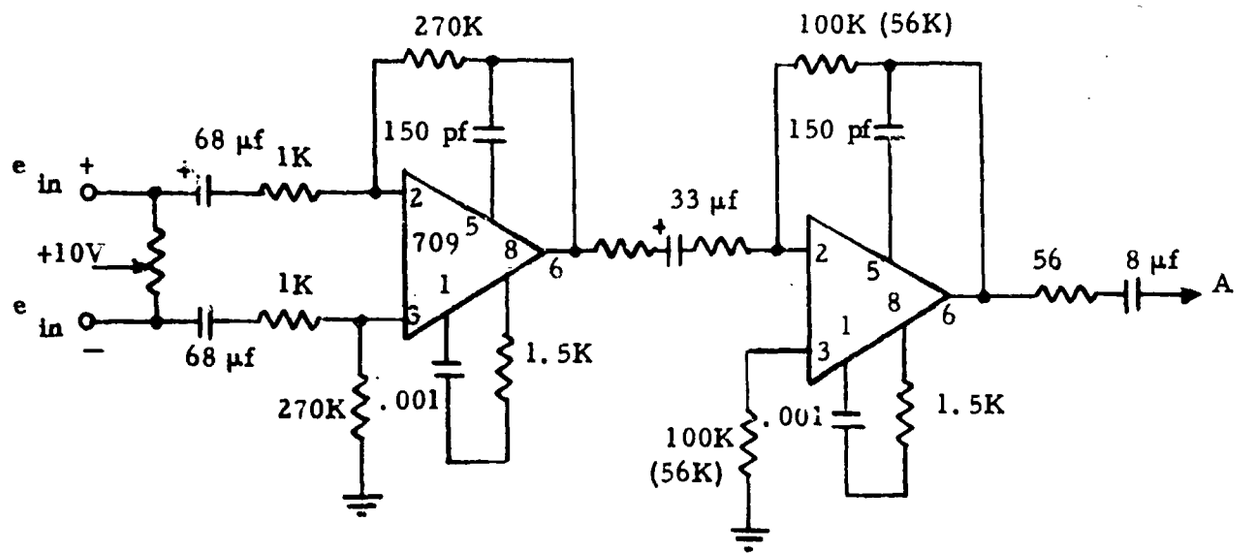

NOTE: ( ) indicates East-West Values

REV STATUS	REV																															
OF SHEETS	SHEET																															

UNLESS OTHERWISE SPECIFIED DIMENSIONS ARE IN INCHES TOLERANCES ON: FRACTIONS ± 1/32 DECIMALS XX ± .02 XXX ± .010 ANGLES ± 0°-30′ MATERIAL:	CONTRACT NO.	Packard Bell Space & Systems	PB
	DRAWN / CHECK / APPD	North-South Channel	
		SIZE A / CODE IDENT NO. 45413	Figure 2-42
		SCALE	SHEET OF

APPLICATION		REVISIONS					
NEXT ASSY	USED ON	LTR	DESCRIPTION	DFT	CHK	DATE	APPR

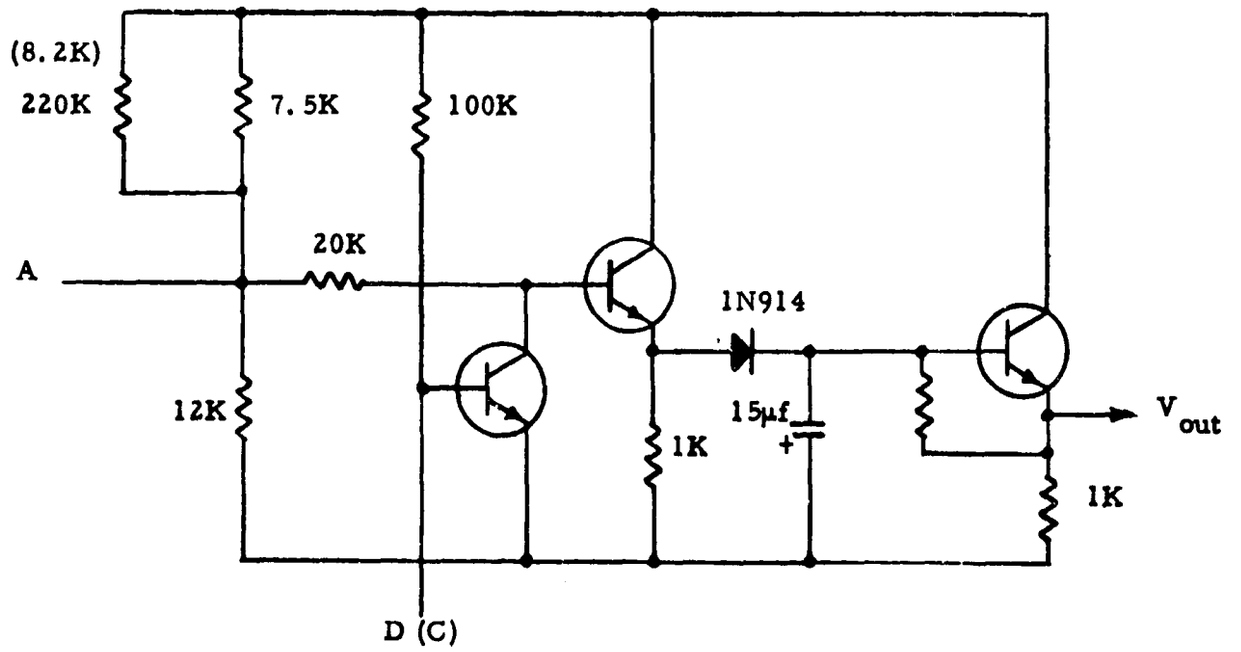

NOTE: ( ) indicates East-West Values

REV STATUS	REV																													
OF SHEETS	SHEET																													

UNLESS OTHERWISE SPECIFIED DIMENSIONS ARE IN INCHES TOLERANCES ON: FRACTIONS ± 1/32 DECIMALS XX ± .02 XXX ± .010 ANGLES ± 0°-30'	CONTRACT NO.	Packard Bell Space & Systems	
	DRAWN / CHECK / APPD	North-South Demodulator	
MATERIAL:		SIZE A	CODE IDENT NO. 45413
		SCALE	SHEET OF

Figure 2-43

APPLICATION		REVISIONS					
NEXT ASSY	USED ON	LTR	DESCRIPTION	DFT	CHK	DATE	APPR

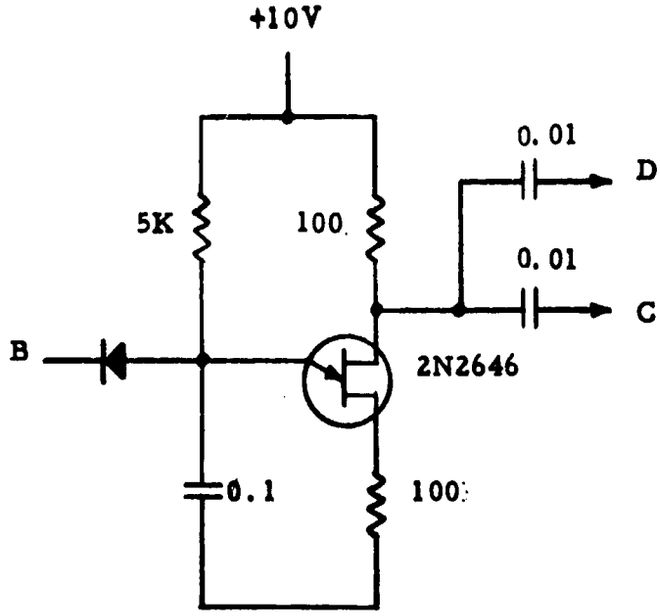

REV STATUS	REV																													
OF SHEETS	SHEET																													

UNLESS OTHERWISE SPECIFIED DIMENSIONS ARE IN INCHES TOLERANCES ON: FRACTIONS ± 1/32 DECIMALS XX ± .02 XXX ± .010 ANGLES ± 0°-30'	CONTRACT NO.	Packard Bell Space & Systems	
	DRAWN / CHECK / APPD	Pulse Generator	
MATERIAL:		SIZE A / CODE IDENT NO. 45413	Figure 2-44
		SCALE	SHEET OF

SECTION III

TEST RESULTS

3.0 This section of the report covers the results of the vehicle flight tests and the communication tests.

3.1 VEHICLE FLIGHT TESTS

3.1.1 PRELIMINARY TEST FLIGHTS

With all the parts fabricated, the first flight vehicle was assembled and tested. A Cessna 172 airplane was chosen as the carrier. A 7- inch diameter tube, 6-feet long, was used as a housing and release tube for the vehicle. The aircraft installation is shown in Figures 3-1 and 3-2. This vehicle was only instrumented with two accelerometers for recording the impact shock.

The deployment vehicle was released from the plane (air speed 60 mph) at 750 feet with the plane headed into a 15-mph wind. The release tube worked ideally and the vehicle cleared the plane and started to tumble, but quickly righted itself to a 30-degree inclination as the main blades caught the air and started rotating. The vehicle fell in a wobbly spiral flight pattern and, as a result, the vehicle impacted the ground at an angle 30 degrees off the vertical and bounced. Also, during the flight, the upper stabilizing blades did not seem to be rotating very fast. Both sets of rotor blades, the main body and one rotating hub were damaged upon impact with the ground.

The following data was collected during flight and impact:

a. Flight time -10 seconds.

b. Target accuracy - within a 200-foot diameter of target center.

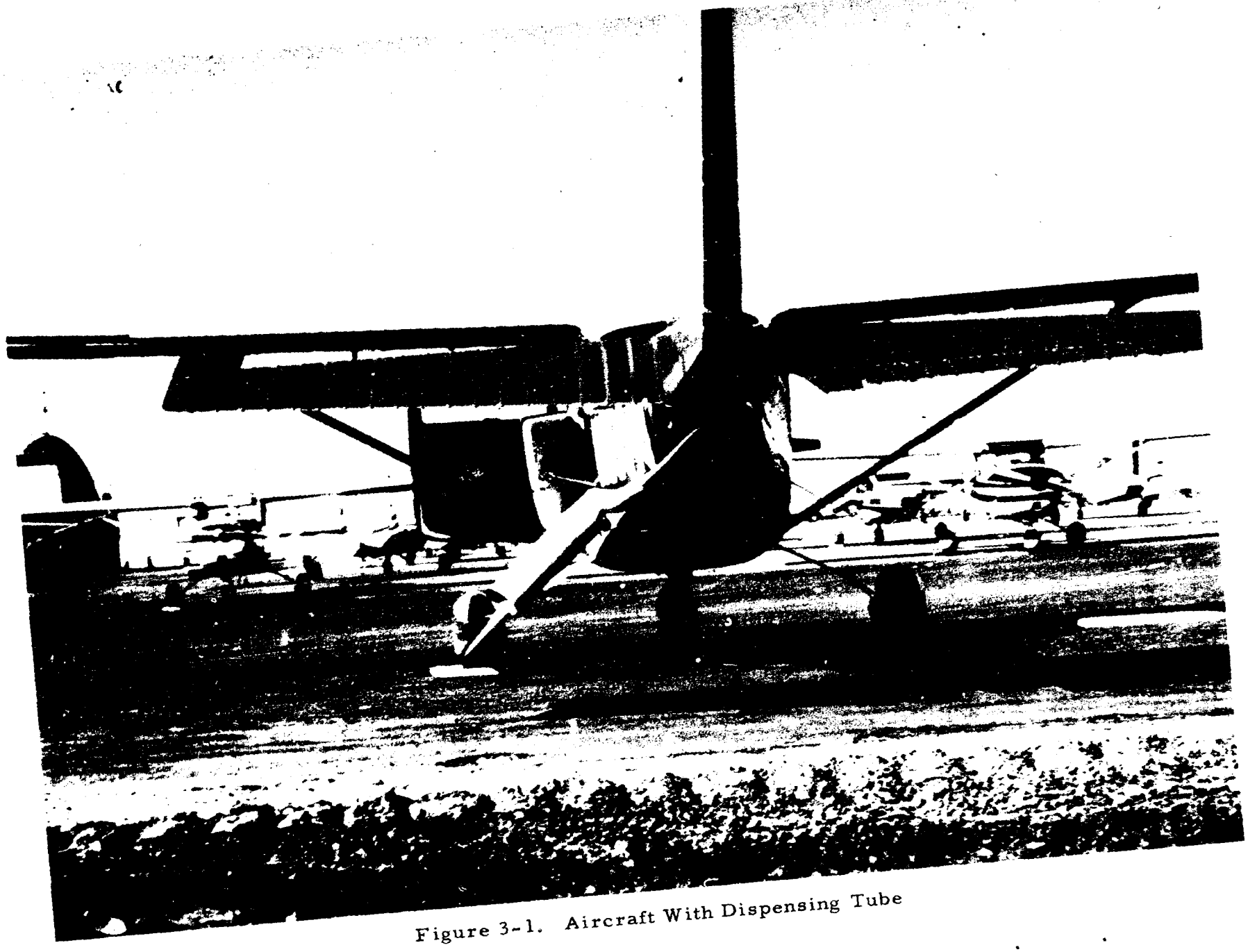

Figure 3-1. Aircraft With Dispensing Tube

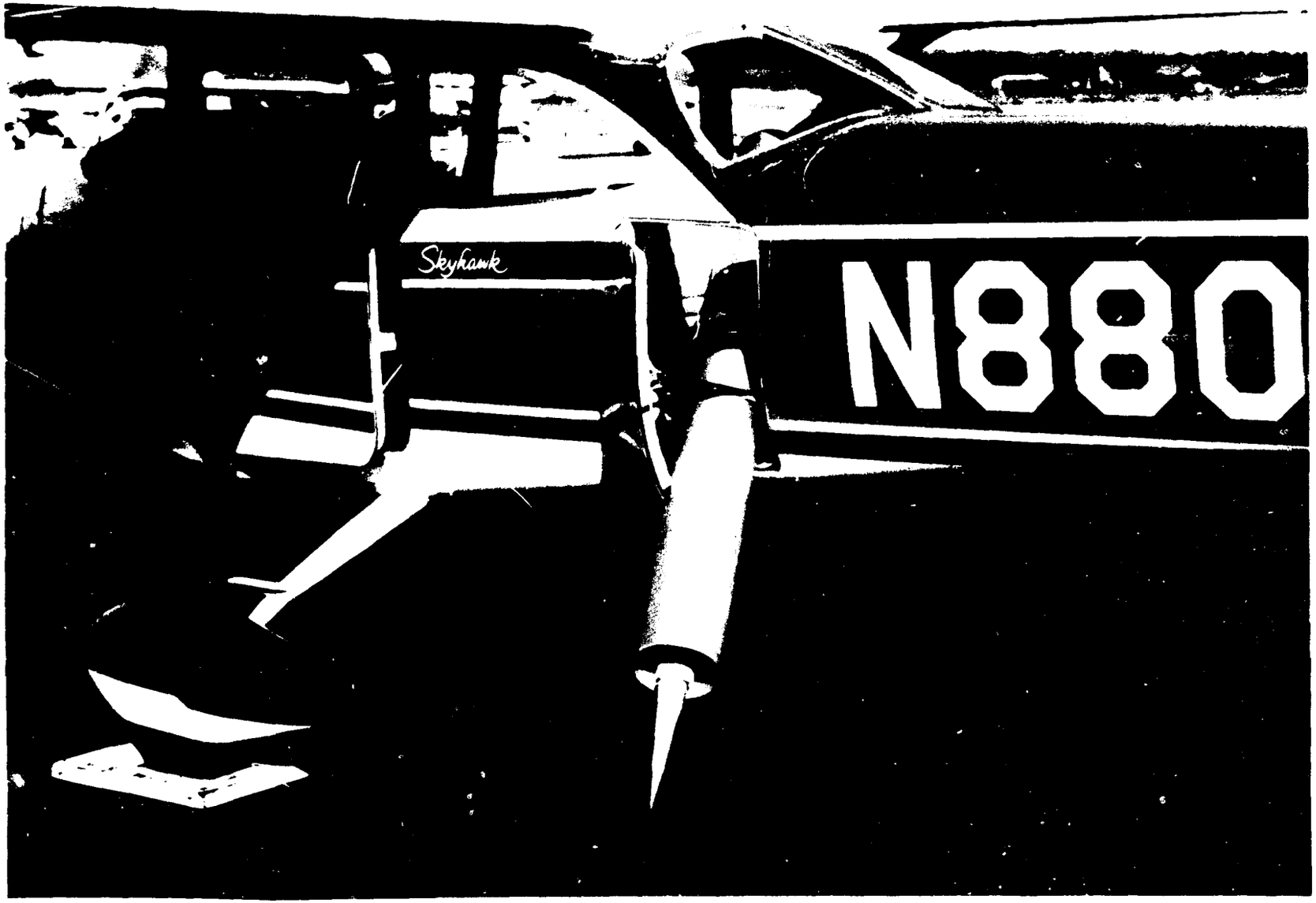

Figure 3-2. Aircraft With Deployment Vehicle Mounted in Dispensing Tube

c. Ejection tube method worked extremely well.

d. Impact shock value -200 G's.

Movies of the flight were thoroughly reviewed and several problem areas were uncovered: (1) the upper set of blades did not appear to be rotating at the proper speed; (2) the vehicle exhibited a distinct wobble during the flight; and (3) the vehicle did not appear to stabilize.

Otherwise, the vehicle as a whole worked quite well with the main problem area being the spiralling flight path of the vehicle during the first flight test. The analysis pointed out that the deployment vehicle was wobbling about the main drag blades (center of buoyancy) in a spiralling path. This was due to the gyroscopic effect caused by the two sets of rotating blades. Each set of blades has a moment of inertia (I) and a spin rate (w). When these are combined, an angular moment of inertia (Iw) is obtained. To evaluate this design, the following terms were used: L_s, M_s, I_s and W_s are the length, mass, moment of inertia and spin rate of the stabilizing blades and L_d, M_d, I_d and W_d are the same for the drag blades. In this design, $L_s = 2\ L_d$ and $M_s = 2\ M_d$ and $W_s = 2\ W_d$. To achieve a vertical flight path and eliminate the gyroscopic effects, the angular moments of inertia of each set of blades have to equal zero, thus $I_s\ W_s + I_d\ W_d = 0$. Rearranging the equation to obtain the spin rate ratio

$$\frac{W_s}{W_d} = \frac{I_d}{I_s}$$

and then substituting the values of moment of inertia into it from the equation

$$I = 1/2\ ML^2$$

we obtain

$$\frac{W_s}{W_d} = \frac{1/3\ M_d}{1/3\ M_s} \left(\frac{L_d}{L_s}\right)^2$$

and simplifying

$$\frac{W_s}{W_d} = \frac{M_d}{M_s} \left(\frac{L_d}{L_s}\right)^2$$

For the present design to have zero gyro effects, the ratio of the spin rates should be

$$\frac{W_s}{W_d} = \frac{2}{1} \left(\frac{2}{1}\right)^2 = 8$$

In actuality, the spin rate ratio which occurred was:

$$\frac{W_s}{W_d} = 2$$

and this is why the gyro effect was present and the vehicle had a wobbling spiralling flight path. To correct this condition, the lengths and masses of the blades were changed from a 1 to 2 ratio to a 2 to 3 ratio, thus,

$$L_s = 2/3\ L_d \text{ and } M_s = 2/3\ M_d$$

Using this new relationship and solving for spin rate ratio

$$\frac{W_s}{W_d} = \frac{2/3\ M_d}{M_s} \left(\frac{2/3\ L_d}{L_s}\right)^2$$

and simplifying

$$\frac{W_s}{W_d} = 3/2 \left(3/2\right)^2 = 3.4$$

If the actual spin rate $\frac{W_s}{W_d}$ is held at 2, the gyro effects can be reduced $4/8 \times 100 = 60\%$ by changing the blade proportions as stated. However, optimum conditions can be achieved by changing the pitch of the drag blades to decrease their angular velocity and by changing the pitch of the stabilizing blades to increase their angular velocity. The goal to be achieved for the spin rate ratio $\frac{W_s}{W_d}$ is 3. This information was utilized and new blades were

designed. A small scale wind machine was devised and, by using a strobe light, the actual spin rate ratio was found to be 3.

As a result, the vehicle was completely rebuilt with the following modifications:

(1) The teflon journal bearings in both sets of rotor blades were changed to ball bearings.

(2) Both sets of blades were moved closer to the top of the vehicle and a weight added to the bottom to lower the center of gravity of the vehicle.

(3) The pitch angle of the stabilizing blades was decreased in order to increase their rotational speed.

With these changes incorporated, a second flight test was conducted. The vehicle was successfully released from the tube in the airplane, but one of the lower drag blades opened in the reverse direction and locked the lower drag blades in a non-rotating position. The vehicle crashed to the ground and fractured the main body tube. These blades were reworked so that they could only open in the forward position and the main body tube was replaced.

Flight testing of the rebuilt vehicle, again instrumented only with accelerometers, was conducted during the first part of August, 1968. The main purpose of this testing was to test the vehicle's flight characteristics and its landing capabilities in the hardened ground of the test site. Since the last series of flight tests, very little rain had fallen and, as a consequence, the ground had become very dry and hard.

On 5 August 1968, three vehicles were flight tested and all of them failed to remain vertical after impact. The 12-inch long impact spear was not able to penetrate the hardened ground deep enough to hold the vehicle vertical. In addition, there were fairly high winds (20 to 30 knots) at the surface that gave the vehicle a horizontal motion in its fall to earth.

3.1.2 IMPACT SPEAR TEST AND REDESIGN

The problem of the hardened earth and horizontal movement of the vehicle due to surface winds was analyzed and a new spear was designed and fabricated. The new spear was manufactured from a 1/2 inch diameter heat-treated rod, 24 inches long.

During the next series of flight tests, these vehicles were equipped with the new impact spear. Upon impact, the spear penetrated to a depth of 20 inches, but the vehicles did not remain vertical. The spears were not strong enough to withstand the horizontal load produced by the surface winds on the vehicle and, therefore, they bent causing the vehicle to tilt at a 45-degree angle.

This problem was again analyzed and this time a spear 1-inch in diameter, 24 inches long and heat treated to a tensile stress of 300,000 pounds per square inch, was fabricated.

This new spear was successfully tested during two flight tests. These tests were conducted from altitudes of 750 feet and 1200 feet. In both cases, the spear penetrated the ground to a depth of 18 to 20 inches and the vehicle remained vertical with respect to ground after impact. A third test was made with the same spear attached to a vehicle 18 inches longer and 10 pounds heavier than the previously tested vehicles. The vehicle remained vertical during its descent but, upon impact, broke the spear into three pieces and fell over on its side. This spear was later analyzed and found to be improperly stress relieved during its heat treating process.

The larger and heavier vehicle was designed and tested since this was the size of the vehicle required to package all of the systems' electronics and power package.

3.1.3 SYSTEM DEMONSTRATION TESTS

At this point in the time schedule, the system was demonstrated to the Air Force. Although a fully implemented AMQ-27 vehicle was not air-dropped,

the system was successfully demonstrated. Two dummy loaded vehicles were successfully flight tested for the demonstration. The electronics and sensors were demonstrated as a system and the data transmitted to the central station and recorded on a strip recorder.

3.1.4 MODIFIED VEHICLE TESTS

Another flight test series was scheduled for the middle of November but, due to wet weather, it was postponed until late in the month. The test vehicles were installed in the Cessna 172 as depicted previously. The deployment vehicle was released at 1500 feet with the plane slowed to 60 mph and flying into a 25-mph wind. The vehicle fell from the plane and did a complete flip, but quickly righted itself to a 15-degree inclination as the main blades caught the air and started rotating. A spiralling flight path was achieved by the vehicle wobbling at approximately 15 degrees about it center line. Upon impact, the vehicle penetrated the ground to a depth of three feet. This depth of penetration was due to the extremely muddy ground in the impact area. Impacting the soft ground at this 15-degree angle allowed the vehicle to tip considerably (the ground could not support the vehicle) and resulted in the main rotor blades hitting the ground, damaging both themselves and the main body.

The following information was collected during flight and impact:

a. Flight time -19 seconds.

b. Target accuracy - within a 200-foot diameter of target center.

c. Ejection tube method worked extremely well.

d. Impact shock value -50 G's.

All of the modifications to the vehicle recommended as a result of the previous flights were incorporated into this flight vehicle. These changes increased the flight stability of the vehicle and, therefore, the vehicle stuck into the ground. The problem of the 15-degree wobble was analyzed and the results incorporated in future flight test models.

3.1.5 TERRAIN EFFECTS ON VEHICLE IMPACT

During this phase of the program, four AN/AMQ-27 vehicles were fabricated, instrumented with accelerometers to measure impact landing, and air dropped. Twenty drop tests were made from aircraft operating between 750 and 1000 feet in altitude over terrain that exhibited different soil characteristics.

The flight test program was initiated with the successful deployment of five vehicles. Four of the vehicles were dropped from an altitude of 1000 feet with the plane slowed to 60 mph. The vehicles were loaded into the plane with the spear pointing towards the sky (this is upside down compared with previous vehicle deployment) so that the sensor end of the vehicle would exit first from the deployment tube. This method of deployment eliminated the complete flip of the vehicle (observed on previous tests) as the blades caught the air. The vehicle emerged from the tube, the blades caught the air and a verticle flight path was achieved on its flight towards the ground. Each vehicle impacted the earth at approximately 45 mph and developed about 65 G's of impact shock. The depth of penetration into the earth was approximately 36 inches and the vehicle remained verticle to within 5 to 10 degrees of a plane normal to the ground. The soil was saturated with water and, therefore, quite muddy but held the impacted vehicles very well. In fact, the vehicles had to be dug out with a shovel.

The last flight vehicle was loaded into the plane in the same manner and was deployed from an altitude of 1000 feet with the plane flying at 125 mph. The vehicle emerged from the deployment tube but, as the blades caught the air, the blades deformed to a permanent set of 30° above a horizontal plane. This blade deformation did not affect the vehicle's flight path, as a verticle flight path was achieved. The vehicle drifted from the target area and landed on a rock covered hill. It penetrated the rocky ground to a depth of 6 inches and remained verticle to within 5 to 10 degrees of a plane normal to the ground. This penetration was not sufficient to withstand a

50 mph wind because the vehicle was easily removed. This particular vehicle impacted the earth at 38 mph with a loading value of 65-70 G's.

The first four vehicles proved that the vehicle design was functional in this type of terrain. The flight path was proper and stability was achieved at impact with a respectable impact shock load. The last flight was experimental to test the present vehicle's aerodynamic characteristics in a more severe environment. The additional wind loading induced into the blades at this greater deployment speed was enough to fracture the blades in the root section. This information will be utilized in the study part of this program to evaluate the present blade root section and suggest improvements in its design.

The rainy weather during February made it impossible to conduct any flight tests. An effort was made to find different test sites so that testing may begin during the month of March. The five test vehicles were assembled and ready for the flight testing program.

The weather cleared in March and the flight testing program resumed. The test site chosen for this series of tests was a rocky hill covered with brush and cactus. A total of six vehicles were assembled for this flight test. Five of the vehicles were loaded into the plane with the spike pointing up and released from an altitude of 1000 feet with the plane slowed to 60 mph. All of the vehicles quickly stabilized after being released from the deployment tube and achieved a vertical flight path as they fell to earth. Three of the vehicles hit rocks with such force upon impact (150-200 G's) that the main body tube buckled and sheared in half about a foot above the impact spear. One of the other vehicles impacted the earth at 200 G's and the spear penetrated to a depth of 24 inches. The vehicle remained intact and in an upright position. The other vehicle impacted at 85 G's and penetrated to a depth of 12 inches. It also remained intact and vertical to the ground. Ground winds of 20 to 30 mph were blowing during the above tests.

The results of these flight tests indicated a high vehicle mortality rate can be expected if the drop area is rocky. The vehicle's impact spear cannot successfully penetrate rocks and, as a result, the achieved energy is dissipated in shearing the body tube. The vehicles that remained intact and achieved penetration had received high impact shock loads. These shock loads will have to be isolated from the vehicle's payload (sensors and electronics) by using the proper materials for shock isolation when these items are ultimately packaged into the flight vehicle.

The last flight test was conducted with a modified vehicle. The upper stabilizing blades were shortened approximately 6 inches so that, in a folded position, the blades did not extend over the lower drag blades. The vehicle was loaded into the plane in the same way as the other five. The vehicle was released from the plane at an altitude of 2000 feet with the plane slowed to 60 mph. The vehicle quickly stabilized and achieved a vertical flight path as it fell to the ground. The drop area was composed of fairly hard ground but the spear penetrated to a depth of 36 inches holding the vehicle in an upright position. The impact loading was approximately 65 G's This test indicated that the upper stabilizing blades could be shortened without affecting the vehicle's flight path and impact stability.

3.1.6 INSTRUMENTED VEHICLE DEMONSTRATION

Prior to the demonstration, the AMQ-27 electronics and sensor packages were checked out. Except for the humidity and precipitation channels, which had been damaged prior to the demonstration flights of last August, all the sensor and RF subsystems were operational. A final calibration of the receiver was also performed. Unfortunately, during final integration of the sensor and electronics packages with the vehicle, excessive voltage was applied to the receiver thereby damaging it. The system packaged into the flight vehicle was ready for the drop test.

The flight testing of the vehicles was conducted at the Moorpark test site. A Cessna 172 was the deploying aircraft flying at an altitude of 1000 feet and slowed to 60 mph prior to releasing the vehicles. Four vehicles were assembled for this test; two dummy vehicles, one with the self-extendible antenna only and, finally, the fully instrumented vehicle.

The first vehicle quickly stabilized after being released from the deployment tube and achieved a vertical path as it fell to earth. It missed the target area by some 300 feet and landed 3 feet from the edge of the road. It impacted to a depth of 36 inches in the sandy soil and remained vertical.

The second vehicle duplicated the flight of the first one. It also missed the target area by some 250 feet and landed in a rocky hillside splitting a rock and penetrating to a depth of 20 inches. The vehicle remained vertical after impact but the self-deployable antenna buckled and collapsed due to the large translation forces it received when the vehicle impacted the ground. This can be corrected by designing a delayed release mechanism for the antenna. The third vehicle was a repeat of the previous vehicle's flight characteristics. It landed within 45 feet of the target zone, penetrated to a depth of 24 inches and remained vertical.

The fourth vehicle was the fully instrumented version and it seemed to take a little longer to stabilize into a vertical flight path. It landed within 150 feet of the target, penetrated to a depth of 24 inches and remained vertical. The horizontal acceleration forces experienced by the vehicle during its impact were much greater than anticipated. The vertical deceleration of 65 G's was within the design specification. Consequently, the large horizontal forces caused a mechanical failure of the upper part of the sensor package. This destroyed the temperature, wind speed and direction sensors as well as the inoperative humidity and precipitation transducers. Also, the antenna was damaged in the same way as the one tested earlier.

The vehicle was brought back to Packard Bell to check out the sensor and RF electronics. Within the vehicle, the compass broke loose from its mounting and severed some of its wires. The remaining electronic modules within the vehicle suffered no damage from the drop. These were checked out and found to be functional along with the RF electronics.

3.1.7 DESERT TEST RESULTS

Arrangements were made to conduct vehicle flight tests in a dry lake bed at El Mirage, California, in the latter part of June. This site tested the vehicle's capability of landing and remaining erect in sand. The flight vehicles were assembled and two of these vehicles contained the delayed antenna release mechanism mounted on them.

On the day the tests were to be conducted, ground winds were blowing between 40 and 60 mph, (i.e. sand storm conditions). The ground crew met the airplane and directed the pilot to land the plane on the dry lake bed near the test site. The wind was still blowing while the airplane was being loaded for the first flight test. The plane was airborne in less than 100 feet and climbed to an altitude of 1,000 feet to release the first flight vehicle. (This vehicle was instrumented.) The flight vehicle was released, caught the air and quickly righted itself for a vertical flight path to the ground. From 1,000 to 500 feet, the flight vehicle fell with very little horizontal movement, while from 500 feet to impact, the flight vehicle increased its horizontal movement tremendously. The vehicle hit the ground at an angle of 15 degrees off a vertical plane normal to the ground. The vehicle's impact force broke the spear and sheared the main body tube into two pieces. It was estimated that the horizontal speed of the vehicle was 40-50 mph at impact. Another flight vehicle was loaded into the plane and, when released, experienced the same conditions as the one in the previous flight test. Further testing was halted to see if the wind would stop blowing and, therefore, produce conditions more favorable to flight testing. Since the wind was still blowing after a considerable period, the remaining flight tests were cancelled.

3.1.8 ANTENNA DEPLOYMENT TEST

The flight testing was conducted on the 15 July 1969 at the Moorpark test site. A Cessna 172 was the deploying aircraft flying at an altitude of 1000 feet and slowed to 60 mph prior to releasing the vehicles. Three vehicles were assembled for this test, one dummy vehicle and the other two had the antennas with the delayed release mechanisms mounted on them. It was a clear day with a 5-10 mph ground wind.

The first vehicle (without an antenna) quickly stabilized after being released from the deployment tube and achieved a vertical path as it fell to earth. It hit a rock and the main body tube sheared into two pieces.

The second and third vehicles (equipped with antennas) duplicated the flight of the first one. They both hit close to the target area and penetrated to a depth of 24 plus inches. The antenna devices survived the 85 G impact landing and released the antennas after a 60-second delay. The cassettes hung up in their release cycles but a slight tap started it again. The stem part of the antennas had been used many times previously and had developed kinks in certain areas thereby causing the cassettes to hang up on them during their release cycles.

3.2 COMMUNICATIONS SYSTEM TESTS

3.2.1 SYSTEM RANGE TESTING

The following parameters for the AMQ-27 unit to base station RF link were important factors in determining the validity of the design parameters; namely,

a. Signal strength vs distance

b. Ambient noise level

c. Signal to noise level

d. Geographic effects on signal strength

The terrain profile graphs presented here aided in showing the topography of the transmission paths for different locations of the range testing program. The charts clearly indicated the direction of the horizontal azimuth for each location with respect to the base station.

In Figure 3-3 it can be seen that the transmission path was obstructed by a peak 700 feet high with respect to the AMQ-27 unit located in Sherman Oaks. This at first, it seemed, might not present any problem, assuming that knife edging would force the signal downward. Knife edging probably did occur, however, since the base station was located in a valley and the signal overshot the last mile or so. What signal was left was consumed in the shadow loss. The beam antenna was pointed directly at the AMQ-27 unit at that time. Scanning the horizon with the antenna, the signal was then picked up on an azimuth almost due north. After an analysis of a terrain map, it was concluded that the signal was bounced back from a mountain peak of about 8,000 feet elevation, 40 miles north from where the AMQ-27 unit was located.

In Figure 3-4 there was almost a line of sight transmission path. In this case, there was no problem in detecting the signal when the antenna was pointed directly at the AMQ-27 unit located in Northridge.

Test number 3 from test area number III (Figure 3-5) was made to ascertain the validity of space wave propagation when the curvature of the earth is neglected for this distance. The signal strength should be inversely proportional to the distance. There were other losses however, but the signal strength was still compatible to the receiver sensitivity requirements.

3.2.2 FUNCTIONAL TESTING

The RF system was tested at close range, with the tests showing that the unit responds to interrogation commands. Figure 3-6 shows the base station discriminator output. The first part shows the presence of

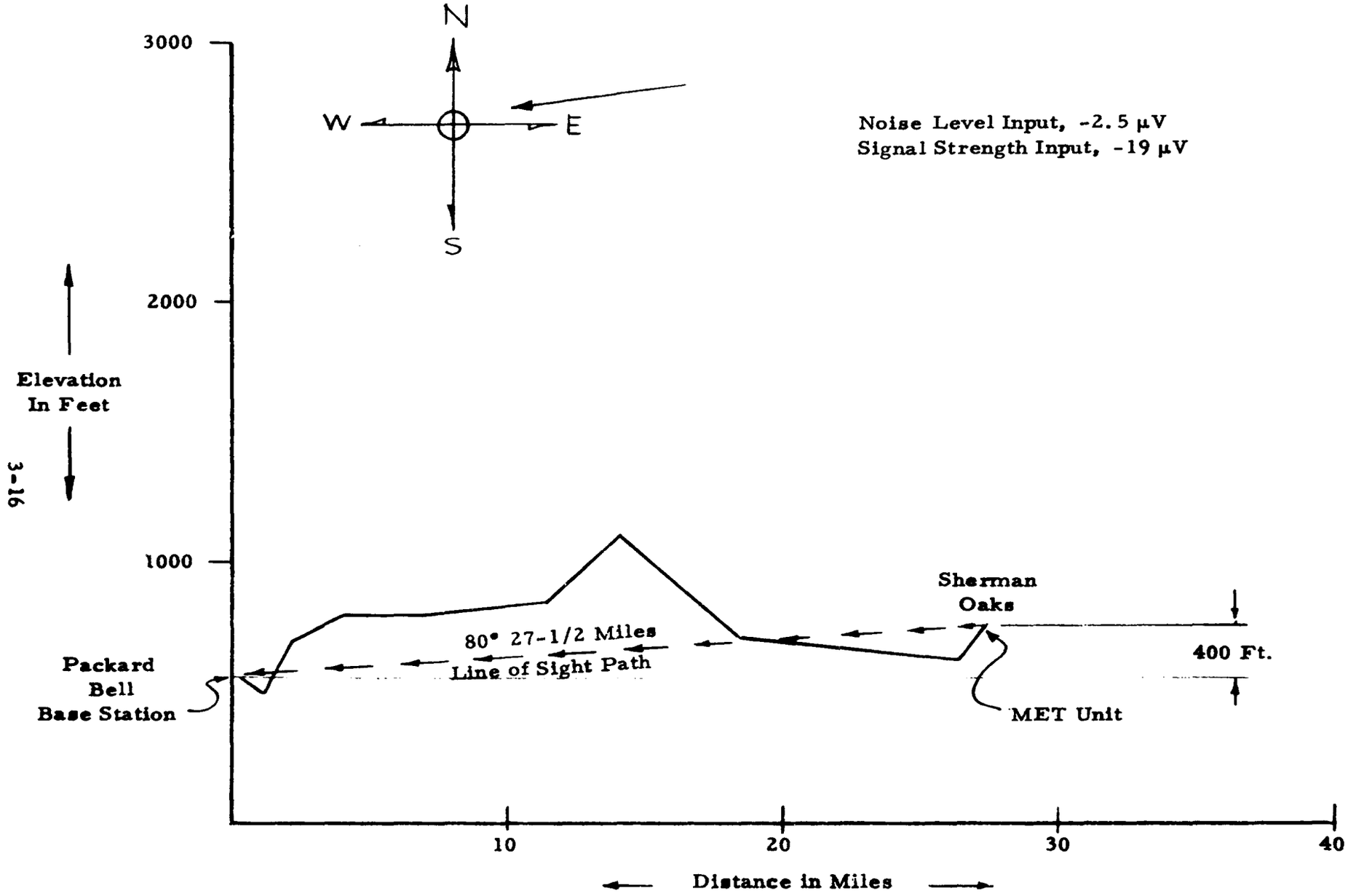

Figure 3-3. Terrain Profile of Test Area Number 1

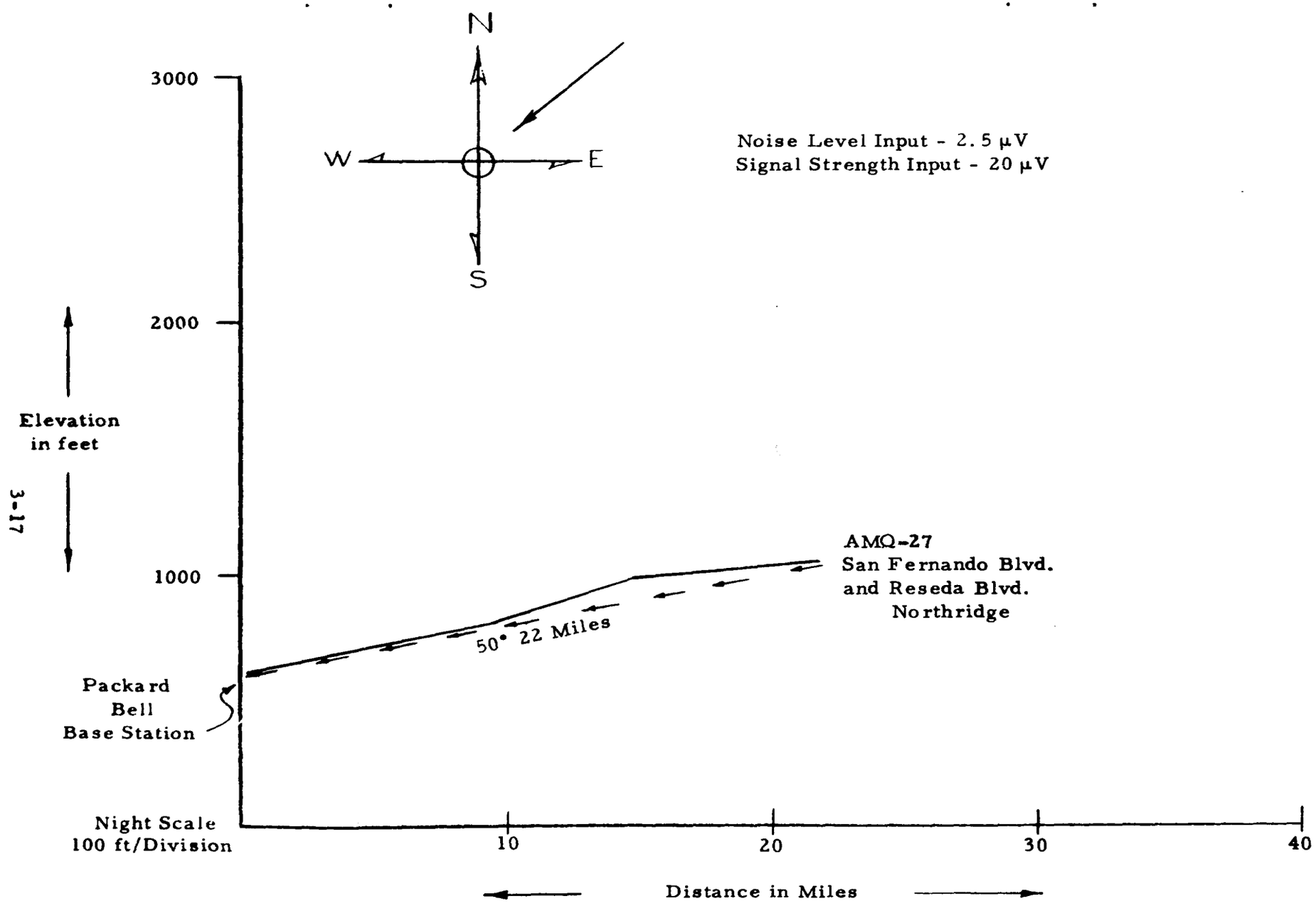

Figure 3-4. Terrain Profile of Test Area Number 2

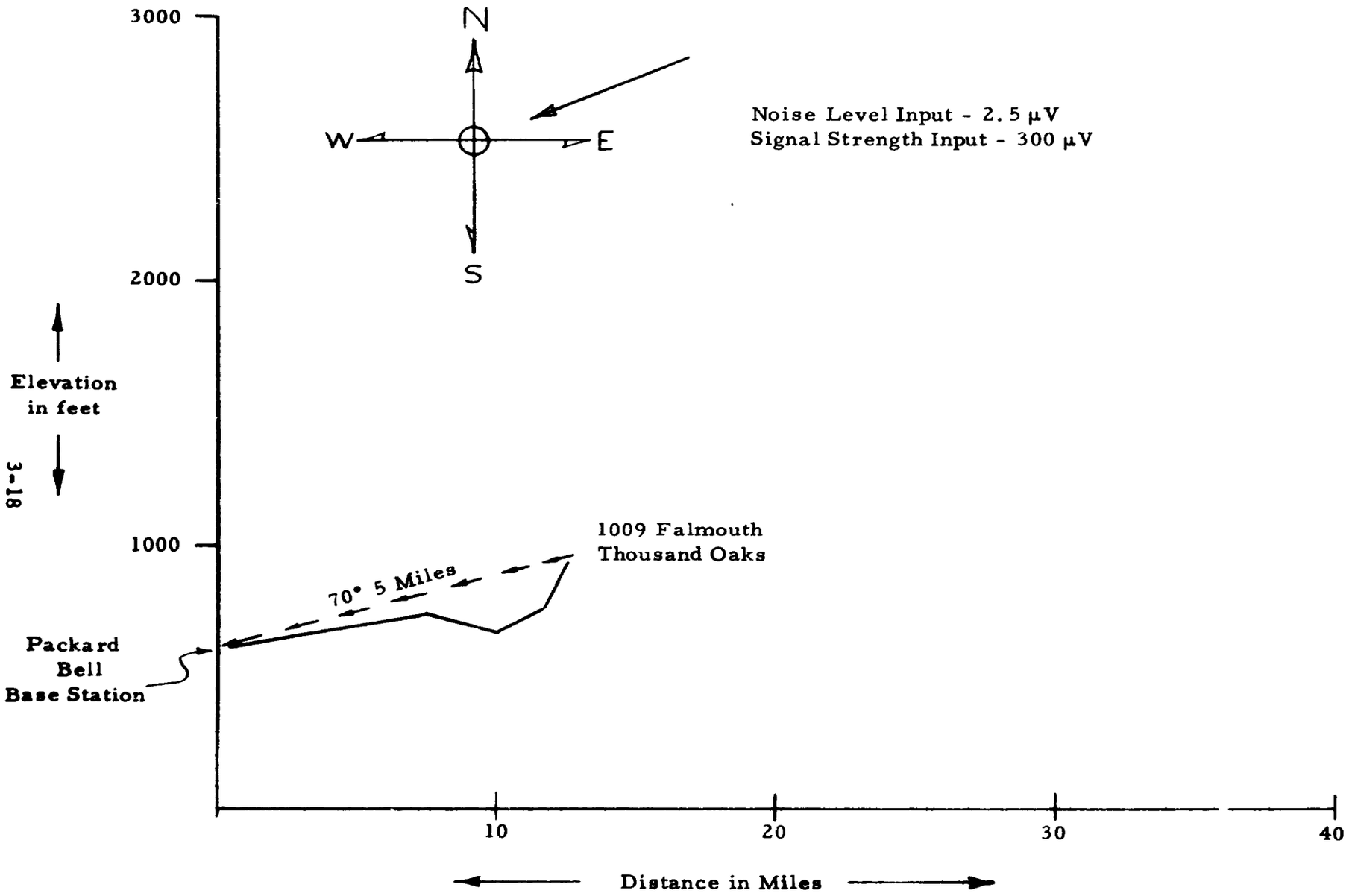

Figure 3-5. Terrain Profile of Test Area Number 3

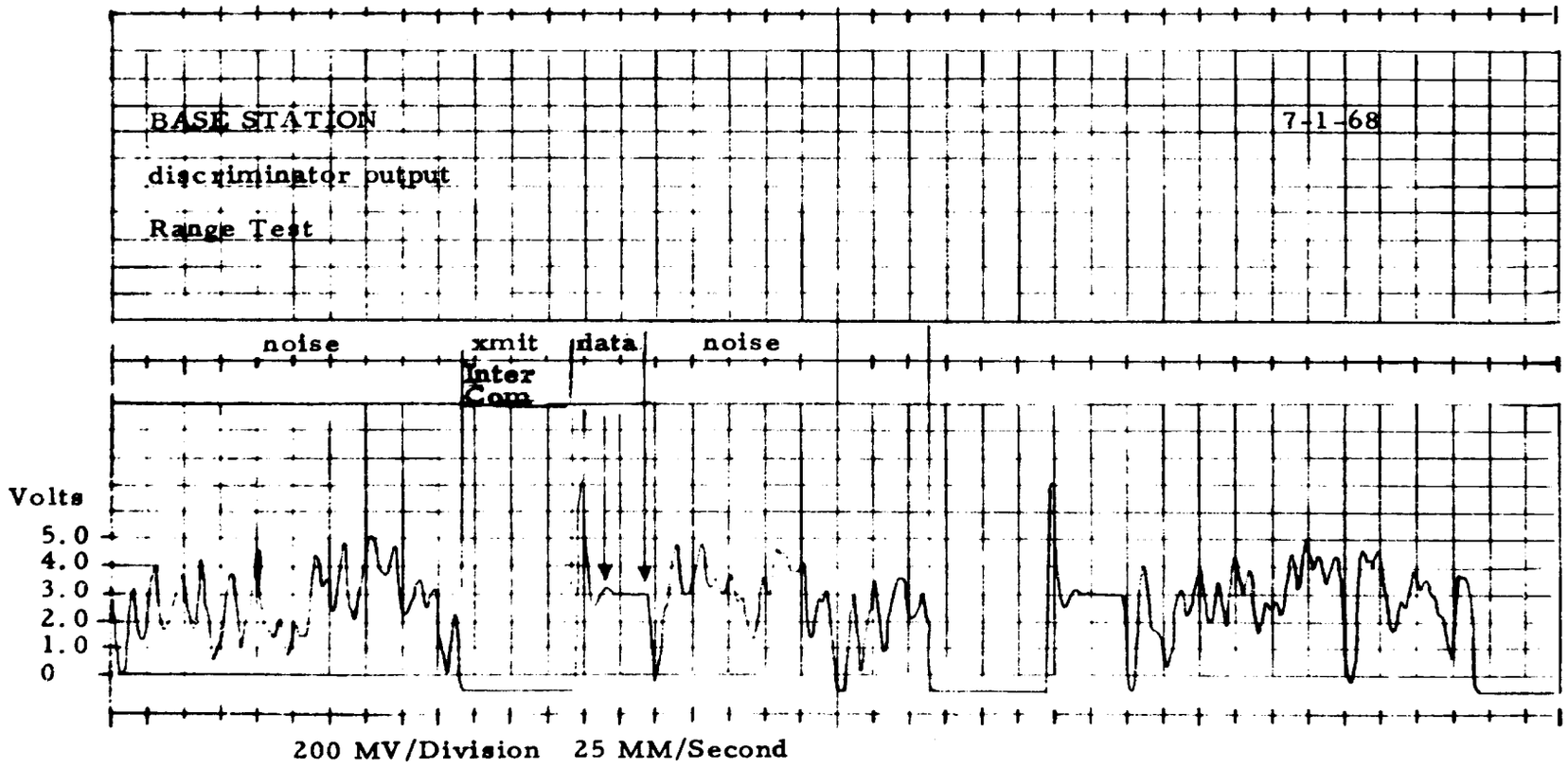

AMQ-27 Unit Output Power 100 MW with 30 DB Insertion
at a Distance of 0.5 Mile

Figure 3-6. Base Station Discriminator Output

noise prior to an interrogate command. During an interrogate command, the base station receiver power was turned off making the output of the sub-carrier discriminator go to some negative value due to lack of signal. When the interrogate command period was over, the receiver power was then turned back on receiving the data, indicating that the AMQ-27 unit had received an interrogate command and had responded with data. At the end of the data period, there was no longer quieting and the receiver again saw the narrow-band noise until the next interrogate command had been received.

3.2.3 RANGE TESTS

The range testing program was successful in proving the system sensitivity requirements under worst case conditions, i.e., that the conductivity of the ground in this area was very poor. Also the topography of the terrain which was selected for the testing was worse than would normally be expected. An aeronautical navigation map was used to select the test range. This type of map was ideally suited for selecting topographical test sites because of the great detail given to terrain elevations, thus allowing one to draw good terrain profiles for a range testing program.

Figure 3-7 shows the locations which were selected for the range tests. The terrain profiles shown in Figures 3-8 through 3-12 with respect to the base station show the transmission path profile again with respect to the line of sight path. The signal strengths indicated show that, for a closer range with less peaks, the signal was somewhat weaker. However, the signal could not be picked up except by aiming the base station antenna directly at the AMQ-27 unit. Knife edging and shadow loss and the earth propagation losses contributed to the weaker signal. The other locations which were further away were not necessarily that much better. In order to pick up the signal, the base station antenna had to be pointing directly at the AMQ-27 unit. The signal in this case was extremely weak. Turning the antenna away from the AMQ-27 unit, the signal was then picked up in the direction of one of the higher peaks surrounding the location of the AMQ-27 unit. This indicated that the

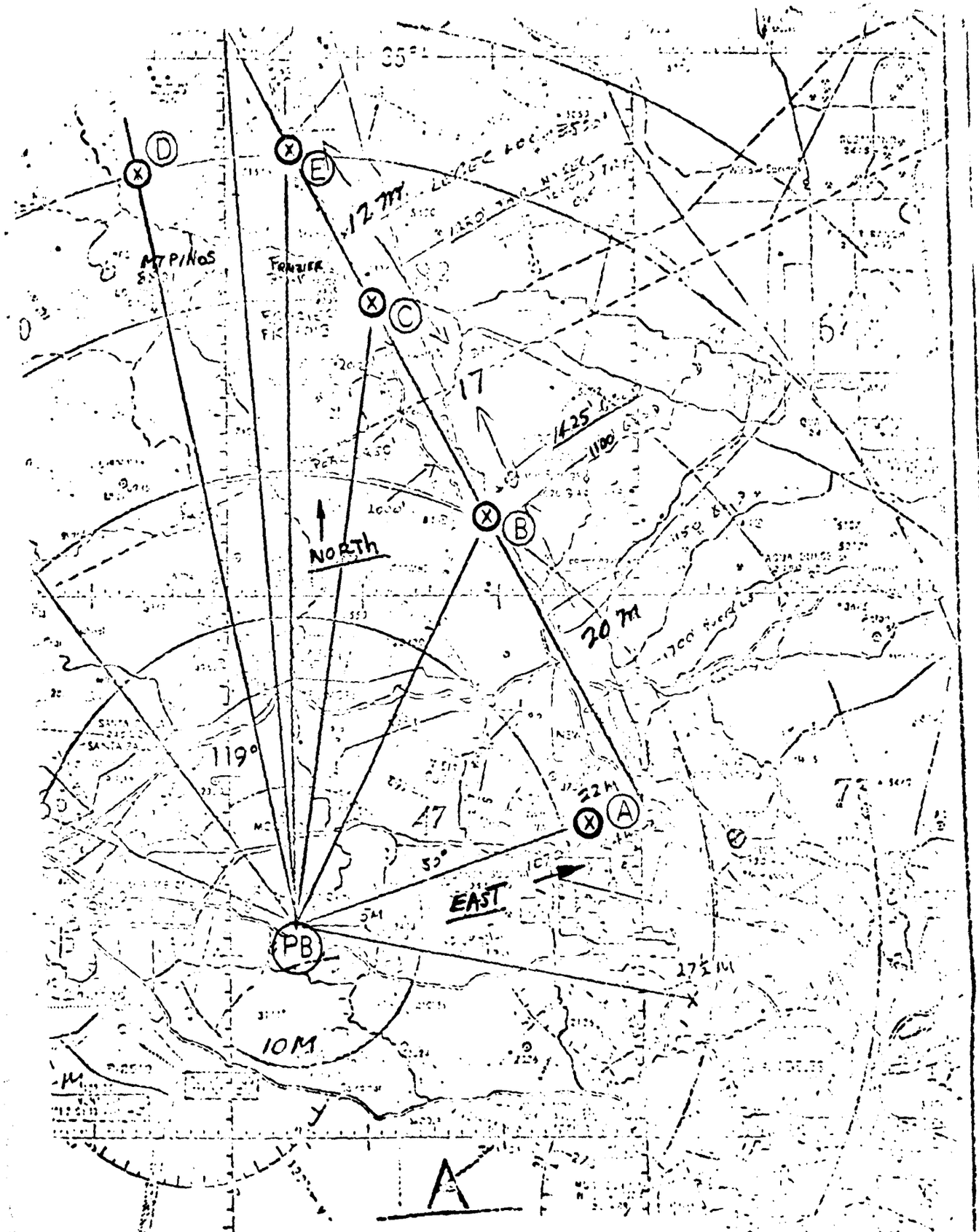

Figure 3-7. Location of Selected Range Sites

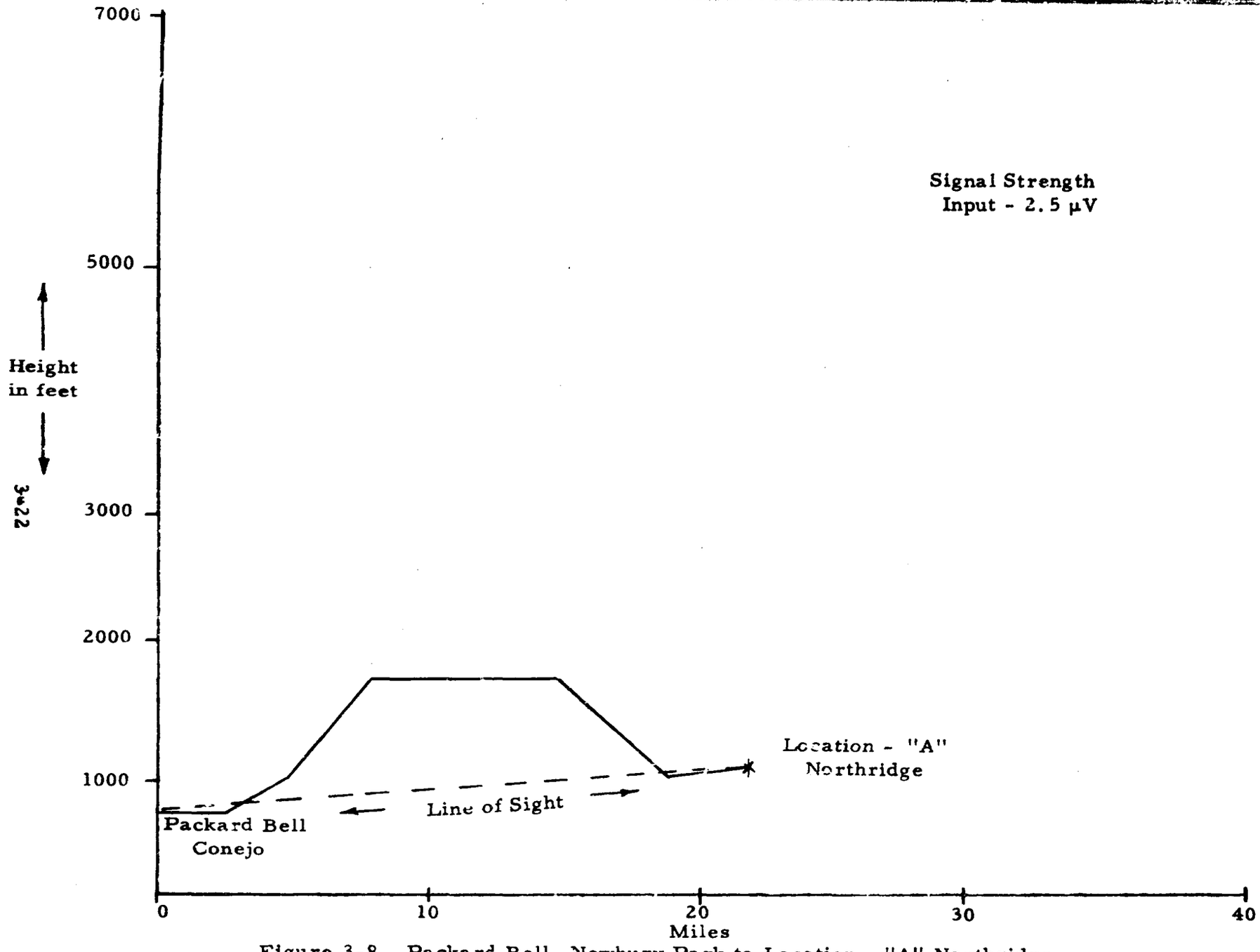

Figure 3-8. Packard Bell, Newbury Park to Location - "A" Northridge

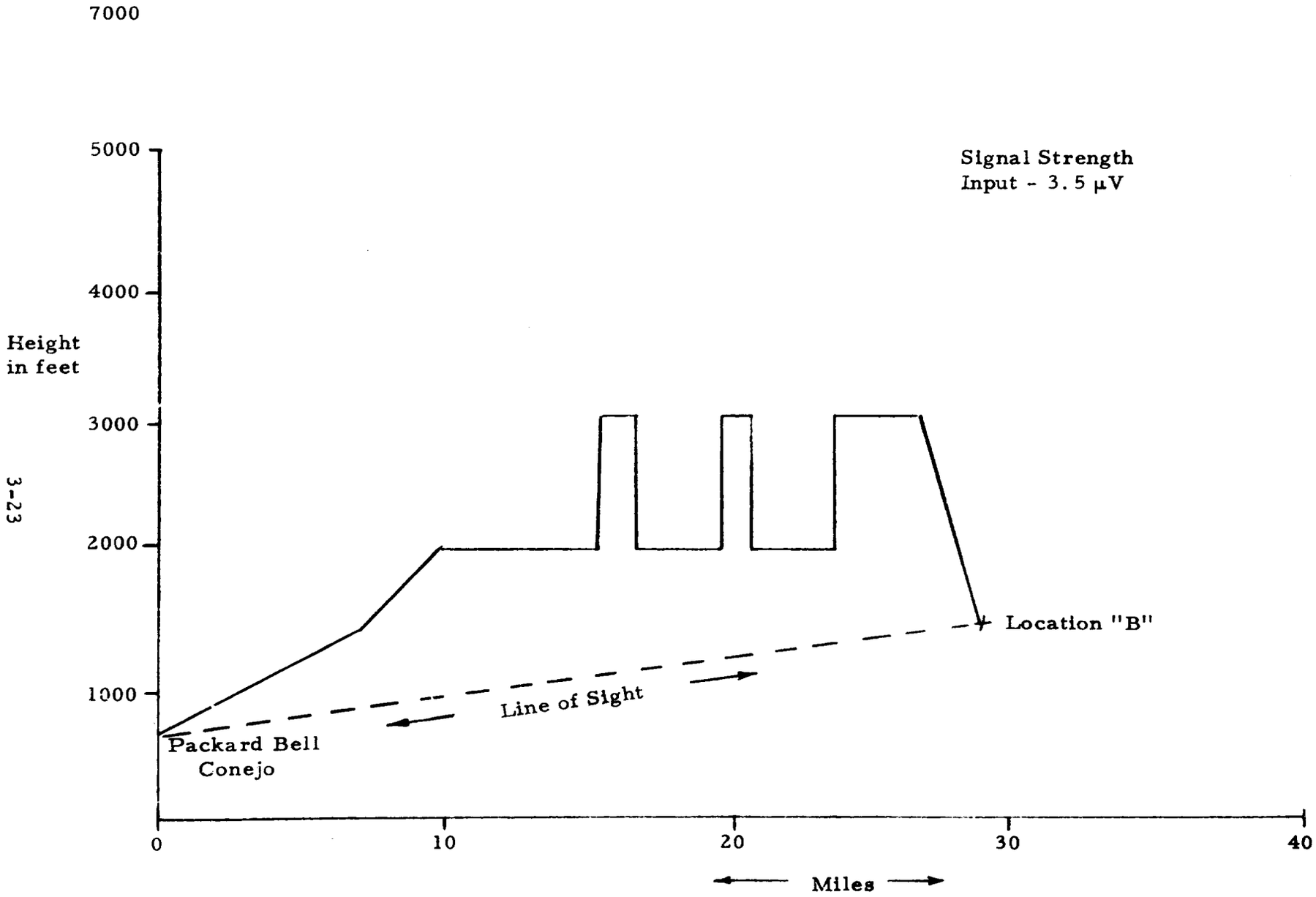

Figure 3-9. Packard Bell, Newbury Park to Location - "B" Near Castaic

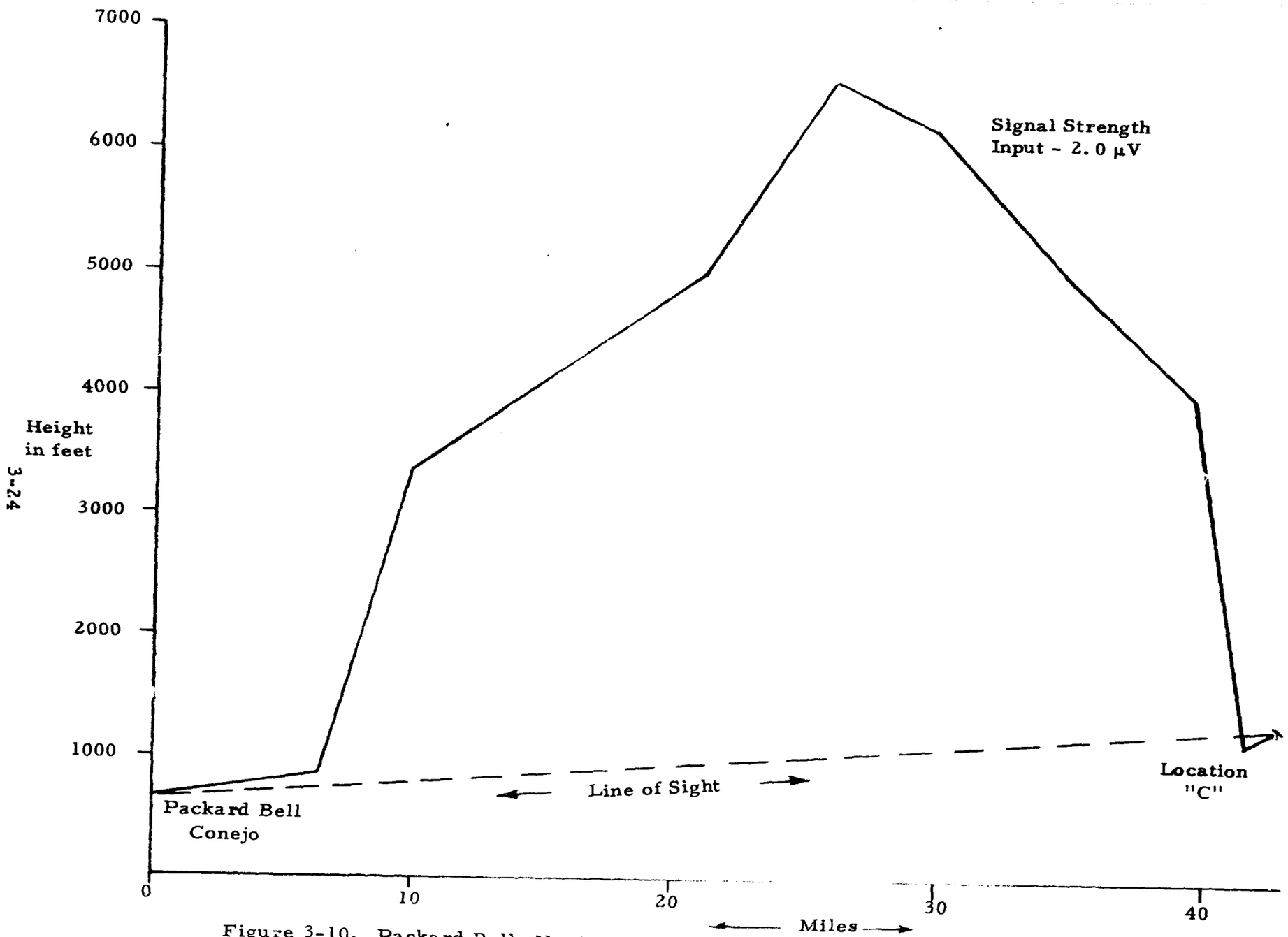

Figure 3-10. Packard Bell, Newbury Park to Location - "C" Near Gorman

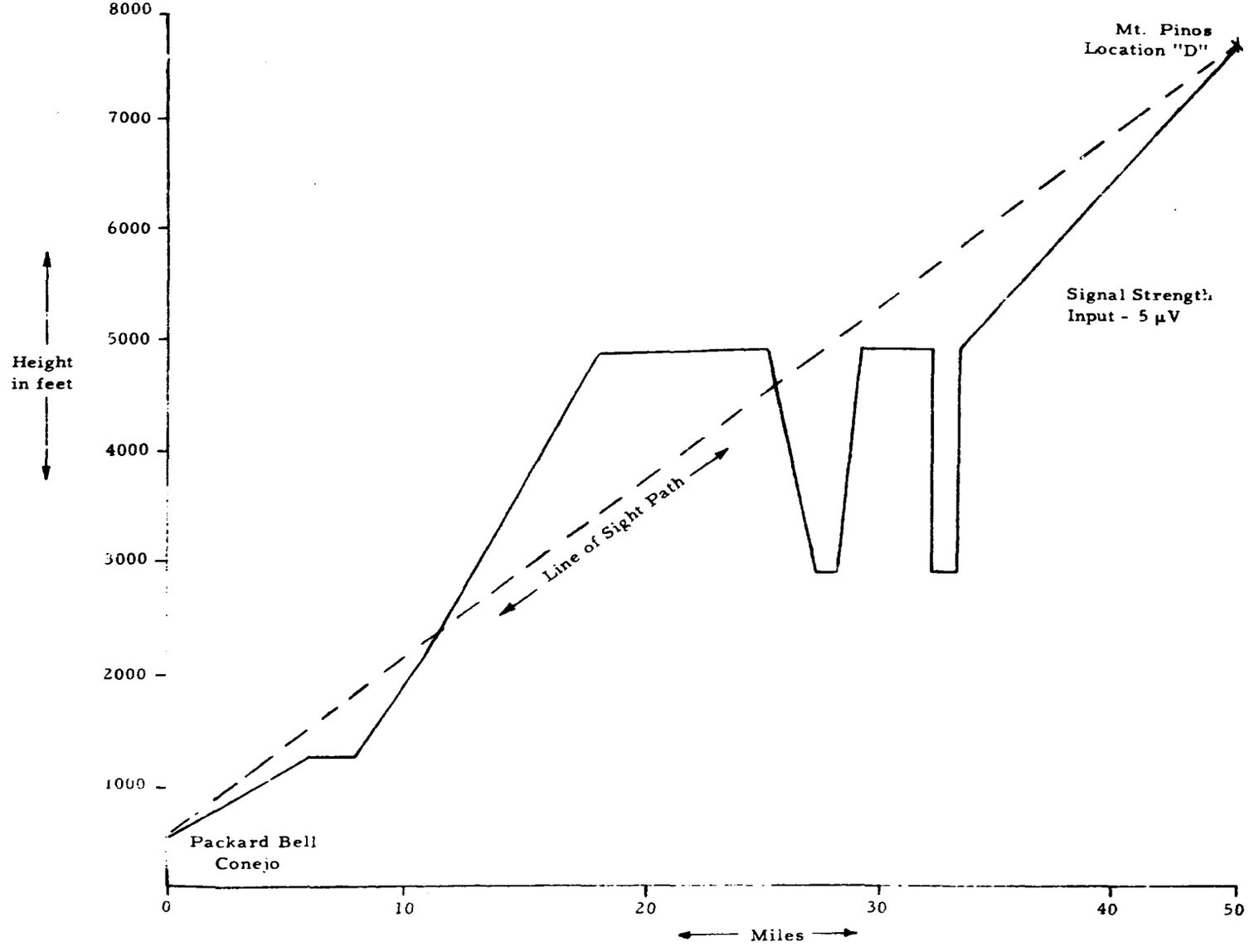

Figure 3-11. Packard Bell, Newbury Park to Mt. Pinos Location - "D"

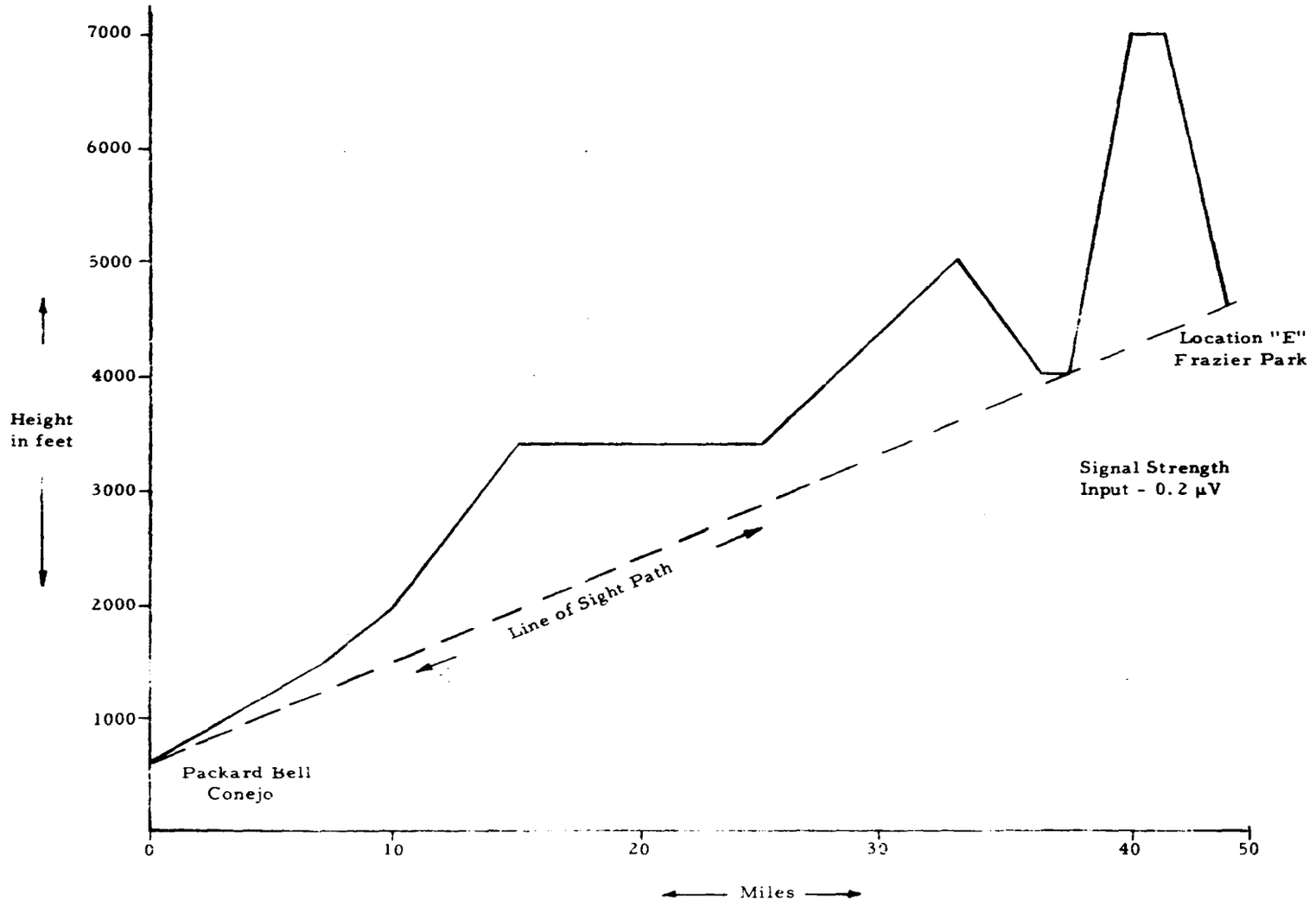

F. ure 3-12. Packard Bell, Newbury Park to Frazier Park Location - "E"

bounce from the higher peaks effectively cleared the terrain in front of the AMQ-27 unit. The signal obtained sufficient surface clearance when the free space loss became a fraction of the surface loss. The free-space loss is given by the expression

$$\delta = 33 + 20 \log_{10} f + 20 \log_{10} d$$

where:

f = frequency in MHz

d = distance in miles

and surface loss, or earth loss is then:

$$\delta = 144 - 20 \log_{10} h_1, h_2 + 40 \log$$

where:

h_1, h_2 = antenna heights, ft.

d = distance in miles

The formula for earth plane loss includes the term $40 \log_{10} d$, which increases the attenuation vs distance twice as fast as the free-space case. This proves that the free-space loss between antennas is controlling, as long as the 0.6 Fresnel zone clearance from obstructions is maintained around the line of sight path. The amount of clearance required in Figure 3-13 is given by the formula:

$$H = 1.316 \sqrt{\frac{D_1 D_2}{f(D_1 + D_2)}}$$

where:

H = clearance height

f = frequency in MHz

D_1, D_2 = distance in miles

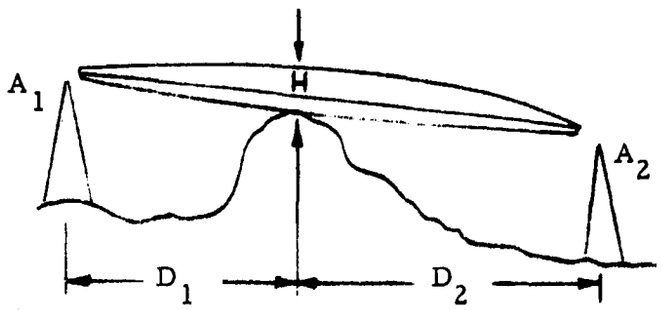

Figure 3-13. Free Space Transmission

This information indicates that the geographical location of a base station is pretty well defined in terms of tactical deployment of AMQ-27 units with respect to a base station. Additional tests were made at the demonstration site and these are shown in terrain profile chart, Figure 3-14.

3.2.4 SUBSYSTEM CALIBRATION

The data shown in the following curves were taken with an RF link to determine the accuracy of the input modulating voltage to the FM transmitter in the AMQ-27 unit.vs the discriminator output at the base station. Figure 3-15 shows the input to the subcarrier oscillator (SCO) vs discriminator output. Figure 3-16 shows the SCO dc input vs output frequency characteristics of the SCO in the AMQ-27 unit. The average accuracy of the discrimination output is 0.2% or best straight line.

3.3 SENSOR TESTS

All sensor signal conditioner prototypes have been fabricated and tested. The prototype modules have all been potted in foam potting compound.

The sensor head assembly and drag cylinder have been shock tested to 75 G's. Some reinforcement of the drag cylinder was required after earlier tests showed cracks in the polystyrene foam webbing. The present design withstood a 75 G vertical impact landing load. All sensors and signal conditioners were integrated with the multiplexer and transmitter subsystems.

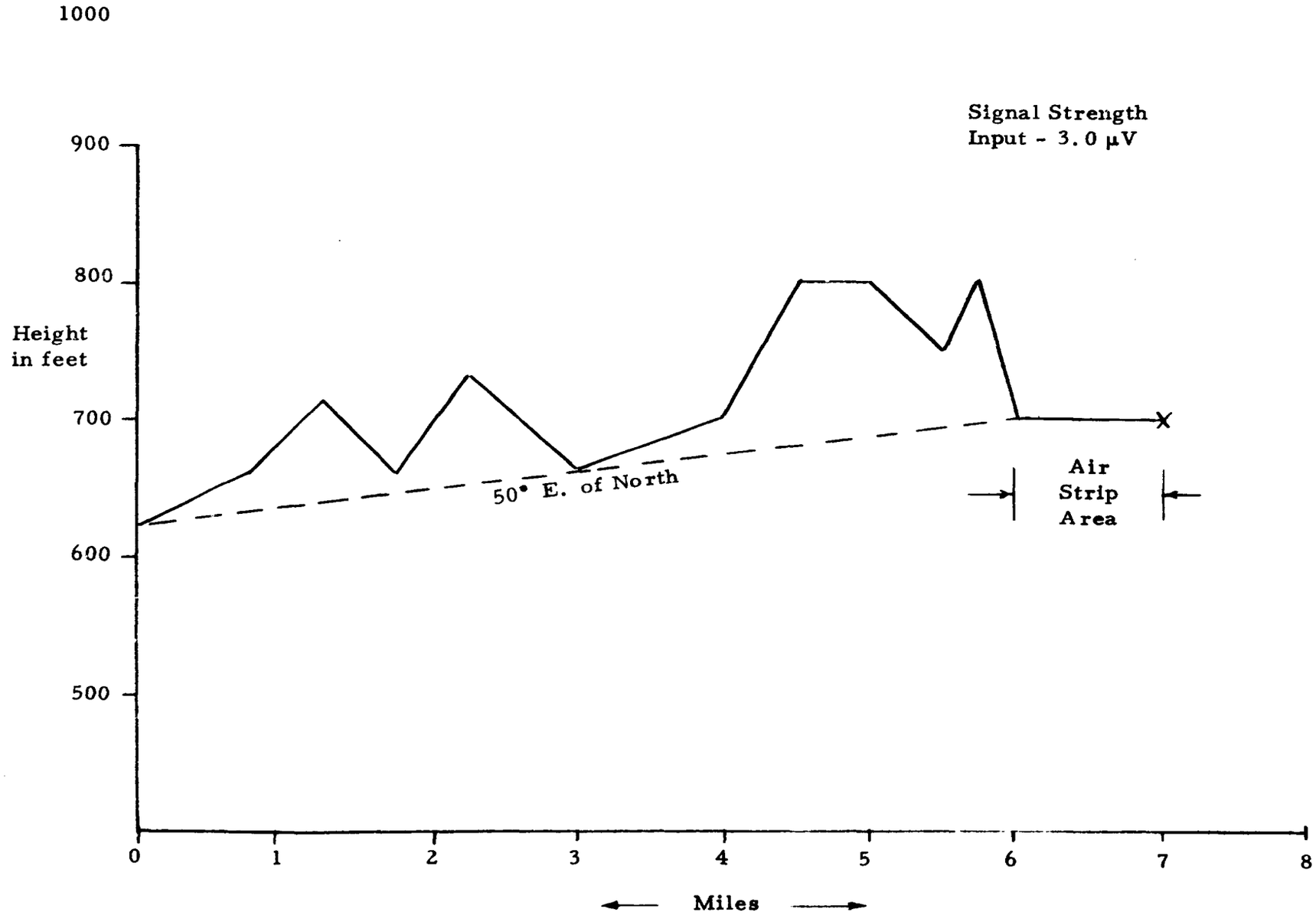

Figure 3-14. Packard Bell, Newbury Park to Everett Airport

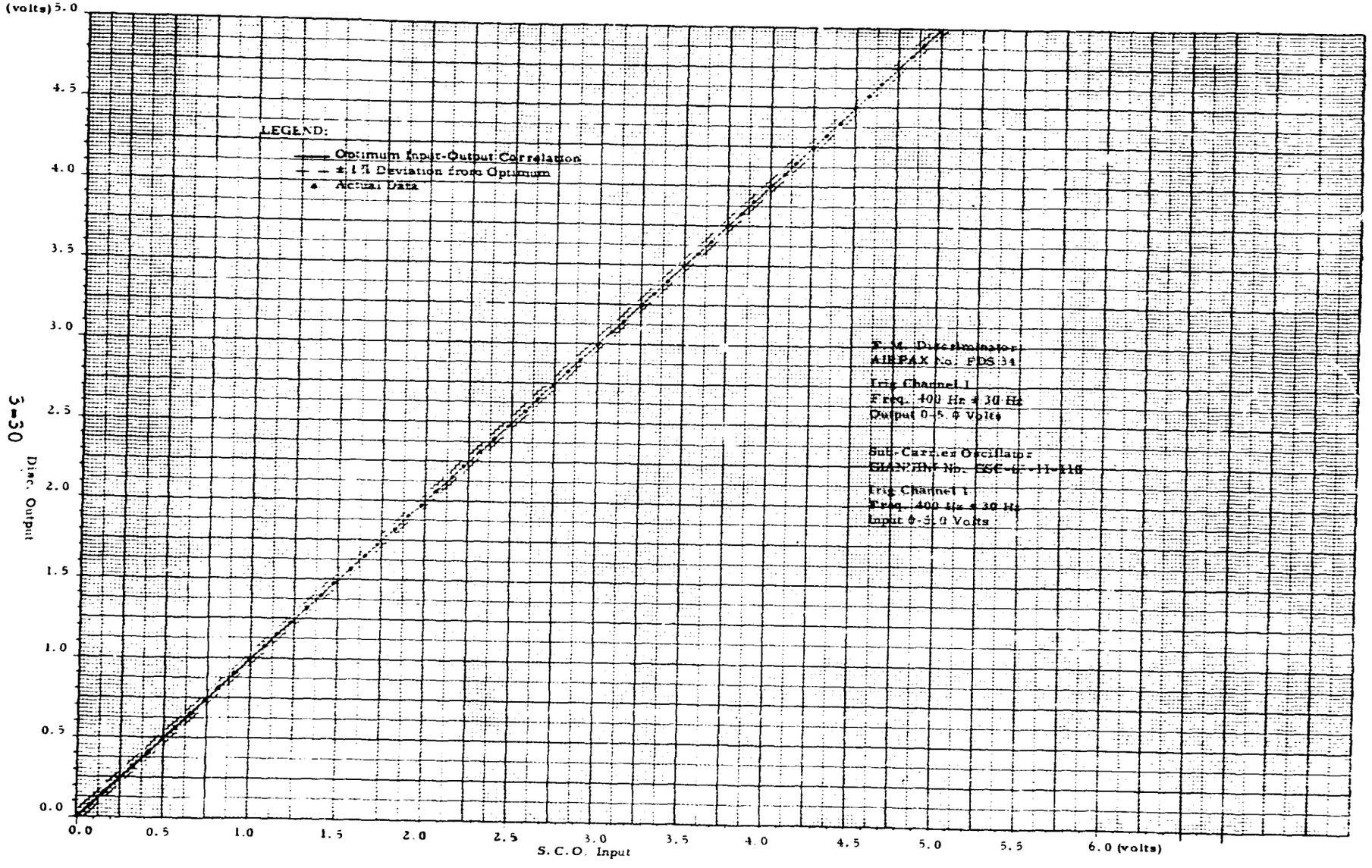

Figure 3-15. Base Station Discriminator Output vs Subcarrier Oscillator Input (Input Coupled to Output via RF Link (41 MHz) (7/30/68)

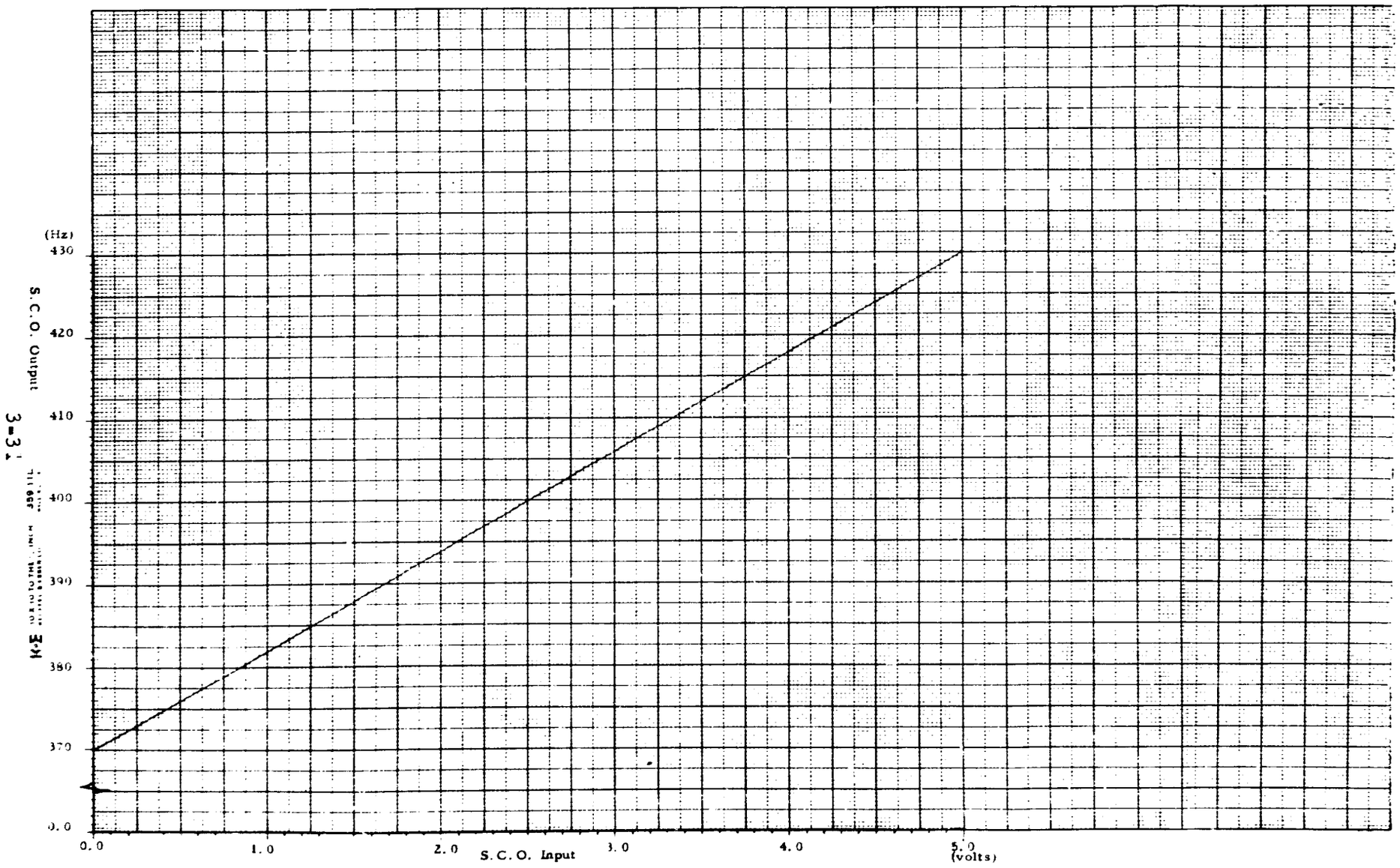

Figure 3-16. Subcarrier Oscillator Input vs Output (7/30/68)

3.4 FINAL TESTS

The following tests were accomplished:

a. AMQ - 27 communications system integration and test.

b. Total communications system integration and test.

c Demonstration of RF command link and data link.

System integration and test of the AMQ-27 included the items indicated in Figure 3-17. The data input lines were simulated DC input levels corresponding to actual levels coming from all of the signal conditioners. The system was then calibrated and rechecked periodically to determine stability of the system.

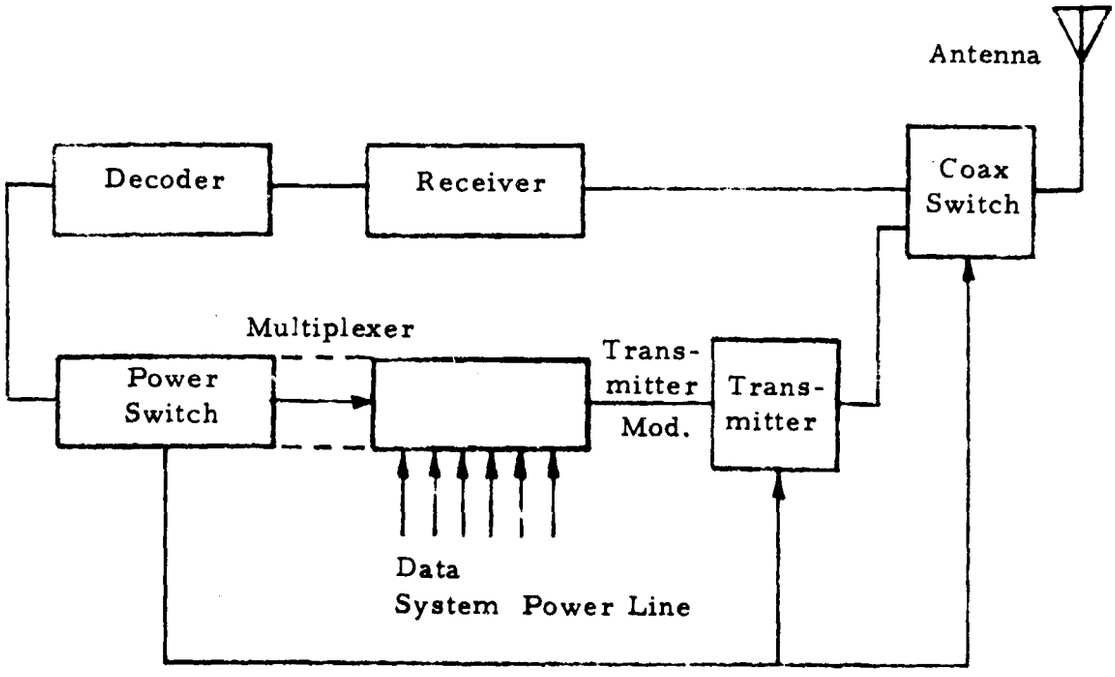

Figure 3-17. System Block Diagram

Figure 3-18 indicates a typical test configuration and measured parameters for an AMQ-27 to base station operation. Figure 3-19 shows the various locations and terrain profile where successful system operation was demonstrated.

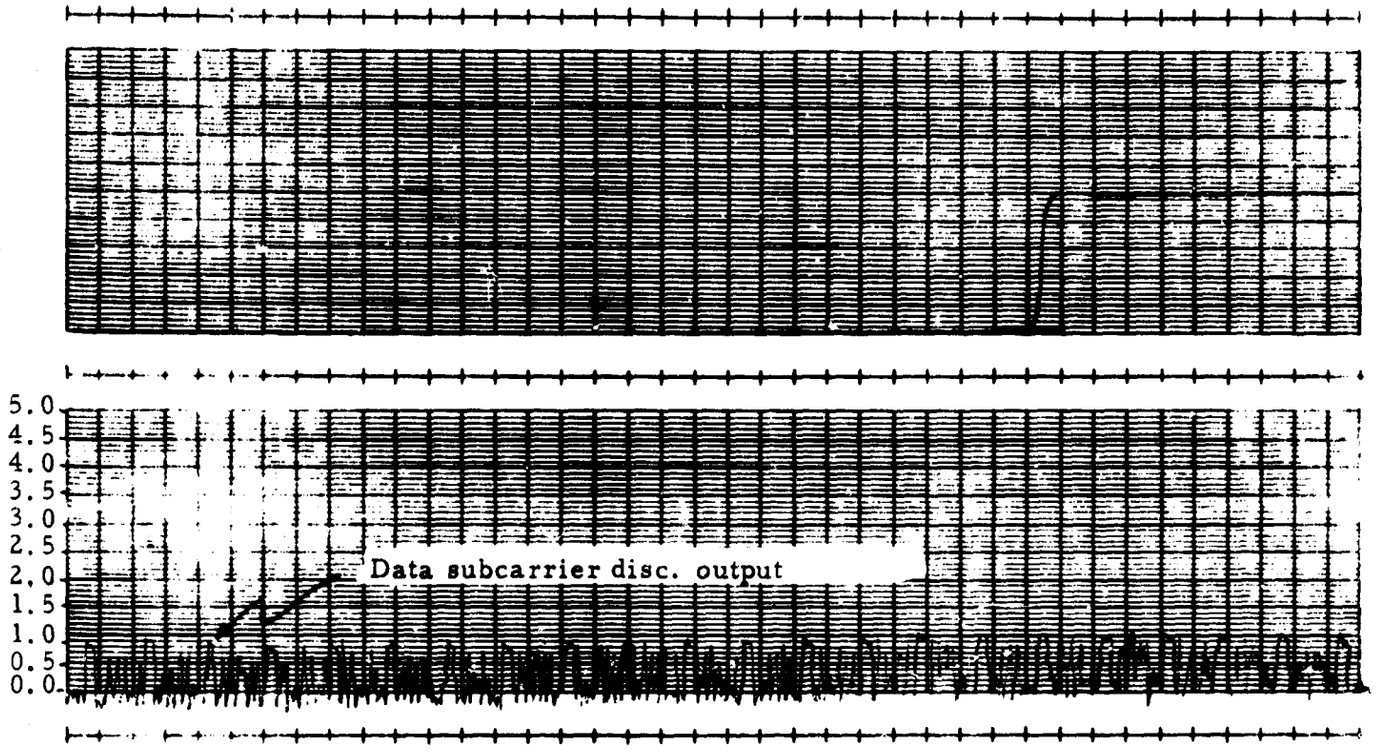

Chart Speed 5 mm/sec.

0.5 V/Division Amplitudes 5.0V full scale

Transmission distance _ _ _ _ _ _ 34 miles

Transmission Power Output _ _ _ _ 50 watts

Antenna _ _ _ _ _ _ _ _ _ _ _ 1/4 wave whip mounted on droppable unit

Transmission period _ _ _ _ _ _ _ 1 Sec. "on" ≈ 8 Sec. "off"

Noise _ _ _ _ _ _ _ _ _ _ _ _ _ Receiver disc. output, -7 dbm into 600Ω

Sig. to noise _ _ _ _ _ _ _ _ _ _ ≈8 db

Base Station

Azimuth _ _ _ _ _ _ _ _ _ _ East (direction of base station antenna)

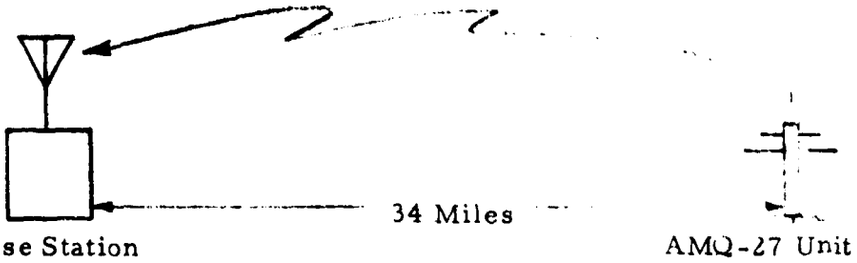

Figure 3-18. AMQ-27 Unit to Base Station Field Test Data

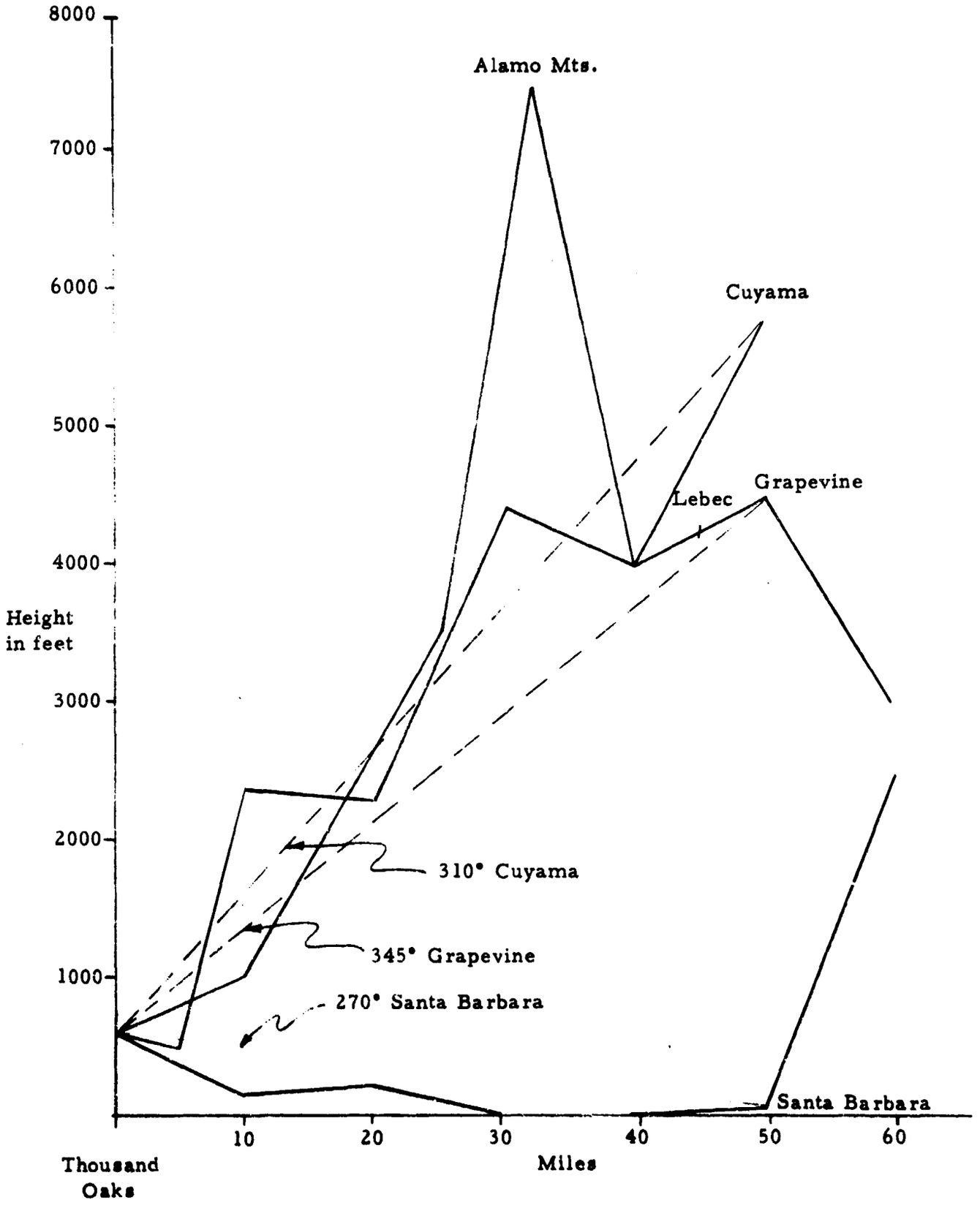

Figure 3-19. Field Test Site Locations for the AMQ-27

SECTION IV

AERODYNAMIC STUDY OF THE DEPLOYMENT VEHICLE CONFIGURATION

4.0 GENERAL

During this phase of the program, a study was performed on the deployment vehicle aerodynamic configuration. The purpose of this study was to determine what system design changes would be required to extend its deployment capabilities to aircraft flying at various altitudes up to 5000 feet at indicated air speeds between 200 and 300 knots per hour.

4.1 AERODYNAMIC EVALUATION

During the last of five test flights on the AN/AMQ-27( ) vehicle in January 1969, the unit was ejected from the aircraft at an indicated airspeed of 144 knots, and at an altitude of 1000 feet. The unit successfully landed as predicted but, upon investigation damage to the blades was discovered. It was evident that this damage, occurring at the spot welds which reinforced the root section of the blade, was due entirely to the slipstream speed at deployment from the aircraft.

Ejection of a vehicle from an aircraft was duplicated in the Laboratory by subjecting the blade to a force parallel to the slipstream application of the centroid of the pressure area. This test was repeated ten times to the point where failure similar to that of the flight unit occurred. The worst condition was chosen and 48 pounds was accepted as the drag force of the blades subjected to the slipstream.

Use was made of the background data developed by J.S. Brown and K. E. McKee in their article - "Wind Loads on Antenna Systems" - viz., "Air in motion possesses considerable kinetic energy. When an object deflects

the air from its free stream path, part of this kinetic energy is transferred into potential energy (i.e., pressure). This pressure acting on the elements of the system produces the wind loads of interest to the designer. These loads depend on the wind velocity, the area and shape of the element, and density of the air. The force acting parallel to the direction of flow of the wind is $F=AC_dq$, where F is the drag force, in pounds; A is the projected area in square feet; C_d is the drag coefficient and q is the pressure in psf."

Using this formula, the coefficient of drag (C_d) for the blade was calculated from the actual test data and the laboratory test data.

$F = 48$ pounds; $q = e\,v^2/2$; $v = 125$ mph $\times$ 5280/3600 = 184 ft/sec

$A = 2 \times 42/144$ sq. ft; at 1000 ft. altitude $e = 0.0744$ lb/cu. ft.

$$e = 0.0744/32.2 = 0.00231 \text{ sec}^2 \text{ lb/ft}^4$$

and $C_d = F/Aq = 48 \times 144 \times 2/84 \times .00231 \times (184)^2 = 2.1$

With this value for C_d, the graph shown in Figure 4-1 was plotted to determine the force on the blades due to changes in altitude and velocity of the aircraft.

The proposed criteria for this study was concerned with the values at an altitude of 5000 feet and between 200 and 300 knots. From the graph, the drag forces experienced by the AMQ-27 unit as it is structured, would be between 80 and 185 pounds.

The derivation of the coefficient of drag (C_D) took under consideration that the unit experienced its maximum stress on the blades the instant that they were presented to the slipstream of the aircraft. The force value evolved by experiment and calculations, could be utilized to establish the proper criteria for calculating the structural integrity of the high speed launch system.

Working with the present design, we first studied the failure mode at slow speed launching, and then extrapolated this information to the higher speeds.

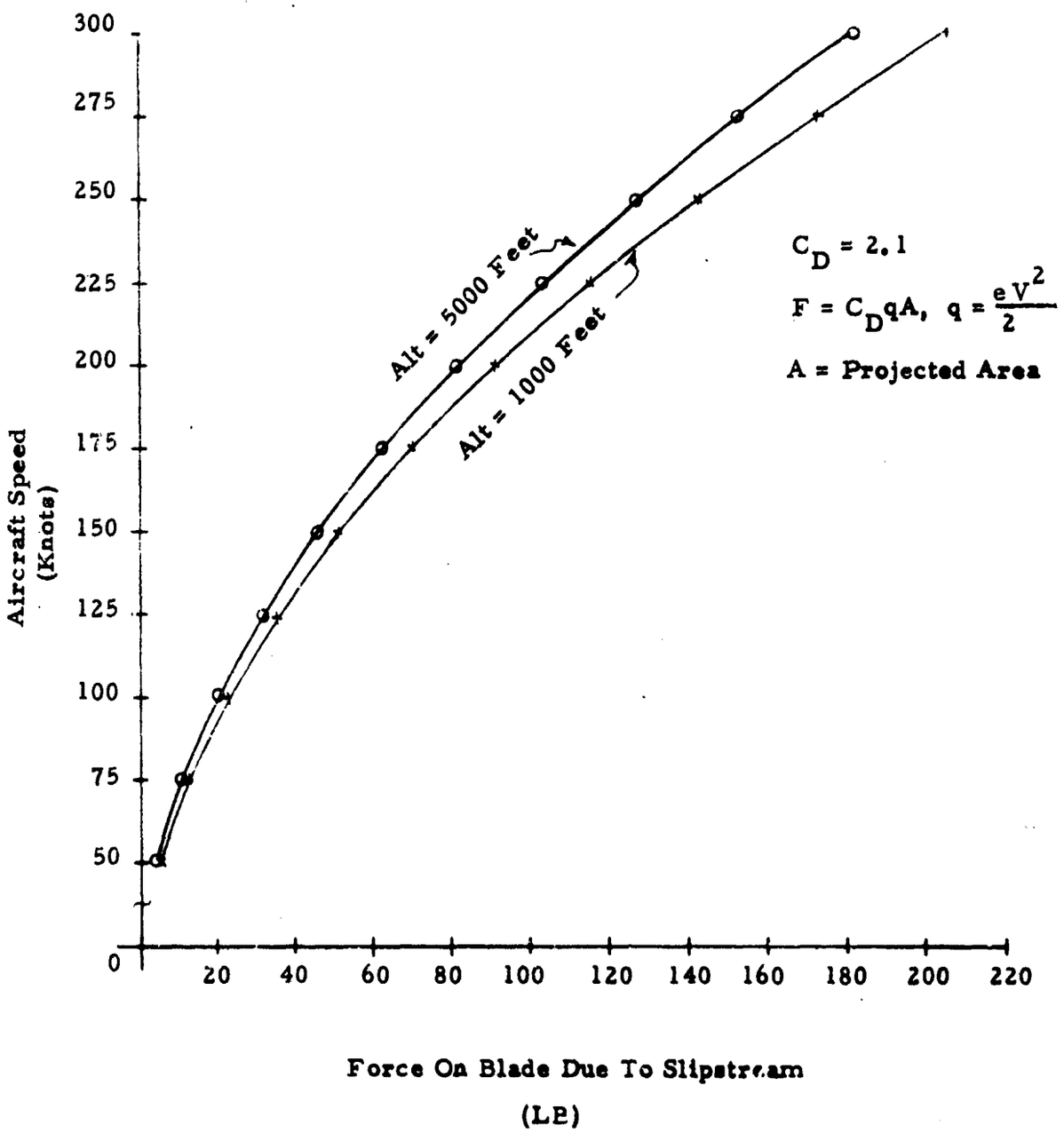

Figure 4-1. Drag Force on Blades in Relation to Aircraft Speed

Using forty-eight pounds as the blade loading at a distance two-thirds the length of the blade from the pivot, and the resisting force at a distance two and one half inches from the pivot, the maximum positive moment developed is

$$M_{\text{max-pos}} = \frac{28 \times 48}{2.5} \qquad \frac{25.5 \times 2.5}{28.0} = 1,223 \text{ in-lb.}$$

In order to be as close as possible on the basic figures, the actual cross-section of the blade at the failure point was used to calculate the section modulus

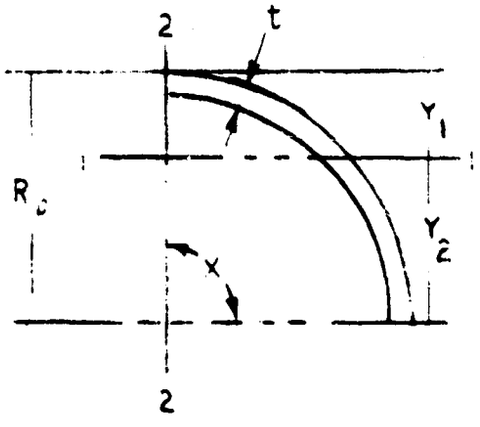

$$Y_2 = R_b\left(\frac{\sin x}{x} - \cos x\right)$$

$$I_{1-1} = \frac{R_b^3 t}{2}\left(x + \sin x \cos x - \frac{2 \sin^2 x}{x}\right)$$

at $x = 90^\circ$: $\sin x = 1$, $x = \pi/2$ rad.

$$\cos x = 0, \quad \sin^2 x = \frac{1-\cos 2x}{2}$$

$$\cos 2x = -1$$

$$Y_2 = 0.64\, R_b$$

$$I_{1-1} = 0.15\, R_b^3 t$$

$$\frac{I_{1-1}}{Y_2} = \frac{0.15\, R_b^3 t}{0.64\, R_b} = \underline{\underline{0.235\, R_b^2 t}}$$

The value of R_b and t were taken from the tubing used to generate the blade shape.

$R_b = 3.125/2 = 1.5625$ inches

$t = .065$ inch

The stress that occurred on the blade was then calculated with the above values

$$S = \frac{M}{I/y} = \frac{1223 \text{ in-lb}}{0.235\,(3.125/2)^2 \quad (.065)} = 32,800 \text{ psi}$$

The material used for the blades was aluminum alloy tubing 6061-T6, which has a yield strength of 35,000 psi. Thus, it was mathematically shown that the blades were marginal for the 125 mph launch, and verified the extent of the damage evident on the test unit.

Since these studies determined the structural integrity of the blades, the next step was to determine the requirements for the high-speed launch.

The stress levels for various section moduli versus the aircraft speed, up to the required maximum speed of 300 knots (IAS) was next investigated. This information enabled us to determine the blade configuration required of the existing design.

First, a determinination of the blades section modulus was calculated. The section modulus is dependent upon the altitude and the speed of launch of the unit. From previous calculations for the coefficient of drag, (C_D), the maximum positive moment for the blades is

$$M_{M-P} = 25.5F \text{ and } F = C_D Aq$$

but

$$C_D A = \text{constant} = 2.1 \times \frac{84}{144} = 1.225$$

and inserting "pressure coefficient", we now have

$$M_{M-P} = 31.2V^2 \left(\frac{q}{V^2}\right)$$

In determining the section modulus, I/Y, we will use

$$S = \frac{M_{M-P}}{I/Y}$$

which leaves us with

$$S = \frac{31.2V^2 \left(\frac{q}{V^2} \right)}{I/Y}$$

Since the pressure coefficient ($\frac{q}{V^2}$) is dependent on the altitude and velocity of launch, various velocities from 50 knots to 300 knots (IAS) and altitudes of 1000 and 5000 feet were used. Using this criteria, a family of lines was obtained which produced the section modulus for a design value of stress dependent upon the material used.

With the value of the section modulus known, the thickness (t) of material required at the stress concentration point from the section modulus formula for the existing blade was found to be

$$I_{1-1}/Y_2 = 0.575\ t.$$

For convenience, the above formulation was added to the chart (Figure 4-2) along with the data for the 5000 ft. altitude. To verify the validity of the charts (Figures 4-2 and 4-3), a sample blade was made which incorporated the existing 42-inch long blade with one lamination from the root 28 inches long, another lamination above that 18 inches long, and a final lamination 10 inches long. The root area of this blade has a thickness (t) from the chart of 0.160 inch plus a safety factor of 1.625 using aluminum, 6061-T6, with a yield point of 35,000 psi. This blade was labelled "Test Blade # 1."

Proposed "Test Blade # 2" was constructed of laminated epoxy with metal sprayed on the upper and lower surfaces for the electrical ground plane. This blade was fabricated by Laminair Incorporated, Gardena, California.

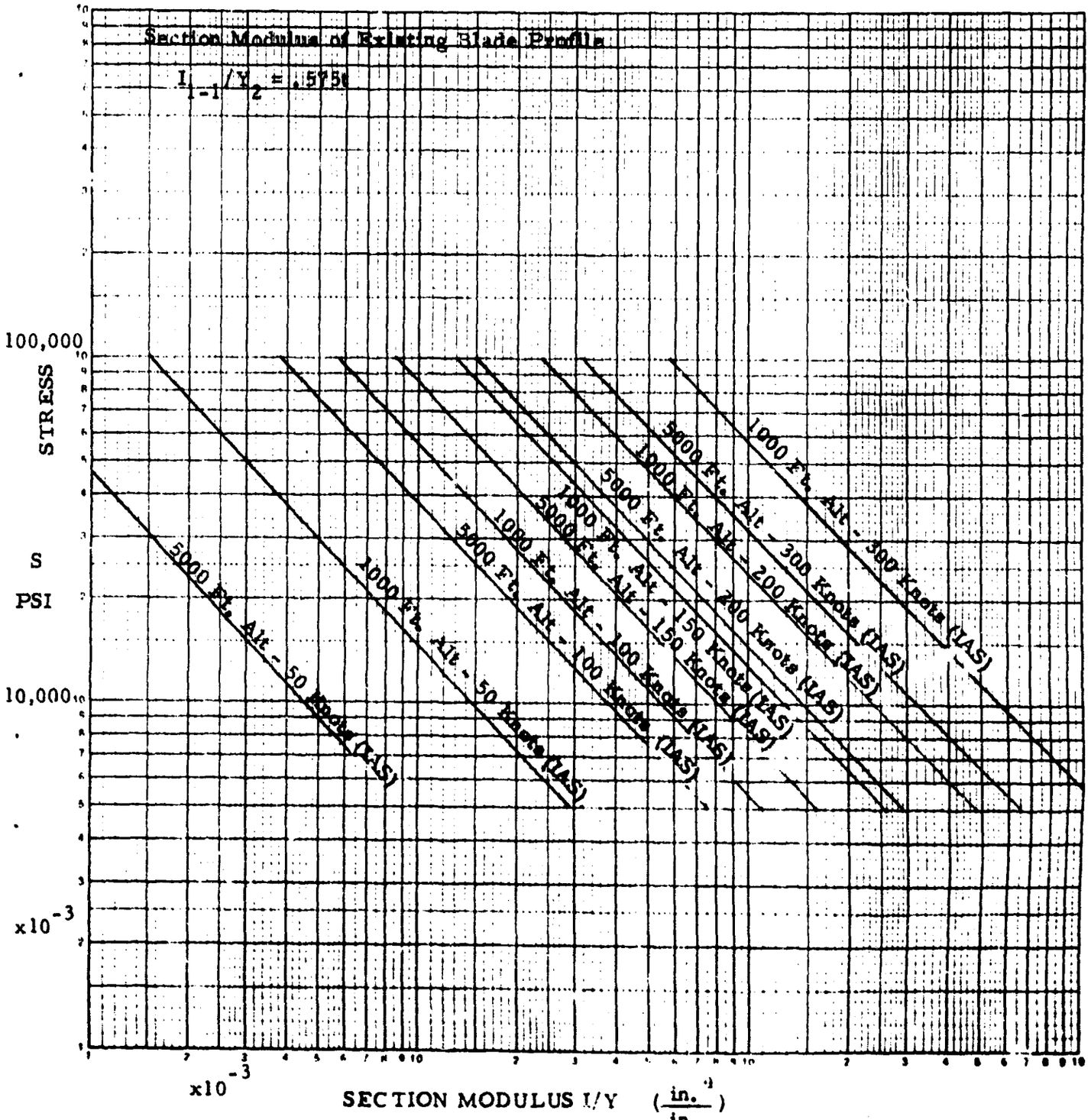

Figure 4-2. Stress Versus Section Modulus

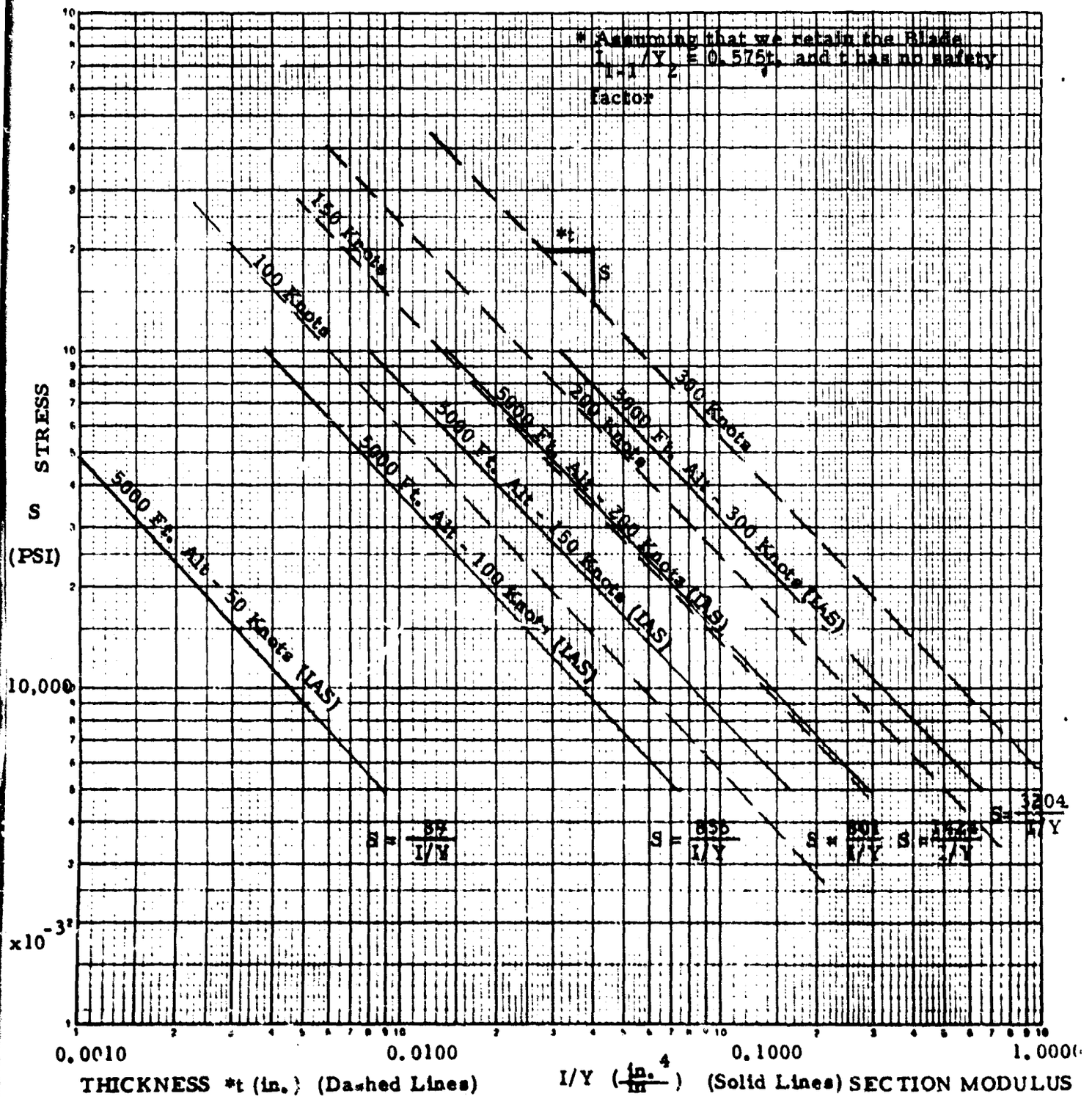

Figure 4-3. Stress in Relation to Section Modulus and Thickness

Test blade #1 was tested by drops on the Barry Drop machine to equal the conditions of actual drop. In order to duplicate the air pressure on the blades equal to the slipstream pressure, the blades deformed a soft foam pad when dropped on the Barry shock testing machine.

It was evident, due to the high speed forces on the blades, that a new and stronger hub area would have to be developed.

Preliminary testing was performed on a test blade using the previously reported data. The blade was made by laminating four (4) blade sections together to develop the root thickness to approximately 0.219 inch. This value includes a safety factor of 1.6.

The predicted load on the blade at 1000 feet altitude and an airspeed of 300 knots was 185 pounds. To effectively test the blade, we first mounted it to the Barry Drop Machine carriage (300 pounds), duplicating the stress areas encountered in actual operation. The blade was then repeatedly dropped onto an immoveable surface softened with foam material. The major force of the falling blade was restricted to an area 17 inches from the mounting bolt. Some deformation was evident, but not enough to effect the flyability of the blade. No material tearing occurred at the critical area between the fulcrum and the mounting bolt.

The drop test verified that the previous calculations were valid and could be used in the construction of an air-droppable unit that could be launched from an aircraft at 300 knots and an altitude between 1000 and 5000 feet.

During the drop test, a different method was used to mount the blade. Instead of a shaft used to support the launching forces, a bridge was made so that the shaft would not be the primary structural part. The forces are absorbed by the bridge through the shaft which can be steel or any other high strength material.

For high production low-cost, the hub could be made of an aluminum extrusion which could be made to include the blade mounting bridge and also one-half of the bearing surface.

The upper stopping area of the hub, which is now 1/8 inch thick aluminum, would have to be increased to twice its thickness in order to sustain the instantaneous loading of the blade at launch; or the material could be changed to steel. (The bending stress on the ledge is 33,400 psi with a thickness of 3/16 inch.)

The conclusion drawn from this study indicates that the most economical and desirable deployment package for the high speed launch system of the AMQ-27 would be a beefed-up version of the existing vehicle. The fact that the test blade used in this last exercise was approximately one pound heavier than the existing blade would indicate that a different material should be used, such as laminated epoxy, as mentioned previously. The treatment of the hub for a high speed launch would indicate that a different configuration could be used that would utilize a high production technique thereby reducing the cost.

All in all, the mechanical package, as now built, seems to have the inherent ability to be adaptable to a high speed launch.

SECTION V

CONCLUSIONS AND RECOMMENDATIONS

5.1 CONCLUSIONS

Packard Bell has developed during the past thirty months a functional breadboard air droppable system which proves the feasibility of the various system elements, i.e., the design described in this report has been functionally tested and meets or exceeds the system parameters.

The sensor package with support electronics is a breadboard system that proved the feasibility of the design. The system measured the various meteorological parameters within the accuracies specified. Although it worked quite well in the laboratory, it was not built strong enough to survive an airdrop.

The transceiver electronics were built and checked out as a single frequency system operating in the range of 40 to 42 MHz with the capability of transmitting over at least 50 miles of range. This system was airdropped and remained functional. Part of this system was the self-extendible antenna with the delayed release mechanism. This antenna was flight tested and proven to be functional.

The flight vehicle's capabilities were demonstrated during development at altitudes of 500 to 2000 feet and at deployment speeds of 60 knots. Increased deployment speeds are practical with a "beefed up" version of the present vehicle. The limiting element on altitudes greater than 2000 feet is the accuracy of the drop zone. Dropping from altitudes lower than 500 feet does not allow enough time for the vehicle to achieve a stabilized flight path and therefore is not practical.

The AMQ-27 vehicle weighs 17 pounds and carries a payload of 15 pounds. When deployed from 1500 feet with the airplane slowed to 60 knots,

it takes 15 to 18 seconds to impact the ground. It will penetrate a medium type of soil 18 to 24 inches and receive an impact shock of 50 to 75 G's.

5.2 RECOMMENDATIONS

Packard Bell suggests the following recommendations for the continuation of the AMQ-27 Program.

a. Improve vehicle to withstand high speed deployment.

b. Develop sensors and support electronics into a tactical system.

   (1) Update design to present state of the art.

   (2) Redesign for reliability and productibility.

c. Improve transceiver equipment design.

   (1) Update design to present state of the art.

   (2) Design for productibility.

   (3) Investigate use of integrated circuits.

d. Improve antenna design for reliability.

e. Develop various types of battery packages to meet environmental conditions in deployment areas.

f. Develop deployment device for cargo type airplanes.

g. Investigate deployment in 50-60 mph wind conditions.

h. Extensive flight testing to develop systems tactical capability.

APPENDIX A

POWER SOURCES

Transmitter	Power Pack Length	9.18"
Receiver	Power Pack Length	2.00"
Sensor	Power Pack Length	1.74"
	Total Length	12.92"

Transmitter	Power Pack Weight	29.4 Oz.
Receiver	Power Pack Weight	8.4 Oz.
Sensor	Power Pack Weight	9.46 Oz.
	Total Weight	47.26 Oz.

Tabulated Weight of Power Sources

Battery, Yardney Cell No. HR-1

Average Voltage
@ 3 Ampere Rate = 1.44V
Wt. = 29.4

21 Cells Required

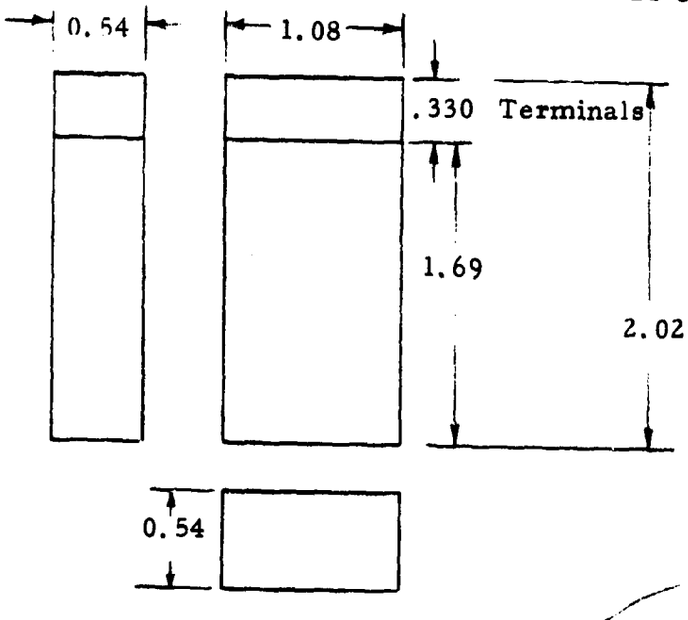

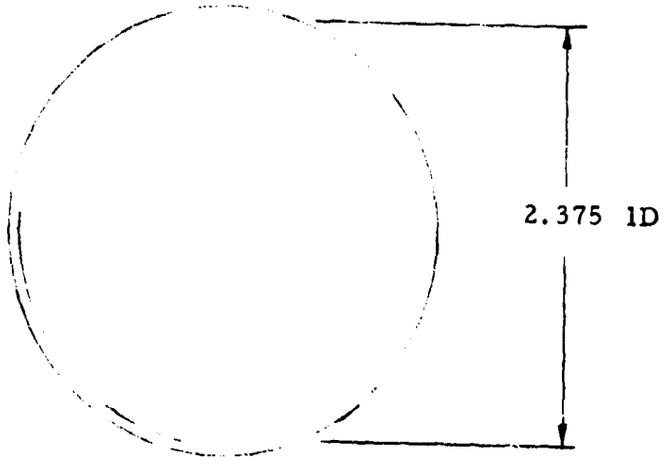

AN/AMQ-27 Unit Barrel Space

Transmitter Power Pack 30.24 Volts

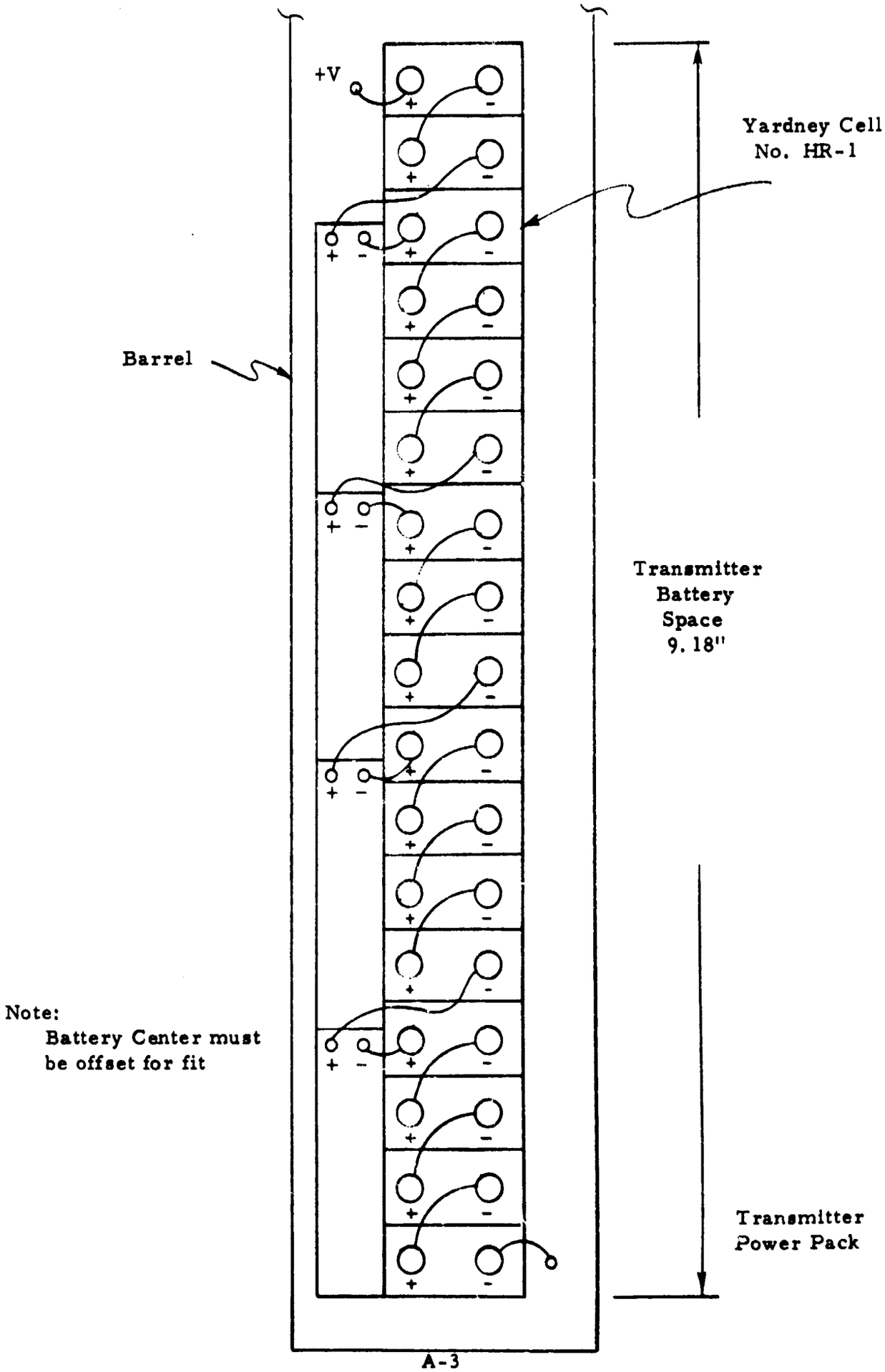

Note:
Battery Center must
be offset for fit

Average Voltage
@ 10 ma hr rate = 1.25 volts
Wt. = 8.4 Oz.
6 Cells

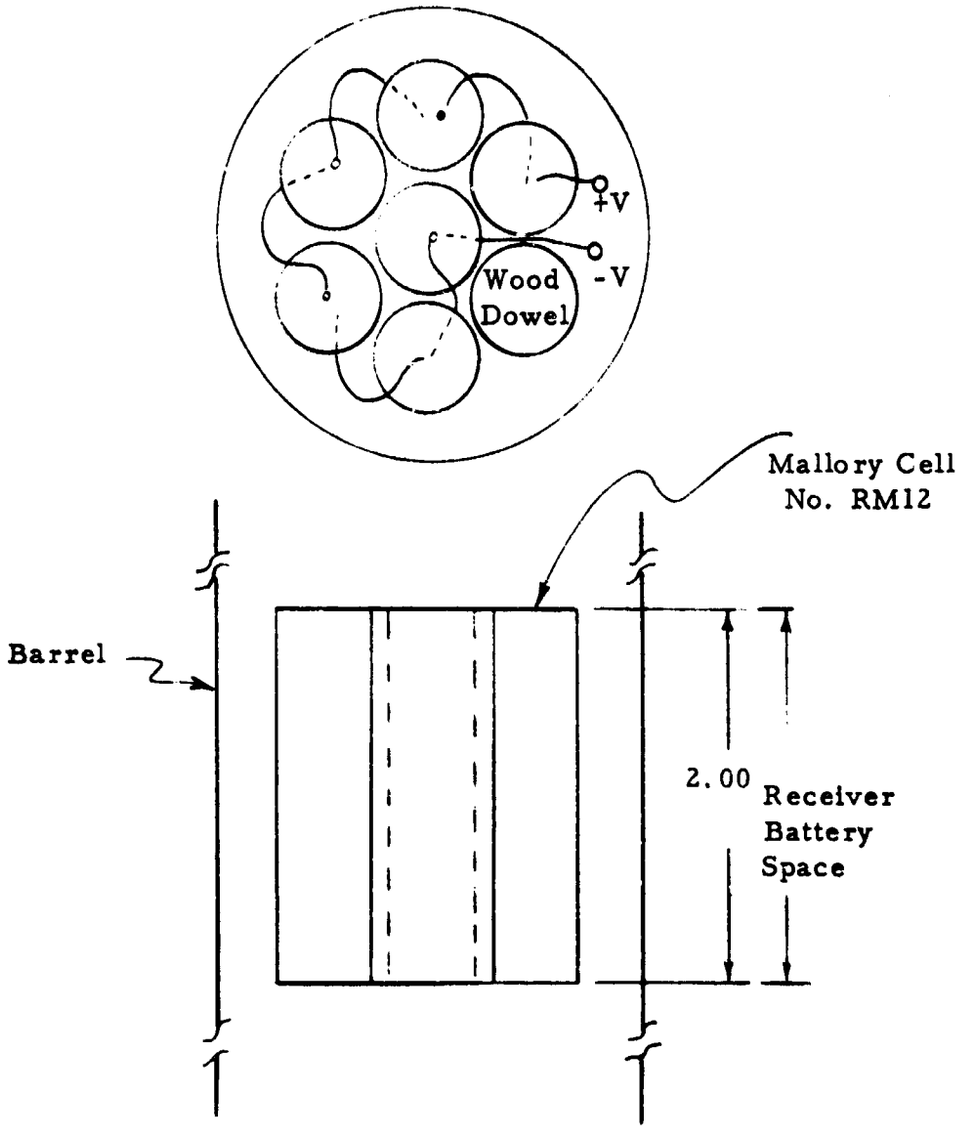

Receiver Power Pack 7.5 Volts

Average Voltage
@ 175 ma hr rate = 1.25 volts
Wt = .43 Oz.
11 Cells for +10V
11 Cells for -10V
} 22 Total

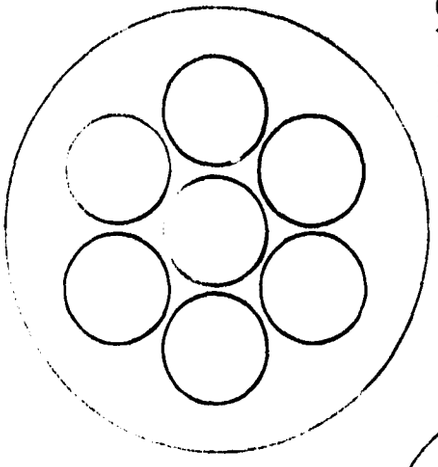

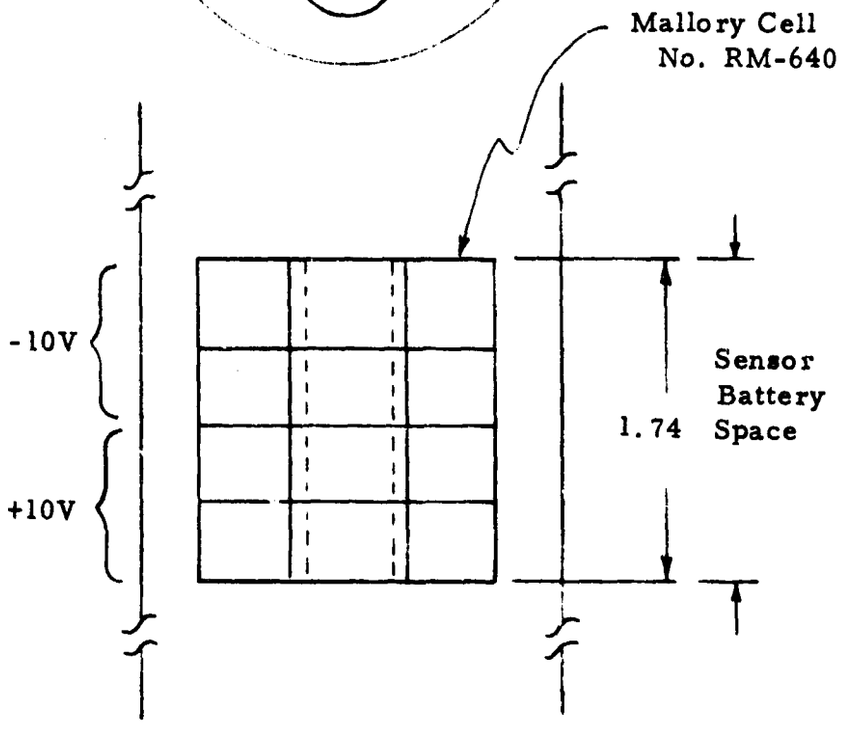

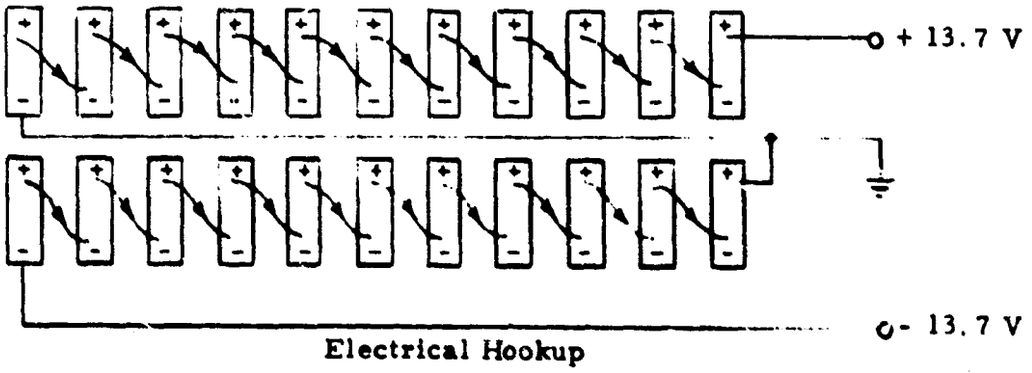

Electrical Hookup

Sensor Power Pack +10V, -10V

Yardney Batteries

20.0	20.
2.0	2.

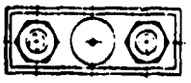

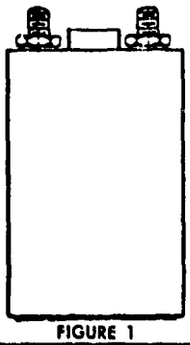

FIGURE 1

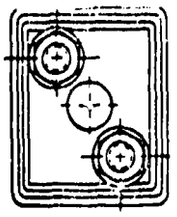

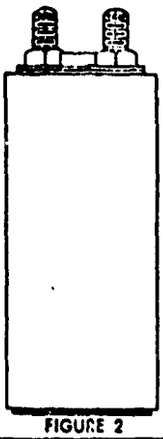

FIGURE 2

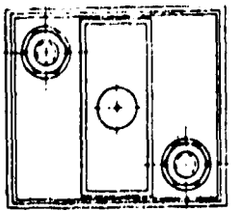

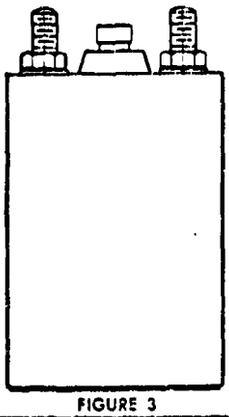

FIGURE 3

20.0	20.
29.0	30.
1.48	1.
49	46
2.8	3.

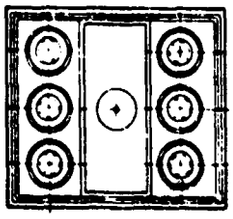

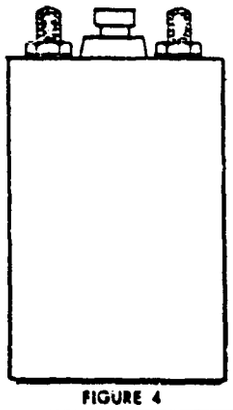

FIGURE 4

60.0	60.
26.0	27.
1.42	
18'	17

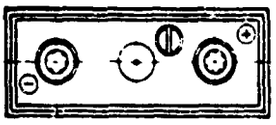

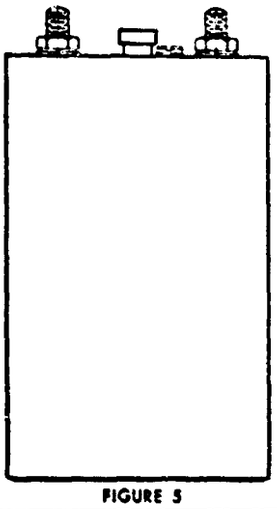

FIGURE 5

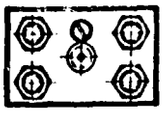

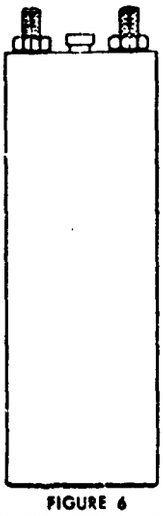

FIGURE 6

120.0	120.
22.0	23.
1.30	1.
8'	6'

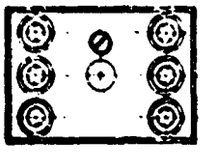

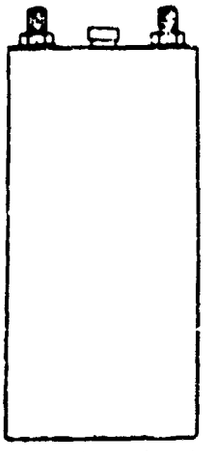

14.0	15.
15.2	13.
4.28	7.
3.64	6.
1.73	2.
2.05	0.
5-16-21	5 16

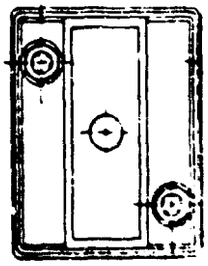

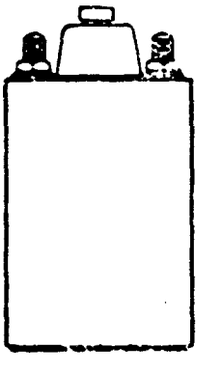

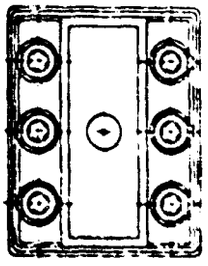

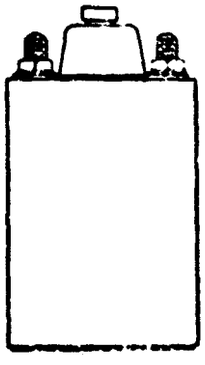

RM640
RM640R

PRIMARY MERCURY BATTERY

SPECIFICATIONS	RM-640
Nominal Voltage	1.40
Rated Capacity	500 mah
Rated Capacity at	15 ma
Diameter	.620±.005 in. 15.8±.13 mm
Height	.435±.005 in. 11.1±.13 mm
Volume	.13 cu in. 2.13 cc
Weight	.28 oz 7.94 gms

VOLTAGE DISCHARGE CURVES VOLTAGE vs. TIME

RESISTANCE VALUES AND EQUIVALENT CURRENT DRAINS AT 1.25 VOLTS

OHMS	MILLIAMPERES
50	25
83	15
125	10

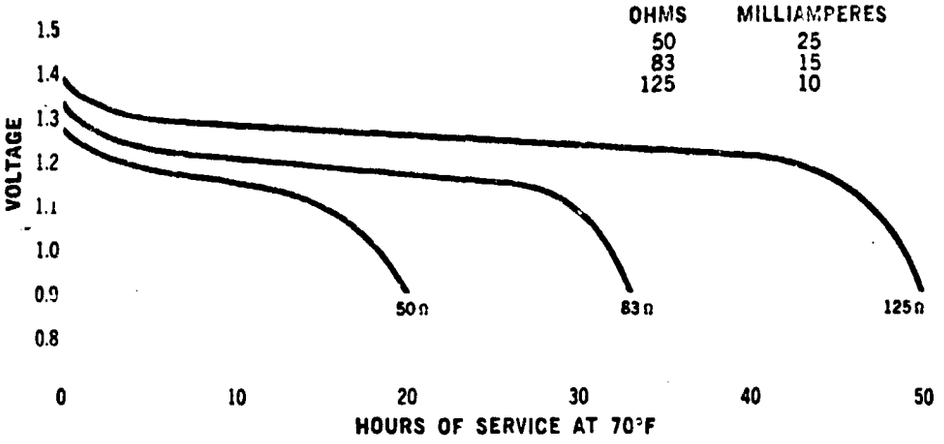

SPECIFICATIONS	RM-640R
Nominal Voltage	1.35
Rated Capacity	500 mah
Rated Capacity at	15 ma
Diameter	.620±.005 in. 15.8±.13 mm
Height	.435±.005 in. 11.1±.13 mm
Volume	.13 cu in. 2.13 cc
Weight	.28 oz 7.94 gms

VOLTAGE DISCHARGE CURVES VOLTAGE vs. TIME,

RESISTANCE VALUES AND EQUIVALENT CURRENT DRAINS AT 1.25 VOLTS

OHMS	MILLIAMPERES
50	25
83	15
125	10

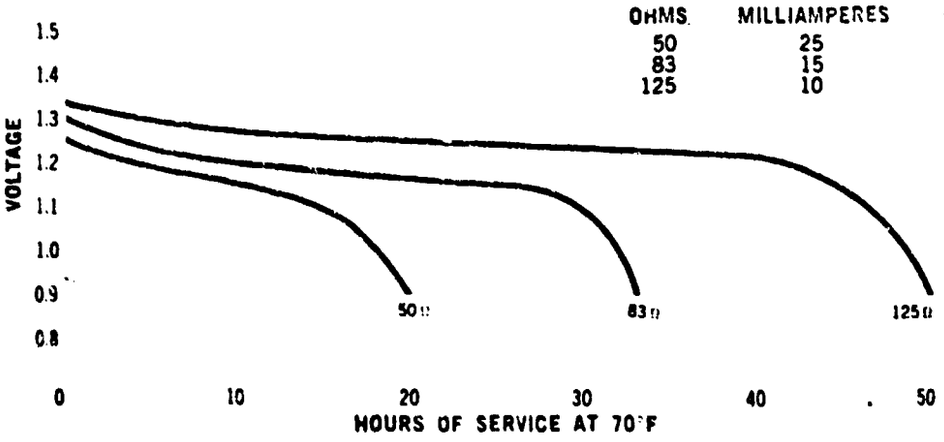

MALLORY BATTERY COMPANY
a division of P. R. MALLORY & CO. INC.
S. Broadway, Tarrytown, New York, 10591; Telephone: 914-591-7000

MALLORY

PRINTED IN U.S.A. 66 13

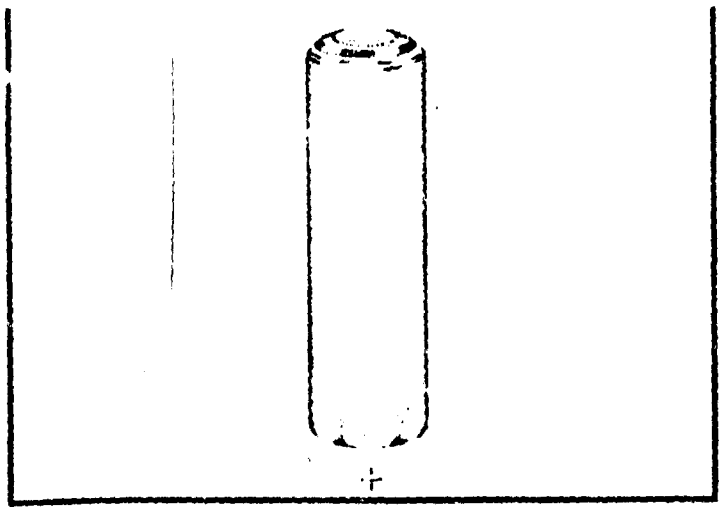

RM12

RM12R

PRIMARY MERCURY BATTERY

SPECIFICATIONS	RM-12
Nominal Voltage	1.40
Rated Capacity	3600 mah
Rated Capacity at	83 ma
Diameter	.622±.005 in. 15.8±.13 mm
Height	1.953±.015 in. 49.6±.38 mm
Volume	.60 cu in. 9.84 cc
Weight	1.4 oz 39.6 gms

VOLTAGE DISCHARGE CURVES

VOLTAGE vs. TIME

RESISTANCE VALUES AND EQUIVALENT CURRENT DRAINS AT 1.25 VOLTS

OHMS	MILLIAMPERES
10	125
20	62
25	50
32	40

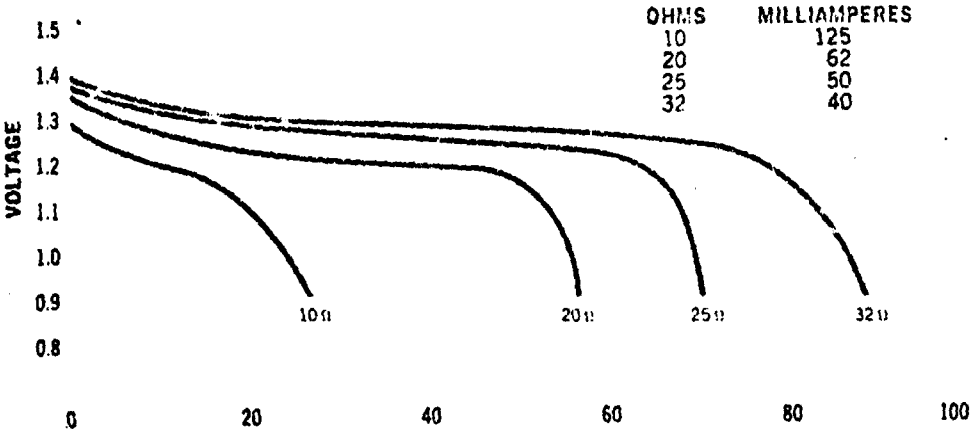

SPECIFICATIONS	RM-12R
Nominal Voltage	1.35
Rated Capacity	3600 mah
Rater Capacity at	83 ma
Diemeter	.622±.005 in. 15.8±.13 mm
Height	1.953±.015 in. 49.6±.38 mm
Volume	.60 cu in. 9.84 cc
Weight	1.4 oz 39.6 gms

VOLTAGE DISCHARGE CURVES

VOLTAGE vs. TIME

RESISTANCE VALUES AND EQUIVALENT CURRENT DRAINS AT 1.25 VOLTS

OHMS	MILLIAMPERES
10	125
20	62
25	50
32	40

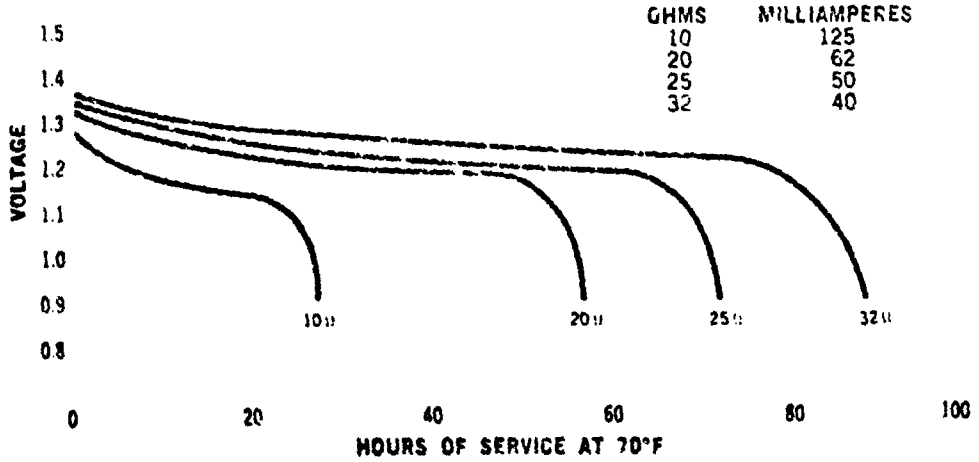

MALLORY BATTERY COMPANY
a division of P. R. MALLORY & CO. INC
S. Broadway, Tarrytown, New York, 10591; Telephone: 914-591-7000

MALLORY

PRINTED IN U.S.A. 66 4

ELECTRICAL CHARACTERISTICS

nominal capacity (ampere-hours)	0.1	0.2	0.5	1.0	1.5	2.0	3.0	4.0	5.0	10.0	15.0
recommended charging rate (amps)	0.01	0.02	0.07	0.10	0.15	0.20	0.30	0.30	0.35	0.75	1.0

TYPICAL APPLICATION DATA (@ 70°F)

A. 60-minute rate discharge discharge rate (amps)	0.1	0.2	0.5	1.0	1.5	2.0	3.0	4.0	5.0	10.0	15.0
ampere-hour output†	0.175	0.22	1.3	1.75	2.5	3.3	5.0	6.0	7.5	12.0	18.5
average voltage	1.45	1.48	1.50	1.50	1.50	1.51	1.50	1.50	1.42	1.44	1.48
watt-hours per pound†	25	23	39	38	43	33	38	39	37	34	44
watt-hours per cubic inch *	1.3	1.2	2.1	2.2	2.7	1.9	2.6	2.7	2.2	2.1	3.0
B. 20-minute rate discharge discharge rate (amps)	0.3	0.6	1.5	3.0	4.5	6.0	9.0	12.0	15.0	30.0	45.0
ampere-hour output†	0.15	0.21	1.1	1.6	2.0	3.0	4.7	5.4	5.9	10.5	16.5
average voltage	1.40	1.35	1.45	1.44	1.40	1.46	1.46	1.49	1.36	1.33	1.44
time limit (minutes)**	16'	15'	20'	20'	20'	20'	20'	20'	20'	18'	15'
C. ten-minute rate discharge discharge rate (amps)	0.6	1.2	3.0	6.0	9.0	12.0	18.0	24.0	30.0	60.0	90.0
ampere-hour output†	0.12	0.17	0.94	1.4	1.5	2.4	4.2	4.8	5.2	8.0	13.0
average voltage	1.32	1.25	1.35	1.35	1.32	1.40	1.37	1.40	1.26	1.26	1.30
time limit (minutes)**	6'	5'	8'	8'	8'	8'	8'	9'	6'	5'	5'

PHYSICAL CHARACTERISTICS

maximum weight filled (ounces)	0.16	0.23	0.8	1.1	1.4	2.4	3.2	3.7	4.6	8.2	10.0
overall volume (cubic inches)	0.19	0.27	0.91	1.18	1.35	2.56	2.90	3.31	4.78	8.26	9.13
overall height (inches)	1.38	1.94	1.56	2.02	2.32	2.53	2.86	3.36	2.91	4.81	4.94
height less terminals (inches)	1.20	1.69	1.20	1.69	1.98	2.16	2.49	3.0	2.49	4.28	4.22
width (inches)	0.63	0.63	1.08	1.08	1.08	1.72	1.72	1.72	2.08	2.32	2.31
depth (inches)	0.22	0.22	0.54	0.54	0.54	0.59	0.59	0.59	0.79	0.74	0.80
terminal threads	1-72	1-72	5-40	5-40	5-40	10-32	10-32	10-32	10-32	1 4-28	5 16 2

† to a final voltage of 1.1V

* calculated using overall volume

** for maximum recyclability observe discharge time limits specified in ... instructions

BATTERY PACK DATA

2-Cell Mallory

Battery #1

Open Ckt Voltage	~16.2V
W/Regulator	~15.8V (4.5 ma)
W/Regulator and 50Ω load	~12.8V (200 ma)

Battery #2

Open Ckt Voltage	~16.2V
W/Regulator	~16.0V (4.5 ma)
W/Regulator and 50Ω load	~12.6V (200 ma)

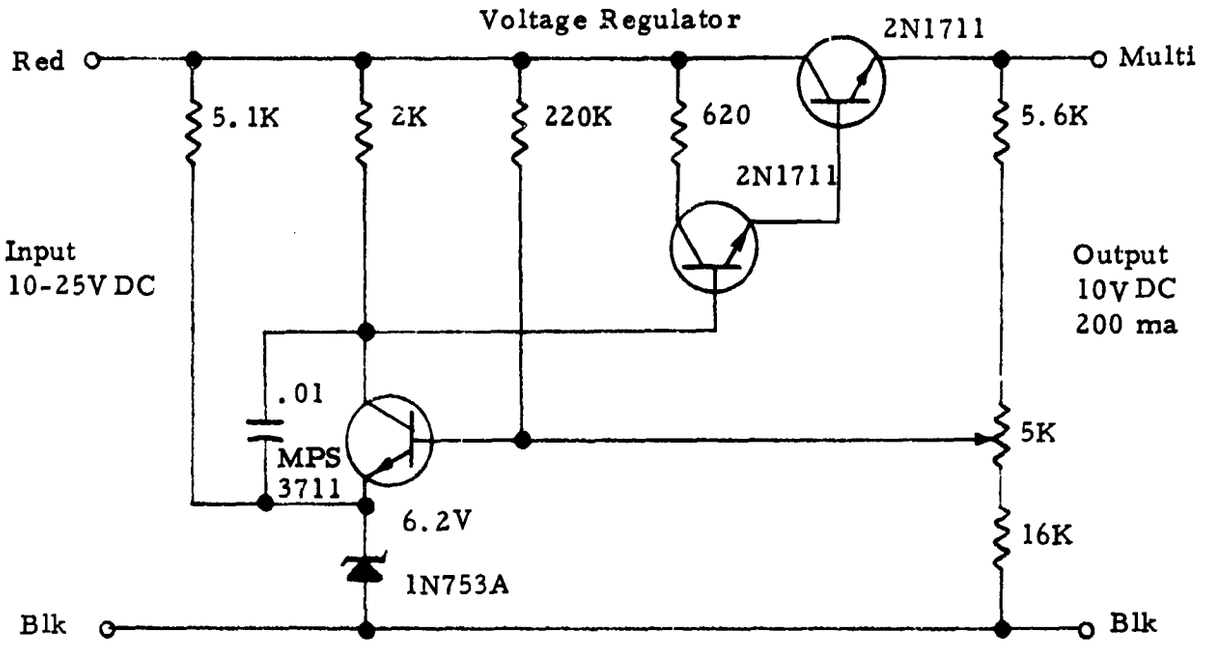

Regulation Range

Reg. Output	Approx. Input Range	
9.5 ± 0.1	11.5 - 25	
10.0 ± 0.1	12.0 - 25	@ 26°C
10.5 ± 0.1	13.0 - 25	
0-200 ma output current		

Temperature Range

Approx. -40°C to 90°C

Current Drain
4.2 ma @ 16V Input
(10.0V regulated output)

Power Req. for Sensor Package

+10 ± 0.1 DC @ 182.1 ma intermittent
+10 ± 0.1 DC @ 12.2 ma continuous

-10 ± 0.1 DC @ 37.5 ma intermittent
-10 ± 0.1 DC @ 3.2 ma continuous

Batt. ~ Open Ckt. - 16.2V / 200 ma load - 12.8V

VOLTAGE REGULATOR TEST DATA

Input Voltage	Output Voltage	
	0 ma load	200 ma load
10.0V	9.00	8.40
11.0V	9.55	9.20
12.0V	9.60	9.59
13.0V	9.60	9.60
14.0V	9.60	9.60
24.0V	9.60	9.60
25.0V	9.50	9.50

@ 26°C

Regulated Output
9.55V

Input Voltage	Output Voltage	
	0 ma load	200 ma load
10.0V	9.10	8.60
11.0V	9.80	9.35
12.0V	9.95	9.90
13.0V	9.98	9.93
14.0V	9.98	9.95
24.0V	9.87	9.95
25.0V	9.87	9.85

@ 26°C

Regulated Output
9.95V

Input Voltage	Output Voltage	
10.0V	9.00	8.40
11.0V	9.95	9.40
12.0V	10.50	10.10
13.0V	10.60	10.55
14.0V	10.61	10.60
24.0V	10.61	10.60
25.0V	10.55	10.53

Regulated Output
10.55V

Output Meter
Simpson 270 VOM (10V Scale)

VOLTAGE REGULATOR TEST DATA

@ 26°C

Current Drain (No Load)	
Input Voltage	Input Current
10V	1.0 ma
11V	1.2 ma
12V	1.6 ma
13V	2.3 ma
14V	3.0 ma
15V	3.8 ma
16V	4.2 ma
17V	4.7 ma
18V	5.5 ma
19V	6.2 ma
20V	6.8 ma

Input Voltage vs Regulated Voltage @ 90°C
@ 0 ma and 200 ma load

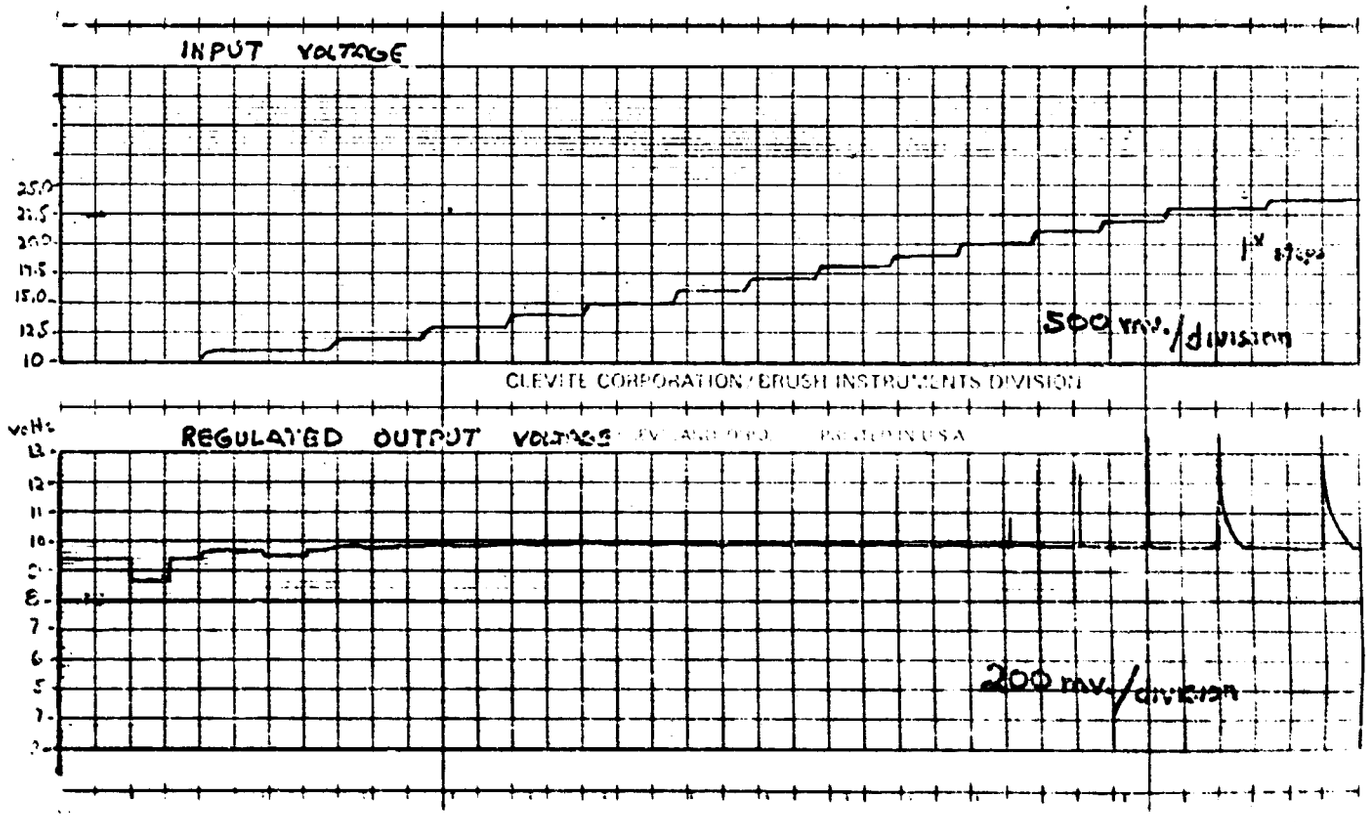

APPENDIX B

RADIO PROPAGATION CONSIDERATIONS

APPENDIX B

RADIO PROPAGATION CONSIDERATIONS

B1.0 TRANSMISSION

The success of radio communications over ranges in the 50-100 mile category, when faced with power and antenna restrictions inherent to any droppable package of size and weight in the area of that applicable to the AN/AMQ-27 ( ), is not clearly definable by even sophisticated mathematical or other paper modeling. The success of communications depends upon the diversity of such variables as terrain, weather conditions, soil conductivity, angle of vehicle penetration, time of day, season of year, sunspot activity, multipath and co-channel interference, etc. All of these elements are variables and cannot be controlled by the equipment user.

In total context, the predominant factor in successful communication is propagation. The selection of operating frequency consequent to fundamental assumption concerning propagation is probably the single most critical design decision. As a preliminary step in frequency selection, radio propagation may be divided into three essentially separate methods as follows:

a. Sky wave (skip)

b. Ground wave

c. Line of sight

In addition, such modes as tropo scatter, meteor burst, Sporadic E, ducting and Aurora also exist, but the power levels required and reliability requirement rule out serious consideration of intentional reliance on these modes.

Of the three propagation methods which are considered, the sky wave mode is unsuitable for consideration because of several factors as follows:

a. The 50-mile range offers insufficient path length for reliable sky wave.

b. Susceptibility to interference from skip stations hundreds or perhaps thousands of miles away.

c. Sky wave propagation is contingent upon and affected by hourly, daily, seasonal and cyclic variations of sunspot activity causing the optimum frequency to change with the ionization of the layers and, thus, requires a very proficient operator or a "smart" system of determining optimum frequency or both. Also, the multipath interference of the transmitted signal can cause serious system design limitations.

Sky wave systems are operable but they are not simple, unattended nor expendable. In essence then, two choices of propagation need to be examined; a line of sight or VHF droppable station, and a ground wave or LF droppable station.

B1.1 VHF COMMUNICATIONS

Communications in the VHF spectrum utilize frequencies ranging from 30 MHz to 300 MHz. The lower portion of this range is considered unusable for the AMQ-27 due to skip and sky wave occurrences. In general, the VHF spectrum can be characterized as predominantly a line of site mode at power levels available in the station. It is also characterized by reflections of the transmitted wave from major topographical features such as mountains, hills, etc.

In the AN/AMQ-27 communication concept, the VHF frequency provides communications in three major conditions:

a. Close-in ground-to-ground conditions.

b. Elevated (line-of-sight) base stations conditions such as aircraft, satellites, or ridge top ground stations or repeaters.

c. Reflective conditions which may exist in a given drop area-to-base station path.

The latter condition cannot be considered as a reliable factor in the VHF communication since it depends upon the geometry of a given air drop to surrounding topographical features and the base station.

In considering VHF power output, an important factor to remember is that the conversion of dc power into VHF rf power is highly inefficient. One hundred watts of input power typically will result in only 20-25 watts of output. Thus, it is extremely costly in terms of battery weight and size to have relatively high VHF transmitting power levels. It also becomes important to minimize average power drain by utilization of short duty-cycle transmissions.

In the AMQ-27, the VHF communications link is operable in two basic conditions (neglecting reflection conditions): a) At short distances where the curvature of the earth or other significant obstruction does not irtroduce sharp attenuation of the transmitted signal, and b) At long distances, where line-of-site conditions prevail. At this point, it is worthwhile to examine the major factors influencing these two conditions of communication.

B1.1.1 Short Distances

Short distance communication is based upon establishing a reasonable ground wave. One of the major factors in this regard is Effective Radiated Power (ERP). Up until the point at which the earth's curvature or a major obstacle introduces sharp attenuation into the ground wave, an increase in ERP will provide a resulting increase in range.

The results of an experiment conducted by Packard Bell is shown in Figure B-1. The test conditions are noted in the Figure. Although this graph is not intended as an absolute or repeatable measurement of VHF performance, it provides insight into the relationship between ERP and range, which approximates one mile per watt of ERP.

FRP depends upon two factors - the obvious factor of rf power output and the gain of the antenna. For a non-directive antenna that is usable with the AMQ-27, a slight loss in ERP over rf power can be anticipated.

Just how far short range transmission with a given ERP can be expected, assuming a fixed receiver sensitivity, depends upon the absorption of the radiated power which primarily is caused by two factors - nearby objects and the ground.

To minimize the effect of nearby objects such as foliage, etc., the first few feet of antenna height are vital. Thus, in addition to providing a "clear-view" for sensors, the deployment vehicle height is maximized to reduce absorption of the radiated signal power.

The second absorption factor is uncontrollable and depends upon the terrain. Absorption over land is greater than over water; increased foliage cover provides more absorption than over a defoliated area; etc.

In terms of the AMQ-27, VHF communications at short range can be expected in distances of 5-10 miles radius from the deployment vehicle unless topographically obstructed. This range of radius assumes transmit and receive antenna heights in the order of six feet.

B1.1.2 Long Distances

The major inhibiting factor for long range transmission is the curvature of the earth. When the curvature of the earth becomes an obstruction between the two stations, the path loss goes up severely, and further

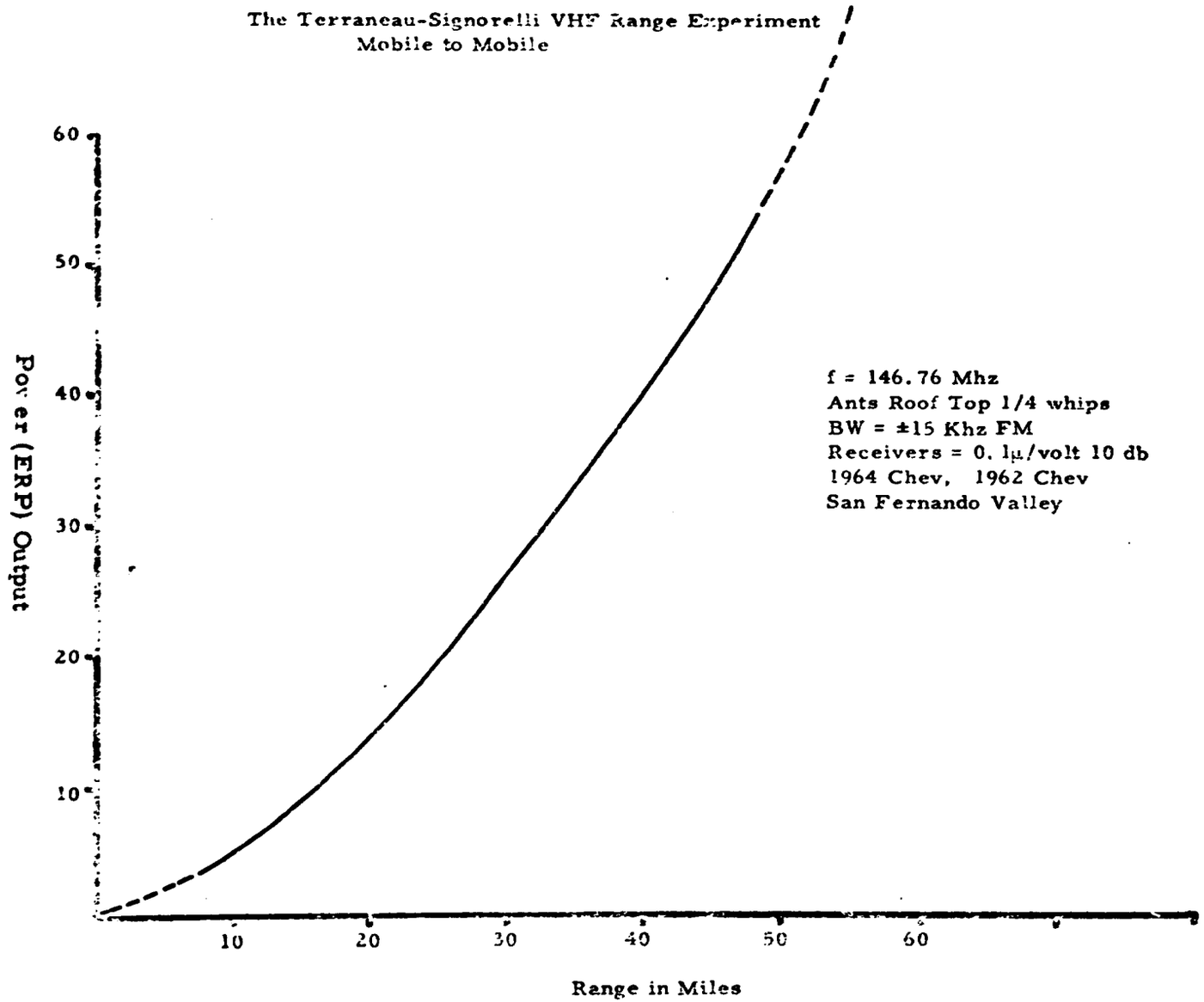

Figure B-1. Vehicle Prototype Development

increases in the distance become very expensive. It is for this reason that the first few feet of antenna height are relatively more important. The cumulative effect of absorption of the low angle of radiation by nearby ground objects plus the requirement for very low effective angles of radiation to counter the curvature of the earth dictate maximum effort to achieve antenna height as a primary goal.

The nature of the droppable station is such that it is always close to the ground. To determine the range from a droppable station, a discussion of the effective angle of radiation and the antenna height at both ends is necessary. In the case of the droppable station, the angle of propagation from the package is affected by the terrain and topography of the drop zone and the topography and conductivity between the droppable station and the base station. In general, the more energy radiated at the lowest angle, the greater the range. The choices of antennas in a droppable package are limited by a direct trade-off between antenna gain and size. The ease of droppability precludes the use of large antennas.

After the droppable station is dropped into whatever terrain exists and the radiation angle is determined or assumed, the range capability is then predominantly determined by the antenna height at the base station. To develop a "feel" for typical distance, it is necessary to make some judicious assumptions about radiation angles from the droppable station and refer to charts such as the one shown in Figure B-2 which predicts range against antenna height at various radiation angles. As an initial step towards evaluating range and for the sake of simplicity, a choice of two types of terrain is suggested. One path chosen over water and the other over gently rolling wooded hills. Next, one makes a judicious estimate of the probable radiation angles from a droppable station over each of these two terrains. The examples chosen assume an angle of radiation from the droppable station of 1/2 degree over water and 1 degree over moderately rolling hills. It

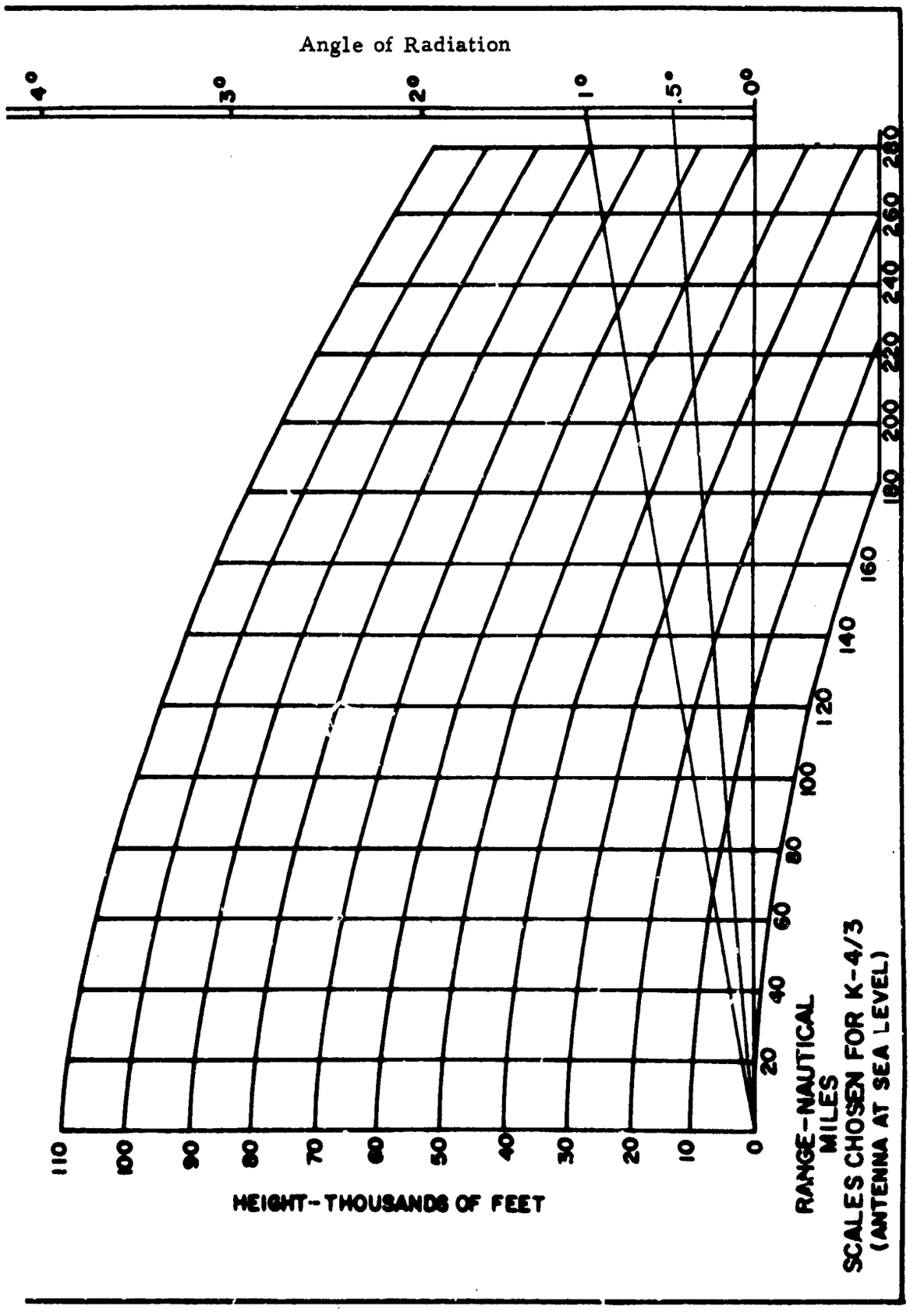

Figure B-2. Line of Sight Range vs Base Station Antenna Height

is emphasized that these angles are representative but not absolute and it is suggested that other angles also be assumed and typical ranges for them also be considered with various base stations antenna heights.

The chart indicates quite clearly the desire for a low radiation angle and also indicates the requirement for height at the base station (receiving) end to achieve long distance communications. Neglecting fortituous reflections, it is obvious that the VHF frequency regime for long distance communications is effectively reserved for what can generally be classed as air-to-ground communication where the receiving station is elevated, either by topography or in an airborne vehicle such as a plane, a repeater balloon, or a satellite.

B1.2 LOW FREQUENCY COMMUNICATIONS

The frequency spectrums from 30 KHz to 300 KHz and 300 KHz to 3 MHz are defined as LF and MF. The propagation characteristics of low frequency are controlled by the following facts:

a. The ground wave attenuation is considerably less than at the higher frequencies.

b. The sky wave penetrates the ionosphere only a slight bit and acts somewhat like a reflecting mirror.

c. The energy absorption in the ionosphere is relatively small and is less for the lower frequency.

Rapid fading at the lower frequencies is not generally observed. Any changes in signal strength occur gradually. At a distance, the field strength is the resultant of a ground wave and wave reflection from the ionosphere. Depending on the distance and frequency, these two waves may add or subtract and their phase relationship will vary with the season and the time of day.

Since sky wave propagation is not always reliable even at the lower frequencies, only ground wave propagation will be considered. The ground wave is that part of the total radiation that is directly affected by the presence of the earth and its surface features. The ground wave is divided into two components; a surface wave and a space wave. The space wave is the result of two components; the direct wave and a ground reflected wave. The ground wave intensity as a function of distance for a given transmitter power depends upon the earth conductivity, the frequency and the antenna configuration. The earth'e conductivity is important. LF communications are substantially improved in transmitting regions of high conductivity such as water, marshlands, etc.

A characteristic of LF communications is noise. Radio disturbances from natural causes such as lightning, electrical storms, etc., are designated variously as static and atmospherics. The effects of such disturbances are also referred to as noise, although this is usually indicated as "man made" electrical disturbances, such as electric razors, power lines, etc. Mountains, desert areas, and the tropics are important sources of static interference. Storm centers, particularly tropical hurricanes are common causes of static. Noise at the lower frequencies has a very high intensity. This is in part because the natural sources of static generate greater intensities at low frequencies and in part because of the very efficient ground wave propagation. Noise will be a major inhibiting factor in the use of low frequency and will result in some periods during which the radio link will not be usable. By using limited bandwidth communications, noise effects can be markedly reduced.

Another facet of LF communications is interference. Interference may be caused by co-channel stations on the same frequency even at some distance. The interfering station(s) may be received by "sky wave" propagation at certain hours of the day or by "extended" ground wave or other

phenomenom. Other interference may be adjacent channel stations, usually nearby with higher power. The only real solution to this type of interference is a careful selection of clear channel frequencies if possible.

A major consideration in LF work is the antenna. Low frequency antennas are quite large and complex due to the long wave lengths involved and the importance of an efficient ground system. However, for moderate range, it was felt that sufficient ERP could be obtained from a loaded short antenna, such as a base loaded whip, helical whip or possibly a loaded wire antenna.

The AMQ-27 scheme for LF communications evolves about driving a necessarily inefficient antenna at high power (at a low duty cycle). To achieve as much noise immunity as possible, and to center maximized power in a minimum frequency spectrum, narrow bandwidth is utilized. A "worst case" graph is shown in Figure B-3. The graph shows the average noise level (1 microvolt per meter dotted line) in a 100 Kz bandwidth and a ground wave curve for an arid geographical location. Propagation of the ground-wave is poor in arid areas and noise is high in the tropics. The dotted line above the tropical noise level line represents the required received power for a 30 db signal/noise output. The ground wave curve is based on a transmitter with 100-w power and an antenna efficiency of 1%. Basically, this "worst case" graph indicates that good communication can be expected up to about 50 miles and that tropic noise combined with ground wave attenuation present a grey area in the 50-100 mile range. The performance indicated in the graph can be improved in three manners: a) increased ERP, b) better (moist) terrain conditions, c) improved receiver performance through filtering and signal enhancement techniques.

Increased ERP is not particularly useful in this application. Although the transformation of dc power into rf power is much more efficient that at VHF by a factor of about 10:1, the antenna efficiency is worse by a

factor in the area of 100:1. Therefore, looking at the total picture, exorbitant amounts of dc power are required to realize even a marginal increase in ERP. However, as pointed out earlier, the LF ground wave propagates markedly more efficiently than a VHF ground wave enabling a small LF ERP to achieve substantial range.

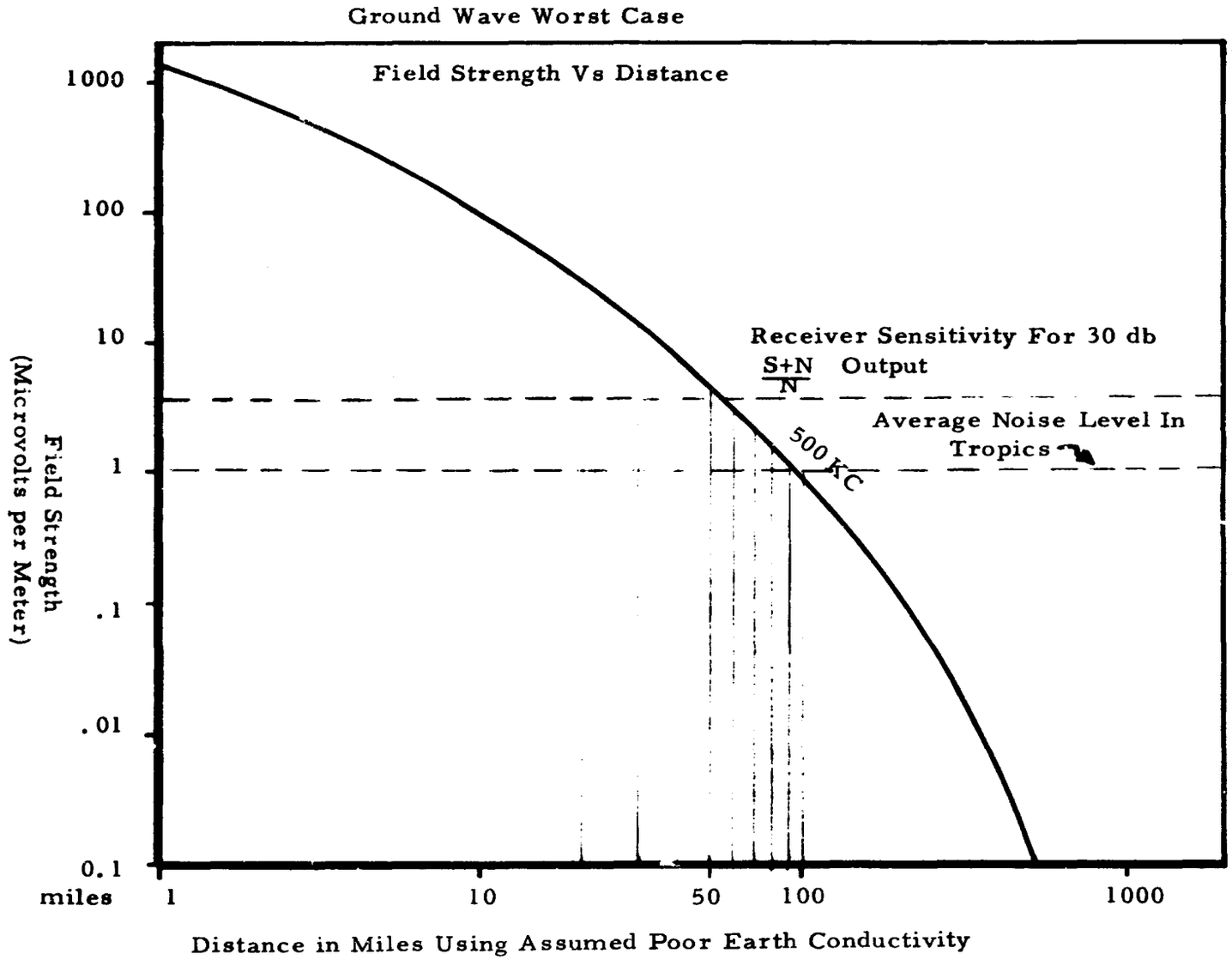

Figure B-3, Signal Field Strength vs Range Figure

APPENDIX C

ANTENNA DESIGN STUDIES

APPENDIX C

ANTENNA DESIGN STUDIES

ANTENNA DATA FROM INITIAL INVESTIGATION WITH DIPOLE ANTENNA

Type	Dipole (whip) 1/4 wave
Frequency	51 MHz
Length	$\lambda = \frac{300}{51} = \frac{5.9 \text{ meters}}{4} = 1.75$ meters
	L (in inches) = 1.475 x 39.4 = 58 inches

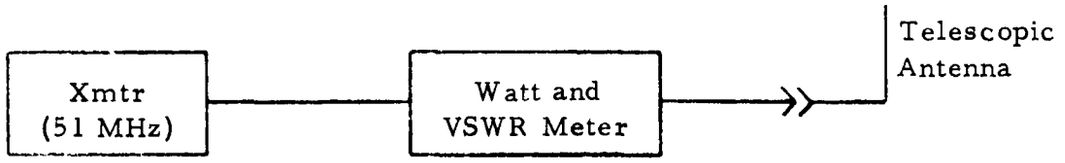

Test No. 1: Optimum Antenna Length

These tests were conducted with the antenna mounted on the AMQ-27 unit and using the rotor blades as the ground plane with the antenna extended the 58-inch calculated length.

The purpose of this test was to determine actual antenna length. The method used for all these tests is a simple one. By using a VSWR meter to measure the referenced power, one can assume that minimum VSWR indicates that: (1) the impedance of the generator output has been matched for maximum power transfer and (2) that the antenna length is, in fact, the proper length to present the characteristic impedance the generator requires.

	Antenna Length	Fwd/Pwr	Refl/Pwr
1.	58"	5.6 W	1.1
2.	56"	3.9 W	0.7
3.	53"	4.0 W	0.3
4.	50"	3.5 W	0.05
5.	44"	4.8 W	1.1

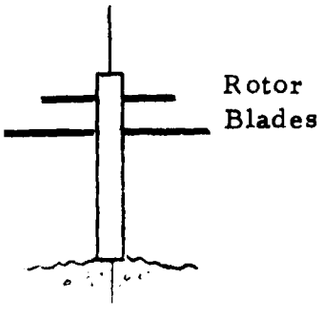

Rotors Extended

For minimum VSWR, 50" is the optimum antenna length.

Test No. 2: Effects of Rotor Blades on Antenna Length

This test was conducted to determine the effects the rotor blades would have on the antenna length if, upon impact, the blades failed to remain in an extended position. Three conditions could exist: (1) the upper blades could collapse, (2) the bottom blades could collapse, and (3) both blades could collapse. All three conditions were tested.

(1) Condition: Upper Rotor Blades Collapsed

	Antenna Length	Fwd/Pwr	Refl/Pwr
	50"	8.0 W	4.0
Test No. 1	60"	5.2 W	1.3
50" Ref.	66"	3.6 W	0.1
	72"	4.8 W	1.2

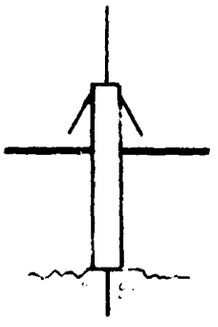

66" optimum, approximately 16" greater than original measurement with both rotors extended.

(2) Condition: Lower Rotor Blades Collapsed

Antenna Length	Fwd/Pwr	Refl/Pwr
50"	8.2 W	5.0
60"	5.3 W	1.5
66"	3.6 W	0.2
72"	5.8 W	1.8

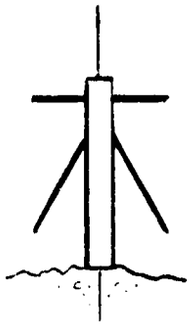

66" optimum, approximately 16" greater than original measurement with both rotors extended.

(3) Condition: Both Blades Collapsed

Antenna Length	Fwd/Pwr	Refl/Pwr
50"	8.4 W	5.0
66"	5.0 W	1.2
71"	4.2 W	0.8
76"	4.0 W	0.7
86"	5.0 W	1.25

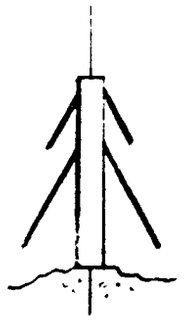

76" optimum, 28" greater than original measurement with both rotors extended.

The preceding tests showed that a large variation exists in the antenna length when ideal conditions are not met.

With the large number of variables which could exist, it would be impossible to transmit the same amount of power from unit to unit. Since there is no guarantee that the conditions in Test No. 2 would not occur, then, the probability of them occurring will have to be assumed.

To overcome any ambiguity in antenna length due to the rotor blades being collapsed, a fixed ground plane was tried starting with six 3-foot radials

spaced 60° from each other and, after extensive testing, reducing the number of radial to three, and then reducing the length to 18 inches. Tests conducted for all conditions in Test No. 2 showed that the antenna length centered at 64" and was not effected by the rotor blades under any conditions.

Test No. 3

These tests were conducted to determine the effects the penetration of the vehicle in the ground would have on VSWR and antenna length. Tests showed that the vehicle could penetrate the ground to the lower blades without significantly effecting the VSWR and antenna length.

Test No. 4: Off-Vertical Angle Effects on Signal Strength

Range tests indicated that the antenna can operate without critically effecting the signal strength as much as 35° off-vertical.

UNCLASSIFIED
Security Classification

DOCUMENT CONTROL DATA - R&D
(Security classification of title, body of abstract and indexing annotation must be entered when the overall report is classified)

1 ORIGINATING ACTIVITY (Corporate author)
Packard Bell Electronics, Space and Systems Div.
649 Lawrence Drive
Newbury Park, California 91320

2a REPORT SECURITY CLASSIFICATION
Unclassified

2b GROUP

3 REPORT TITLE
THE AN/AMQ-27( ) METEOROLOGICAL STATION, AUTOMATIC

4 DESCRIPTIVE NOTES (Type of report and inclusive dates)
Scientific Final February 1967 - August 1969 Approved 10 Sept 1969

5 AUTHOR(S) (Last name, first name, initial)
Lee G. Buhr Jan Rampacek
Octavio Galindo

6 REPORT DATE	7a TOTAL NO. OF PAGES	7b NO. OF REFS
6 August 1969	166	1

8a CONTRACT OR GRANT NO.	9a ORIGINATOR'S REPORT NUMBER(S)
F19628-67-C-0174	
b PROJECT NO. 6670-02-01	
c DOD ELEMENT 62101F	9b OTHER REPORT NO(S) (Any other numbers that may be assigned this report)
d DOD SUBELEMENT 681000	AFCRL-69-0374

10 AVAILABILITY/LIMITATION NOTICES
Distribution of this document is unlimited. It may be released to the Clearinghouse, Department of Commerce, for sale to the general public.

11 SUPPLEMENTARY NOTES
TECH, OTHER

12 SPONSORING MILITARY ACTIVITY
Air Force Cambridge Research Lab. (CRE)
L. G. Hanscom Field
Bedford, Massachusetts 01730

13 ABSTRACT

Packard Bell has successfully completed a program that developed an expendable, air droppable weather station (the AN/AMQ-27( ) Meteorological Station, Automatic) for the Air Force Cambridge Research Laboratories (AFCRL) under contract number F19628-67-C-0174. The Station grew out of a requirement for meteorological measurements in hostile or inaccessible areas. Packard Bell investigated this problem and devised a system that met the program's objectives of cost, reliability and covertness. The Station's deployment vehicle mimics an autogyro when dropped from an aircraft. The main rotor blades control descent rate, while a set of counter rotating blades provide vertical stability. Upon touchdown, the impact spear embeds itself in the earth, thereby, keeping the system upright. Since there are no highly mechanized devices required for arming the system, the station is operational at impact. This report covers in detail, the problems and their solutions that were encountered as this program progressed to its completion.

DD FORM 1473

UNCLASSIFIED
Security Classification

14 KEY WORDS	LINK A		LINK B		LINK C	
	ROLE	WT	ROLE	WT	ROLE	WT
Automatic Weather Stations						
Meteorological Sensors						
Anenometers						
Barometers						
Hygrometers						
Thermistors						
Precipitation gauges						
Airdrop Systems						
Aerodynamic Deceleration						
Air Launched Vehicles						
Telemetry						
VHF Communications						
Antennas						
Power Sources						

INSTRUCTIONS

1. ORIGINATING ACTIVITY: Enter the name and address of the contractor, subcontractor, grantee, Department of Defense activity or other organization *(corporate author)* issuing the report.

2*a*. REPORT SECURITY CLASSIFICATION: Enter the overall security classification of the report. Indicate whether "Restricted Data" is included. Marking is to be in accordance with appropriate security regulations.

2*b*. GROUP: Automatic downgrading is specified in DoD Directive 5200.10 and Armed Forces Industrial Manual. Enter the group number. Also, when applicable, show that optional markings have been used for Group 3 and Group 4 as authorized.

3. REPORT TITLE: Enter the complete report title in all capital letters. Titles in all cases should be unclassified. If a meaningful title cannot be selected without classification, show title classification in all capitals in parenthesis immediately following the title.

4. DESCRIPTIVE NOTES: If appropriate, enter the type of report, e.g., interim, progress, summary, annual, or final. Give the inclusive dates when a specific reporting period is covered.

5. AUTHOR(S): Enter the name(s) of author(s) as shown on or in the report. Enter last name, first name, middle initial. If military, show rank and branch of service. The name of the principal author is an absolute minimum requirement.

6. REPORT DATE: Enter the date of the report as day, month, year, or month, year. If more than one date appears on the report, use date of publication.

7*a*. TOTAL NUMBER OF PAGES: The total page count should follow normal pagination procedures, i.e., enter the number of pages containing information.

7*b*. NUMBER OF REFERENCES: Enter the total number of references cited in the report.

8*a*. CONTRACT OR GRANT NUMBER: If appropriate, enter the applicable number of the contract or grant under which the report was written.

8*b*, &, & 8*d*. PROJECT NUMBER: Enter the appropriate military department identification, such as project number, subproject number, system numbers, task number, etc.

9*a*. ORIGINATOR'S REPORT NUMBER(S): Enter the official report number by which the document will be identified and controlled by the originating activity. This number must be unique to this report.

9*b*. OTHER REPORT NUMBER(S): If the report has been assigned any other report numbers *(either by the originator or by the sponsor)*, also enter this number(s).

10. AVAILABILITY/LIMITATION NOTICES: Enter any limitations on further dissemination of the report, other than those imposed by security classification, using standard statements such as:

(1) "Qualified requesters may obtain copies of this report from DDC."

(2) "Foreign announcement and dissemination of this report by DDC is not authorized."

(3) "U. S. Government agencies may obtain copies of this report directly from DDC. Other qualified DDC users shall request through

_____."

(4) "U. S. military agencies may obtain copies of this report directly from DDC. Other qualified users shall request through

_____."

(5) "All distribution of this report is controlled. Qualified DDC users shall request through

_____."

If the report has been furnished to the Office of Technical Services, Department of Commerce, for sale to the public, indicate this fact and enter the price, if known.

11. SUPPLEMENTARY NOTES: Use for additional explanatory notes.

12. SPONSORING MILITARY ACTIVITY: Enter the name of the departmental project office or laboratory sponsoring *(paying for)* the research and development. Include address.

13. ABSTRACT: Enter an abstract giving a brief and factual summary of the document indicative of the report, even though it may also appear elsewhere in the body of the technical report. If additional space is required, a continuation sheet shall be attached.

It is highly desirable that the abstract of classified reports be unclassified. Each paragraph of the abstract shall end with an indication of the military security classification of the information in the paragraph, represented as *(TS)*, *(S)*, *(C)*, or *(U)*.

There is no limitation on the length of the abstract. However, the suggested length is from 150 to 225 words.

14. KEY WORDS: Key words are technically meaningful terms or short phrases that characterize a report and may be used as index entries for cataloging the report. Key words must be selected so that no security classification is required. Identifiers, such as equipment model designation, trade name, military project code name, geographic location, may be used as key words but will be followed by an indication of technical context. The assignment of links, rules, and weights is optional.